Article:
Colombera, L orcid.org/0000-0001-9116-1800 and Mountney, NP orcid.org/0000-0002-8356-9889 (2020) Accommodation and sediment-supply controls on clastic parasequences: a meta-analysis. Sedimentology, 67 (4). pp. 1667-1709. ISSN 0037-0746

https://doi.org/10.1111/sed.12728

Accommodation and sediment-supply controls on clastic parasequences: a meta-analysis

Luca Colombera*, Nigel P. Mountney

School of Earth & Environment, University of Leeds, LS2 9JT, Leeds, UK

*) corresponding author. l.colombera@leeds.ac.uk

ABSTRACT

This study combines data from many published case studies to undertake a quantitative characterization of clastic parasequences, with the aim to determine how accommodation, sediment supply and autogenic sediment-storage dynamics are recorded in their sedimentary architecture and stacking patterns. Results of this study are used to critically evaluate the validity of paradigms and models that are routinely used to explain and predict trends in the anatomy and arrangement of parasequences. Data on 957 parasequences from 62 case studies of clastic, shallow-water successions were coded in a relational database, which includes outcrop and subsurface datasets of ancient and Quaternary examples. These units cover the preserved records of both river-dominated deltas and wave-dominated coasts, representing shoreline transits over a breadth of timescales, likely of both local and regional extent. The role of extant accommodation, rates of creation of accommodation (A) and rates of sediment supply (S) in determining parasequence architecture is assessed through analysis of relationships between (i) proxies of these variables at different scales (rates of aggradation and progradation, facies-belt shoreline trajectories, systems-tract type, parasequence-set stacking patterns, parasequence progradation angle and stratigraphic rise, size of feeder rivers), and (ii) parameters that describe the geometry and stacking style of parasequences, and associated shallow-water sand bodies. Statistical analyses of database outputs indicate which proxies of accommodation, sediment supply and A/S ratio are significant as predictors of parasequence architecture, and which allow for interpretations of the importance of allogenic and autogenic factors. The principal results of this study reveal the following: (i) parasequence thickness varies as a function of water depth, accommodation generation and erosional truncation, and these variations are also reflected across types of systems tracts and parasequence sets; (ii) the dip length of parasequence sand bodies demonstrates scaling with measures of A/S ratio at multiple scales, partly in relation to the possible effect of sediment supply on progradation rates; (iii) in systems tracts, stratigraphic trends in parasequence stacking due to autogenic mechanisms or to acceleration or deceleration in relative sea-level fluctuations are not revealed quantitatively; (iv) some association is seen between the abundance of deltaic or river-dominated parasequences and progradational stacking; (v) positive but modest correlation is observed between measures of river-system size and the dip length of shallow-marine parasequence sand bodies. The resulting insights can be applied to guide sequence stratigraphic interpretations of the rock record and the characterization of sub-seismic stratigraphic architectures of subsurface successions.

Keywords: sequence stratigraphy; shallow marine; sand body; shoreline; shelf; sedimentary architecture.

INTRODUCTION

Parasequences are widely applied in the description of clastic shallow-marine strata and are commonly regarded as the fundamental building blocks of sequence-stratigraphic interpretations. Current knowledge of geological controls on parasequence architectures is supported by empirical understanding originating from studies of the rock record (e.g., Garrison & van den Berg, 2004; Olariu et al., 2012; Hampson, 2016), and by insight from physical or numerical experiments (e.g., Ross et al., 1995; Charvin et al., 2011; Straub et al., 2015). Yet, interpretations of shallow-marine successions are still largely guided by basic thought experiments, typically depicted as idealized cartoons (e.g., Posamentier et al., 1988; Van Wagoner et al., 1988; Embry, 2009). It is widely assumed that parasequence architectures are influenced by accommodation and rates of creation thereof, by rates of

sediment supply to formative palaeo-shorelines, and by autogenic processes, but the relative importance of these different factors still needs to be elucidated. Furthermore, factors other than accommodation and sediment-supply rates (e.g., process regime, grainsize calibre) are likely to affect resulting architectures (cf. Swift & Thorne, 1991; Swift et al., 1991; Rodriguez & Meyer, 2006; Reynolds, 2009; Patruno & Helland-Hansen, 2018).

Further investigation of controls on parasequence architectures is therefore warranted, and quantitative assessments undertaken on large datasets and with consideration of the origin and geological context of parasequences can improve understanding of the significance of controlling factors (cf. Ainsworth et al., 2018, 2020; Colombera & Mountney, 2020).

The aim of this work is to investigate how accommodation and sediment supply are recorded in the parasequence architecture of clastic successions at multiple scales. Specific research objectives are as follows: (i) to present a synthesis of properties that describe the geometry, lithology, stacking pattern, interpreted origin, and rates of evolution of clastic parasequences described in the scientific literature, (ii) to test hypotheses on the importance of controlling factors by means of a statistical approach, and (iii) to discuss the applied significance of the findings in view of their possible predictive use in subsurface studies.

First, this work provides a brief synopsis of current views on controls on parasequence architectures. The work then presents the results of a meta-study of published datasets so as to attempt to ascertain and elucidate the role of accommodation and sediment supply in controlling the stratigraphic record of shallow-marine successions.

BACKGROUND

Parasequences: definitions and application

The progradation of linear coasts and deltas into shallow open seas is typically recorded as a succession of offshore to littoral deposits arranged into a coarsening- and shoaling-upward trend (Fig. 1A). Resulting regressive packages are commonly capped by flooding surfaces and may be overlain by transgressive deposits, which together represent a response to increases in water depth that may be widespread and allogenic in origin (e.g., eustatic) or local and autogenic (e.g., due to delta drowning driven by river avulsion) (Reading & Collinson, 1996, and references therein). The recognition and correlation of apparently cyclically arranged stratal packages of shallow-marine sand or sandstone tongues encased in marine muds or mudstones and bounded by surfaces recording marine flooding predates the advent of sequence stratigraphy as a recognized discipline (e.g., Hollenshead & Pritchard, 1961; Coleman & Gagliano, 1964; Harms et al., 1965; Frazier, 1974). However, the formalization of units of this type in sequence-stratigraphic practice was first proposed by Van Wagoner (1985), who defined a parasequence as "a relatively conformable succession of genetically related beds or bedsets bounded by marine flooding surfaces and their correlative surfaces", and a flooding surface as a surface "across which there is evidence of an abrupt increase in water depth" (Van Wagoner et al., 1988, p. 39).

Parasequences were considered to arise from variations in the balance between sediment supply and relative sea-level change, but were originally defined as units that only develop under conditions of non-negative accommodation (Van Wagoner et al., 1990; Kamola and Van Wagoner, 1995), i.e., that are the product of sedimentation during a sea-level stillstand (a 'paracycle' *sensu* Vail et al., 1977) or during a phase when the rate of sediment supply outpaces the rate of accommodation generation. Thus, by their original definition, parasequences record normal regression (Fig. 2A). Notwithstanding, shoaling-upward packages have sometimes been termed 'parasequences' despite being part of successions accumulated during forced regression (Fig. 2A) and having characters that contrast with the definition of a parasequence *sensu* Van Wagoner (1985): where shallowing-upward units – organized in down-stepping patterns – record shelf transit during stillstands of falling stages, flooding surfaces should not develop between consecutive instances of these. Furthermore, the term has even been used to refer to units developed during relative sea-level fall (cf. Plint, 1991; Catuneanu et al., 2010; Li et al., 2011a). Uncertainty on whether a sedimentary unit represents a true parasequence is also caused by criteria for identifying forced regression, such as downstepping stratal geometries, since

these may be difficult to recognize in outcrop and across wells and below the resolution of seismic datasets. Other issues with the definition and diagnostic criteria of parasequences, discussed in detail elsewhere (Swift et al., 1991; Posamentier and James, 1993; Arnott, 1995; Christie-Blick & Driscoll 1995; Kamola & Van Wagoner, 1995; Zecchin, 2007, 2010; Embry & Johannessen, 2017; Catuneanu, 2019a, 2019b; Colombera & Mountney, 2020), make the recognition of parasequences partly subjective: resulting inconsistencies in their application must be acknowledged when adopting these units as the basis for interpreting controls on the stratigraphic record. An issue that is of particular significance to the analyses presented below is the fact that parasequences can be defined for stratal patterns that develop at different scales, in sedimentary units that can be nested hierarchically, even in the same succession (cf. Fig. 1B; Ainsworth et al., 2019; Colombera & Mountney, 2020; and references therein).

Nonetheless, clastic parasequences are considered here because they enable, in principle, a comparative analysis of many shallow-marine regressive tongues. By adhering to the original broad definition of parasequence (Van Wagoner et al., 1988), insight can be derived from meta-analysis that is relevant to situations where a more detailed classification of sedimentary units cannot be made with confidence (e.g., in subsurface interpretations supported by limited datasets, where parasequences may be varied in origin and sedimentary hierarchy). Herein, the focus is particularly on the role of accommodation and sediment supply as controls on parasequence architectures. A synthesis of many examples of parasequences aiming to offer some insight into their geological significance is presented in a companion paper (Colombera & Mountney, 2020).

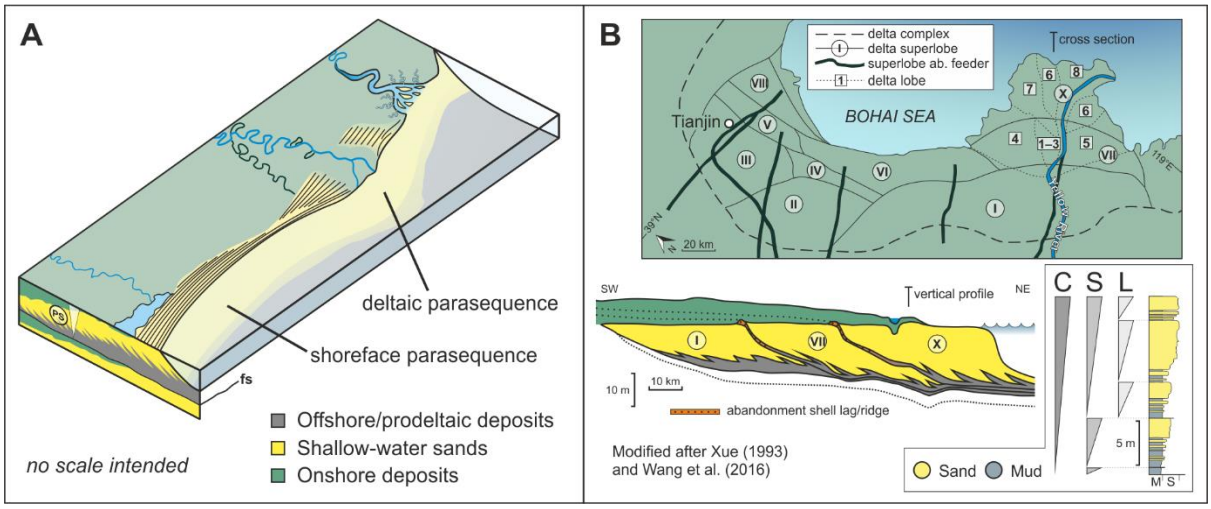

Figure 1: Definition and architecture of shoreface and deltaic parasequences (A). Part B illustrates a planview map and a cross-section of the accretionary history of the Yellow River delta (China), which serves as an example of how the sedimentary architecture of deltaic successions could be variably formalized into parasequences. The planform extent of deltaic constructional units of different hierarchies (delta complex, delta superlobe, and delta lobe, in order of descending scale; Xue, 1993; Wang et al., 2016, and references therein) on the delta plain is shown in map, together with the location of their now abandoned feeder channel belts. The idealized vertical log exemplifies the possible facies sequence of these units (C = complex; S = superlobe; L = lobe), which may variably be treated as deltaic parasequences, to highlight the challenge of defining parasequences in datasets with limited observations (cf. Fig. 2 in Ainsworth et al., 2019). Arabic numerals indicate delta 'lobes' (Wang et al., 2016); Roman numerals indicate delta 'superlobes' (Xue, 1993).

Parasequence controls: accommodation and sediment supply

Inferences of the controls exerted by accommodation and sediment supply based on sequence stratigraphic interpretations are commonly guided by theoretical predictions of how these factors affect stratal architectures at the scales of parasequences and parasequence sets (e.g., Posamentier et al., 1988; Galloway, 1989; Van Wagoner et al., 1990; Schlager, 1993; Wehr, 1993; Soreghan & Dickinson, 1994;

Posamentier & Allen, 1999). Some of these basic concepts have been substantiated in the following ways: (i) by outcrop and subsurface studies of the stratigraphic record where variations in accommodation and sediment supply can be constrained or inferred and compared with parasequence architectures, (e.g., Kidwell, 1993; van den Berg & Garrison, 2004; Aschoff & Steel, 2011; Carvajal & Steel, 2012; Hampson, 2016); (ii) by results of physical experiments and of process-based or geometric numerical-modelling exercises (e.g., Burgess & Allen, 1996; Houston et al., 2000; Kim et al., 2006; Charvin et al., 2011; Burpee et al., 2015); and (iii) by studies of the evolution of modern shoreline-shelf systems (e.g., Rodriguez & Meyer, 2006; Wolinsky et al., 2010; Tamura, 2012; Hein et al., 2016).

Accommodation is recognized to control the geometry of individual parasequences (Fig. 2B). At a fundamental level, the water-depth and gradient of the shelf or ramp into which a shoreline builds out determine the (decompacted) thickness of a parasequence and influence the rate and amount of shoreline progradation it records (Heward, 1981; Jervey, 1988; Emery & Myers, 2009; Reynolds, 2017; Ainsworth et al., 2018, 2020). The seabed bathymetry is itself a function of the rate at which accommodation is generated and of spatial variations thereof, and is also influenced by the rate of sediment supply and by type and energy of the process regime operating therein (Swift & Thorne, 1991). In some cases the three-dimensional nature of the pre-existing accommodation into which parasequences develop may be complex, for example where parasequences are generated as bayhead-delta cycles within the confines of incised valleys (cf. Thomas & Anderson, 1994; Bartek et al., 2004; Amorosi et al., 2008; Simms & Rodriguez, 2015). In these cases palaeo-topographies will control how sediment is distributed to a shoreline and the resulting lateral and downdip extent of parasequences, and can even act to determine or prevent autogenic parasequence generation, for example by dictating accommodation changes through progressive flooding of terraced profiles (cf. Rodriguez et al., 2005) and by suppressing trunk-river avulsion (Bhattacharya et al., 2019), respectively.

At parasequence scale, the rates of creation of accommodation resulting from subsidence and eustatic fluctuations control the thickness of parasequences by driving aggradation and causing burial of older deposits (Wehr, 1993; Emery & Myers, 2009; Ainsworth et al., 2018; Fig. 2B). However, when an increase in accommodation outstrips sediment supply leading to transgression, reduction of parasequence thickness can occur in the form of erosional beheading by wave or tidal ravinement (Posamentier & Allen, 1999; Cattaneo & Steel, 2003; Jordan et al., 2016; Zecchin et al., 2019).

Temporal changes in rates of creation of accommodation through a relative sea-level cycle are expected to determine variations across systems tracts and parasequence sets, with regards to the likelihood of development of units classifiable as parasequences and to their geometry. For example, paracycles are thought to be more likely during highstand and under conditions of overall shoreline progradation (Carter et al., 1998; Helland-Hansen & Hampson, 2009). Parasequences are also thought to be thicker on average in transgressive systems tracts because of the relatively higher rate of accommodation generation under which they form (Reynolds, 2017). In a basin, spatial variability in rates of creation of accommodation is expected to simultaneously affect parasequence geometry and stacking style (i.e., whether a parasequence set is ‘progradational’, ‘aggradational’, or ‘retrogradational’, according to the definitions by Van Wagoner et al., 1988); this could be expressed, for instance, in the lateral along-strike transition from thicker parasequences organized in an aggradational set to a progradational set of thinner parasequences towards regions undergoing slower subsidence (Fig. 2C; cf. Van Wagoner et al., 1990; Wehr, 1993; Martinsen & Helland-Hansen, 1994; Krystinik & DeJarnett, 1995; Zecchin et al., 2006; Madof et al., 2016). Modes of sediment accommodation also vary across types of basins in relation to the magnitude and direction of subsidence gradients. Whether a sedimentary basin undergoes back-tilting or fore-tilting, or whether it presents syndepositional flexural bulges, will have an influence on sediment distribution and therefore on parasequence thickness, progradation distance and style of stacking (cf. Bhattacharya & Posamentier, 1994; Herbert, 1997; Emery & Myers, 2009; Hajek et al., 2014; Leva López et al., 2014).

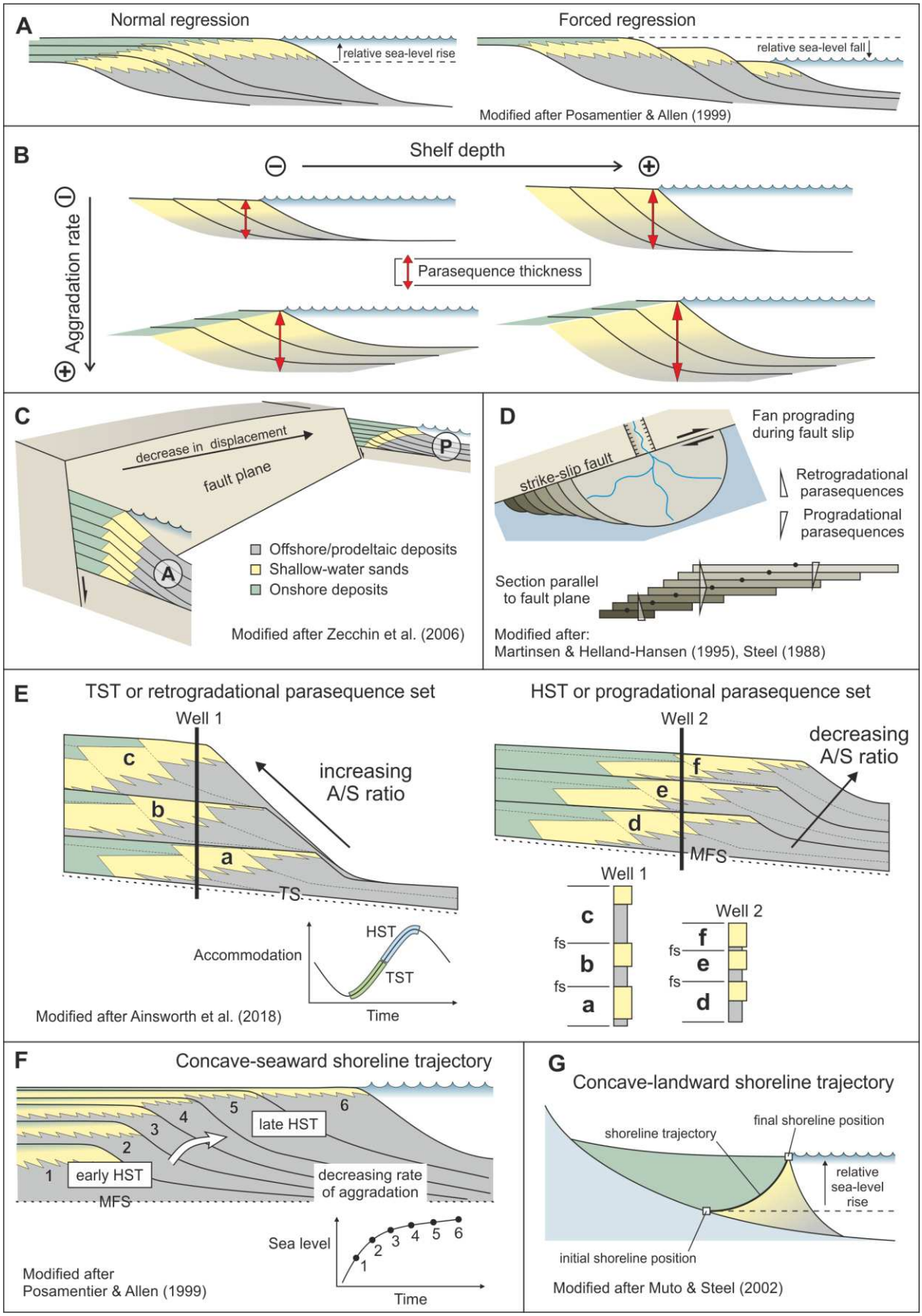

Figure 2: Accommodation and sediment-supply controls on the architecture of shoreface and deltaic parasequences. Part A illustrates stacking styles associated with normal and forced regression. Part B summarizes the expected influence of extant shelf accommodation (water depth) and rates of accommodation creation (aggradation rate) on parasequence thickness. Part C shows along-strike variation in parasequence

stacking patterns, from aggradational (A) to progradational (P), and the associated change in parasequence thickness resulting from spatial decrease in rate of creation of accommodation in extensional basins (Zecchin et al., 2006). Part D shows spatio-temporal changes in parasequence stacking patterns arising from progressive displacement of the position of a sediment entry point feeding a fan-delta system undergoing progradation, in response to strike-slip tectonics (Martinsen & Helland-Hansen 1995; cf. Steel, 1988). Part E shows parasequence thickness trends that can be predicted to develop in systems tracts based on acceleration or deceleration in the rate of relative sea-level rise. Parts F and G illustrate how concave-seaward (E) or concave-landward (F) shoreline trajectories can develop across sets of parasequences under constant rates of sediment supply, specifically in relation to decreasing rates of sea-level rise and to autogenic dynamics of linked depositional systems. Key shown in Fig. 1A applies to all parts of figure. See text for details.

The control operated by the rate of sediment supply to depositional shorelines (S) is commonly considered relative to that of the rate of creation of accommodation (A), and expressed in terms of A/S ratio. The stratigraphic record of changes in A/S ratio is manifested over a range of scales. Variations in A/S ratio during deposition of a parasequence are expected to affect its geometry and internal anatomy. Temporal changes in sediment influx affect accretion dynamics in the nearshore, which should control the amount of progradation experienced by the shoreline during the geological history of the parasequence, as well as its internal bedset architecture (cf. Houston et al., 2000; Storms & Hampson, 2005; Forzoni et al., 2014; Li et al., 2015). Accordingly, the magnitude of A/S, by regulating the relative amount of nearshore aggradation and shoreline progradation, should be reflected in the regressive shoreline trajectory of a parasequence (Helland-Hansen & Martinsen, 1996; Hampson, 2000; Løseth et al., 2006; Helland-Hansen & Hampson, 2009). It is also postulated that rates of sediment supply might control the fraction of sand or sandstone of a parasequence, and that, therefore, the ratio between parasequence thickness and sand fraction (T/SF ratio) should represent a proxy of A/S (Ainsworth et al., 2018; 2020). Moreover, the A/S ratio determines the preservation potential of normal-regressive units (Cattaneo & Steel, 2003; Zecchin et al., 2019), and is also thought to control the proportions and vertical trends of lithofacies and facies associations in parasequences, by affecting the relative degree of preservation of different facies belts (Swift et al., 1991; Cant, 1993; Helland-Hansen & Hampson, 2009). At the scale of multiple genetically related parasequences, temporal variations in A/S ratio are recorded in the stratigraphy in the form of changes of stacking pattern, which is itself a defining attribute of parasequence-set and systems-tract types (Van Wagoner et al., 1990; Wehr, 1993; Neal et al., 2016; Catuneanu, 2019a). Similarly, strike-oriented spatial variations in A/S associated with along-shore gradients in the rate of sediment supply can determine lateral changes in type and timing of development of parasequence stacking patterns (Fig. 2D; Van Wagoner et al., 1990; Schlager, 1993; Martinsen & Helland-Hansen, 1995; Forzoni et al., 2015).

Parasequence architectures are also controlled by inherent dynamics in the way accommodation and sediment supply change through time. Under conditions of sinusoidal sea-level fluctuations, the rate of sea-level rise is expected to be typically accelerating through late lowstand and transgressive conditions and decelerating through highstand (cf. Posamentier et al., 1988; Catuneanu, 2019a). Notwithstanding possible variations in sediment supply, this should result in predictable parasequence arrangements and stacking patterns, by determining stratigraphic variations in the amount of aggradation recorded in consecutive parasequences and in their regressive shoreline trajectories. So, for example, parasequence aggradation is expected to progressively increase through transgression and progressively decrease through highstand (Ainsworth et al., 2018; Fig. 2E), whereas the regressive shoreline trajectories of successive parasequences are expected to portray a concave-seaward trajectory in highstand systems tracts and a concave-landward trajectory in lowstand systems tracts (Posamentier et al., 1988; Posamentier & Allen, 1999; Catuneanu, 2019a; Fig. 2F). Parasequence characteristics may also be controlled by autogenic behaviours related to coastal progradation. Continental environments that increase in extent because of delta growth sequester a progressively larger volume of sediment inducing a decrease in sediment influx to the deltaic shoreline, which itself requires more sediment to maintain the rate of offshore progradation if the delta builds out into deeper waters and its subaqueous portion increases in area. An autogenic decrease in rate of progradation is therefore expected in deltas subject to constant accommodation and sediment-supply rates, and this should be reflected in a concave-landward shoreline trajectory (Jervey 1988; Muto & Steel, 1992, 1997, 2002; Fig. 2G). It is then

assumed that a concave-landward shoreline trajectory may also develop in parasequence sets and systems tracts arranged according to a progradational stacking pattern (Hampson, 2016). Potentially, a positive feedback may also exist whereby relative sea-level rise, by driving floodplain aggradation and thereby reducing the rate at which sediment reaches the shore, progressively enhances the rate of transgression (Kamola & Van Wagoner, 1995).

These considerations are not necessarily comprehensive of all possible ways in which accommodation and sediment supply are believed to control the geometry and arrangement of parasequences, but are particularly important because they are widely considered in interpretations of the stratigraphic record. These assumptions form testable hypotheses, whose investigation is rendered possible by geological data arising from the description of parasequences in subsurface and outcrop studies conducted in the last four decades, and which lend themselves to a quantitative assessment through a meta-analysis.

DATA AND METHODS

A compound analysis has been undertaken of many datasets collated from the scientific literature, and stored in a SQL relational database, the Shallow-Marine Architecture Knowledge Store (SMAKS; Colombera et al., 2016). SMAKS stores data on sedimentary units of different types, for marine and lacustrine shallow-water and paralic depositional systems, and on the depositional context, geological boundary conditions, and metadata of datasets and systems. SMAKS includes data on sequence stratigraphic units and surfaces, among other entities (Colombera et al., 2016). As of November 2019, SMAKS contained data on tens of thousands of sedimentary units, including over 2,000 sequence-stratigraphic units, of which 1,163 were parasequences that had originally been detailed in 64 case studies (Colombera & Mountney, 2020). Data on 957 parasequences from 62 case studies (Tab. 1) are used in this work. These units are recognized in sedimentary basins that collectively cover a range of tectonic and physiographic settings.

Parasequences defined according to the definition of Van Wagoner et al. (1990) are coded in SMAKS following the interpretations provided in the original literature sources. No reinterpretation is attempted of the original datasets by defining flooding surfaces, parasequences or other sequence stratigraphic units. The main implication of this approach is that the collated data are geologically heterogeneous (see below; cf. Fig. 1B). For datasets released over multiple publications, more recent interpretations are favoured over older ones (e.g., Simpson & Eriksson, 1990; Eriksson et al., 2019). Original interpretations are discarded if they contrast with the database standard; so, for example, units termed ‘parasequences’ in the literature sources but recognized to record shallowing-deepening cycles (e.g., Bowman, 2003) or displaying deepening-upward trends (e.g., Blondel et al., 1993) are not considered herein.

In SMAKS, hierarchical and spatial relationships between different types of genetic units are recorded (Colombera et al., 2016). This allows tracking the relative containment of parasequences into parent sequence stratigraphic units, including parasequence sets and systems tracts (cf. Fig. 1D), and to characterize spatial trends. Where multiple orders of systems tracts and parasequence sets are recognized in the original literature sources, parent systems tracts and parasequence sets employed in the analyses represent units that build third-order sequences *sensu* Vail et al. (1977). The hierarchical containment of parasequence bounding surfaces, typically flooding surfaces, into large-scale facies belts, termed ‘depositional tracts’ (Colombera et al., 2016), allows querying relationships between attributes of both types of units.

In SMAKS, parasequences are characterized employing several attributes, including genetic classifications of their deposits (Colombera & Mountney, 2020); interpretations by the original authors are relied upon. The interpreted depositional environment of parasequences is classified as ‘deltaic’, ‘shoreface’ *sensu lato* (i.e., the preserved expression of non-deltaic linear coasts, such as those of strandplains or barrier systems), or as ‘deltaic-shoreface’ (in cases where both deltaic and shoreface *s.l.* systems are interpreted to have formed the units; cf. Fig. 1A). SMAKS parasequences are also classified on the interpreted dominant process regime, according to classes that define the interpreted relative importance played by wave, tidal and fluvial processes on their accumulation, largely based on the

scheme by Ainsworth et al. (2011; e.g., 'F' = river dominated; 'Wf' = wave dominated, river influenced; 'Twf' = tide dominated, wave influenced, river affected). Deposits of uncertain attribution are left unclassified.

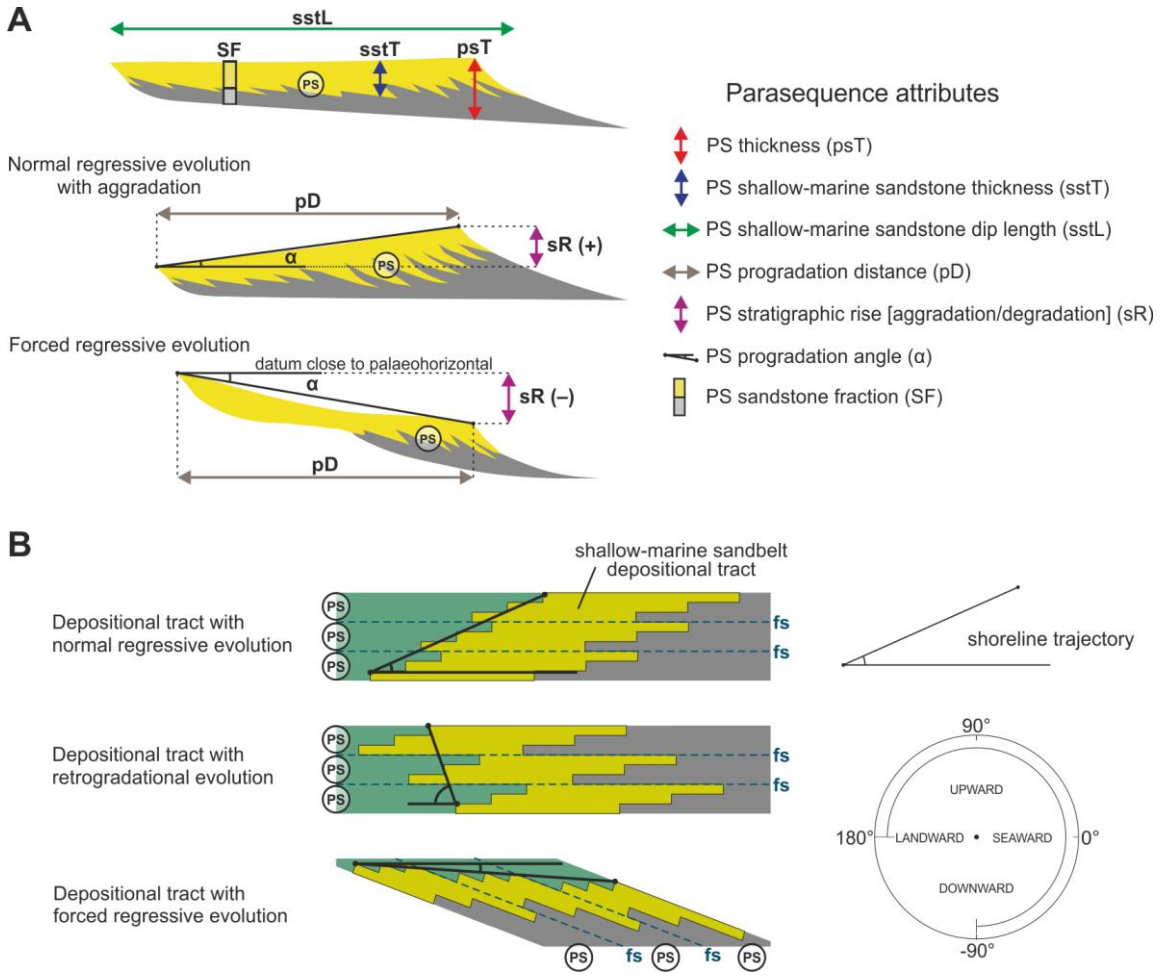

Figure 3: Definition diagram for quantities discussed in this article. (A) Parameters recorded in SMAKS (Colombera et al., 2016) to describe the anatomy of parasequences and of associated shallow-water sand belts. (B) Idealized examples illustrating shoreline trajectories (Helland-Hansen & Martinsen, 1996) for SMAKS depositional tracts across which multiple parasequences are recognized (Colombera et al., 2016). Labels 'PS' and 'fs' indicate parasequences and flooding surfaces, respectively.

Quantitative data on the geometry of parasequences (Fig. 3A), extracted from the original sources, include: the thickness of the parasequence, the thickness and downdip length of its shallow-water sand belt, and quantities that describe its regressive evolution, consisting of its progradation distance (i.e., the length of shoreline progradation recorded in the parasequence), its stratigraphic rise (i.e., the amount of aggradation at the shoreline) and the resulting progradation angle (i.e., the angle that tracks the direction of progradation of the parasequence relative to the palaeo-horizontal, that is, its regressive shoreline trajectory; Cant, 1991; Helland-Hansen & Martinsen, 1996). Values of thickness and dip length are classified by observation type, as 'true', 'apparent', 'partial' (when the location of termination of a unit at one end is unknown), or 'unlimited' (when the location of termination of a unit at both ends is unknown; Geehan & Underwood, 1993). This allows for analyses to be performed with consideration of possible bias arising from differences in observation types. No correction for sediment compaction has been applied to the thickness of sedimentary units. The estimated length of time (duration) and order of magnitude in timescale over which parasequences were accumulated are recorded, considering chronostratigraphic frameworks reported by the original authors and based on radiometrically dated

horizons within the successions or correlated through biostratigraphy.

Table 1: Summary of the 62 case studies of sequence stratigraphic interpretations considered in this work. A case study is a dataset on a particular succession, by some author or research group, as presented in a published source or Thesis (or in a set of related publications). References to the consulted literature sources that contain the sequence-stratigraphic interpretations and associated data are reported. The asterisk denotes a lacustrine succession; all other successions are paralic to shallow marine in origin. N indicates the number of parasequences considered in this work for each case study; a larger number of parasequences may be described in each case study. The data from each of these studies are recorded in the Shallow-Marine Architecture Knowledge Store (SMAKS) database, the structure of which allows for sophisticated querying to examine possible relationships (see Colombera et al., 2016).

Succession	**Location**	**Age**	**Data types**	**N**	**Sources**
Battfjellet Formation	Spitsbergen, Norway	Eocene	Outcrop	15	Gjelberg (2010); Helland-Hansen (2010)
Bell Island Group	Newfoundland, Canada	Lower Ordovician	Outcrop	8	Brenchley et al. (1993)
Blackhawk Formation	Utah, USA	Upper Cretaceous	Outcrop	38	Reynolds (1999); data from: Balsley (1982); Taylor & Lovell (1992); Van Wagoner (1992); O'Byrne & Flint (1993)
Bouzergoun Formation	Morocco	Lower Cretaceous	Outcrop	3	Nouidar & Chellaï (2002)
Cliff House Sandstone	New Mexico, USA	Upper Cretaceous	Outcrop	11	Jordan et al. (2016)
Ferron Sandstone 'Last Chance Delta'	Utah, USA	Upper Cretaceous	Outcrop	44	Garrison & van den Bergh (2004); van den Bergh & Garrison (2004)
Ferron Sandstone 'Notom Delta'	Utah, USA	Upper Cretaceous	Outcrop	43	Li et al. (2010, 2011a, 2011b, 2012); Zhu et al. (2012)
Foreknobs Formation	Virginia/West Virginia, USA	Upper Devonian	Outcrop	5	McClung et al. (2013, 2016); Eriksson et al. (2019)
Frontier Formation	Wyoming, USA	Upper Cretaceous	Outcrop	8	Feldman et al. (2014)
Gallup Formation	New Mexico, USA	Upper Cretaceous	Outcrop	61	Lin et al. (2019)
Gelincik Formation	Turkey	Miocene	Outcrop	32	Ilgar (2015)
Gros Morne Formation	Trinidad	Pliocene	Outcrop	13	Bowman (2003)
Hosta Tongue	New Mexico, USA	Upper Cretaceous	Outcrop	1	Sixsmith et al. (2008)
Jurassic of East Greenland	Greenland	Lower to Upper Jurassic	Outcrop	13	Surlyk (1991); Dam & Surlyk (1995); Larsen & Surlyk (2003); Engkilde & Surlyk (2003); Vosgerau et al. (2004)
Lajas Formation	Argentina	Middle Jurassic	Outcrop	7	McIlroy et al. (2005)
Mayaro Formation	Trinidad	Pliocene	Outcrop	16	Bowman (2003, 2016); Bowman & Johnson (2014)
Mesaverde Group	Wyoming, USA	Upper Cretaceous	Outcrop	9	Fitzsimmons & Johnson (2000)
Mulichinco Formation	Argentina	Lower Cretaceous	Outcrop	19	Wesolowski et al. (2018)
Neill Klinter Group	Greenland	Lower Jurassic	Outcrop	8	Eide et al. (2016)
Oligocene-Early Miocene of northern Taiwan	Taiwan	Oligocene to Miocene	Outcrop	55	Teng & Tai (1996)
Pilmatué Member, Agrio Formation	Argentina	Lower Cretaceous	Outcrop	11	Isla et al. (2018); Schwarz et al. (2018)
Pliocene of Dacian	Romania	Pliocene	Outcrop	10	Jorissen et al. (2018)

Basin					
Pliocene of Val d'Orcia Basin	Italy	Pliocene	Outcrop	4	Ghinassi (2007)
Point Lookout Sandstone	Colorado, USA	Upper Cretaceous	Outcrop	16	Crandall (1992); Katzman & Wright-Dunbar (1992); Wright-Dunbar et al. (1992)
Potrerillos Formation of Mexico	Mexico	Paleocene	Outcrop	29	Shelley & Lawton (2005)
Star Point Sandstone	Utah, USA	Upper Cretaceous	Outcrop	5	Hampson et al. (2011)
Straight Cliffs Formation	Utah, USA	Upper Cretaceous	Outcrop	11	McCabe & Shanley (1992)
Uppermost Kubang Pasu Formation	Malaysia	Cisuralian	Outcrop	8	Hassan et al. (2013, 2017)
Yenimahalle Formation*	Turkey	Miocene	Outcrop	12	Ilgar & Nemec (2005)
Battfjellet Formation	Spitsbergen, Norway	Eocene	Outcrop and subsurface	19	Grundvåg et al. (2014)
Blackhawk Formation and Castlegate Sandstone	Utah, USA	Upper Cretaceous	Outcrop and subsurface	29	Hampson & Storms (2003); Hampson & Howell (2005); Hampson et al. (2008); Charvin et al. (2010); Hampson (2010)
Blackhawk Formation and Castlegate Sandstone	Utah/Colorado, USA	Upper Cretaceous	Outcrop and subsurface	29	Pattison (2010, 2018, 2019a, 2019b)
Brejning Formation and Ribe Group	Denmark	Miocene	Outcrop and subsurface	6	Rasmussen et al. (2004); Rasmussen & Dybkjær (2005); Hansen & Rasmussen (2008); Rasmussen (2009)
Cozzette Sandstone	Utah/Colorado, USA	Upper Cretaceous	Outcrop and subsurface	6	Madof et al. (2015, 2016)
Emery Sandstone	Utah, USA	Upper Cretaceous	Outcrop and subsurface	17	Edwards et al. (2005)
Fox Hills Formation	Wyoming, USA	Upper Cretaceous	Outcrop and subsurface	10	Carvajal & Steel (2009); Olariu et al. (2012)
Frontier Formation	Utah/Colorado/Wyoming, USA	Upper Cretaceous	Outcrop and subsurface	7	Hutsky et al. (2016); Hutsky & Fielding (2016, 2017)
Mesaverde Group	Wyoming, USA	Upper Cretaceous	Outcrop and subsurface	17	Klug (1993)
Muskiki and Marshybank formations	Alberta, Canada	Upper Cretaceous	Outcrop and subsurface	15	Plint (1990, 1991); Plint & Norris (1991)
Point Lookout Sandstone	New Mexico, USA	Upper Cretaceous	Outcrop and subsurface	9	Devine (1991)
Quaternary of Paraná coastal plain	Brazil	Pleistocene to Holocene	Outcrop and subsurface	2	Angulo et al. (2009); Souza et al. (2012); Berton et al. (2019)
Rio Bonito and Palermo formations	Brazil	Cisuralian	Outcrop and subsurface	9	Holz (2003); Ketzer et al. (2003); Holz & Kalkreuth (2004); Holz et al. (2006)
Second Frontier sandstone, Frontier Formation	Wyoming, USA	Upper Cretaceous	Outcrop and subsurface	7	Vakarelov & Bhattacharya (2009)
Upper Almond Formation	Wyoming, USA	Upper Cretaceous	Outcrop and subsurface	21	Merletti et al. (2018)
Upper Sego Sandstone and Iles Formation	Colorado, USA	Upper Cretaceous	Outcrop and subsurface	24	Kirschbaum & Hettinger (2004); Kirschbaum & Cumella (2015)
Wall Creek Member, Frontier Formation	Wyoming, USA	Upper Cretaceous	Outcrop and subsurface	9	Lee et al (2005, 2007a, 2007b); Gani & Bhattacharya (2007); Sadeque et al. (2009)
22 Sand of	Trinidad	Pliocene	Subsurface	15	Bowman (2003)

Columbus Basin					
Arida and Diba formations	Libya	Oligocene	Subsurface	7	Gruenwald (2001)
Barrow Group	Northwest Shelf, Australia	Lower Cretaceous	Subsurface	40	Ainsworth et al. (2018)
Brigadier Formation	Northwest Shelf, Australia	Upper Triassic	Subsurface	16	Ainsworth et al. (2016, 2018)
Calcasieu incised valley	Louisiana, USA	Pleistocene to Holocene	Subsurface	3	Nichol et al. (1996)
Dunvegan Formation	Alberta, Canada	Upper Cretaceous	Subsurface	19	Bhattacharya (1989, 1992); Bhattacharya & Walker (1991a, 1991b); Bhattacharya & MacEachern (2009)
Gulf of Cádiz shelf	Spain	Pleistocene to Holocene	Subsurface	4	Lobo et al. (2001); Gonzales et al. (2004)
Gulf of Lion, inner shelf and Rhone Delta	France	Pleistocene to Holocene	Subsurface	10	Boyer et al. (2005); Labaune et al. (2005; 2008); Berné et al. (2007); Jouët (2007)
Gulf of Lion, outer shelf	France	Pleistocene	Subsurface	7	Berné et al. (1998); Rabineau et al. (2005); Jouet et al. (2006); Bassetti et al. (2006; 2008)
Hazad Member, Ankleshwar Formation	India	Eocene	Subsurface	21	Jaiswal et al. (2018)
Holocene of the Po Plain	Italy	Holocene	Subsurface	8	Amorosi et al. (2005, 2017); Campo et al. (2017)
Krossfjord and Fensfjord formations	Norway	Middle Jurassic	Subsurface	8	Holgate et al. (2013, 2015); Holgate (2014)
Late Quaternary of Tuscany	Italy	Pleistocene	Subsurface	3	Amorosi et al. (2008, 2013); Rossi et al. (2017)
Palaeo-Changjiang delta	China	Pleistocene to Holocene	Subsurface	3	Zhang et al. (2017)
Plover and Laminaria formations	Timor Sea	Middle Jurassic	Subsurface	23	Ainsworth (2005); Ainsworth et al. (2008)
Viking Formation	Alberta, Canada	Lower Cretaceous	Subsurface	19	Boreen & Walker (1991), Pattison (1991, 1992)

Values of parasequence ‘sand fraction’ (cf. Ainsworth et al., 2018, 2020) are computed based on the ratio between the maximum observed thickness of the parasequence shallow-water sand belt and the maximum observed thickness of the parasequence (Fig. 3A). Because these thickness values might have been observed at different locations, the parasequence ‘sand fraction’ does not necessarily correspond to the value of actual sand or sandstone proportion at either location, and is not necessarily an accurate measure of the global proportion for the parasequence. Values of parasequence thickness-to-sand-fraction ratios (cf. T/SF ratio of Ainsworth et al., 2018, 2020) are also computed accordingly, meaning that these metrics differ substantially from the T/SF ratios of Ainsworth et al. (2018, 2020), in two ways: (i) the downdip variability in volumetric sand fractions within individual parasequences is not characterized: estimations of sand fractions are less accurate than they would be if it was (as done by Ainsworth et al., 2018, 2020); (ii) the maximum, rather than the mean, parasequence thickness is considered.

In SMAKS, units termed ‘depositional tracts’ are defined that represent large-scale facies belts (e.g., shallow-marine sand belts); these units, which may span several stacked parasequences, are characterized based on several attributes (Colombera et al., 2016). The only parameter employed in this work is the depositional-tract ‘shoreline trajectory’, i.e., the angle that defines the direction of migration of a depositional shoreline-break relative to the palaeo-horizontal (cf. Helland-Hansen & Martinsen, 1996), over the entire vertical extent of the depositional tract (Fig. 3B). This allows a quantitative description of parasequence stacking patterns, even in cases where parasequence sets are not formally

defined in the original literature datasets.

Statistical analyses of the data were conducted in R 3.5.1 (R Core Team, 2018). Transformations of variables are sometime applied to meet assumptions of normality or to assess relationships that may be non-linear. Pearson's correlation coefficients are used to quantify sign and magnitude of linear correlation. To test for statistical significance of differences among groups, analysis of variance (ANOVA) with Welch's correction is applied, followed by non-parametric Games-Howell post-hoc tests (Welch, 1951; Games & Howell, 1976). An alpha value of 0.05 is considered when testing statistical significance, unless stated otherwise.

Limitations

Some limitations to the current study that should be remarked before presenting the results are briefly summarized as follows.

- All sequence-stratigraphic categories used in this article are interpretive, and the segmentation of a succession into parasequences is a heuristic process and is to some degree arbitrary. The parasequences considered in this study may vary widely with respect to their original formative mechanisms, and may represent different hierarchies of stratal packages (cf. Fig. 1B). These units are interpreted to represent pulses of shoreline progradation at both local and regional scales, and covering a broad spectrum of timescales. A discussion of how geological variability can affect the studied properties is offered by Colombera & Mountney (2020).
- The present compilation includes both outcrop and subsurface case studies, and for each of these data types the datasets vary with respect to data dimensionality, density, and geographic coverage. Physical correlation of parasequences and bounding surfaces is inherently uncertain, especially across wells, and this might affect parasequence definition in studies that employ subsurface data. The orientation and extent of outcrop exposures is variable across the considered outcrop studies, which affects parasequence characterization. A discussion of how the studied attributes are seen to vary across datasets of different types, with consideration of how the architecture of parasequences varies along their depositional dip profile, is provided by Colombera & Mountney (2020).
- Any error that affects the primary data sources (e.g., error in radiometric dating and in correlation of dated horizons, error in depth conversion) is inherited by the meta-analysis. In particular, estimations of parasequence durations are likely affected by age extrapolation being attempted without constraints on the duration of hiatuses (cf. Sadler, 1981; Colombera & Mountney, 2020).
- In parasequences, the transition between offshore or prodeltaic muds or mudstones and shallower-water sands or sandstones is commonly gradational. For attributes of parasequence sand belts, corresponding to littoral or delta-front deposits, the sand-mud boundaries placed in the original works were considered, but criteria for their placement may vary across datasets.
- Uncertainty in the recognition of the true orientation of a depositional-dip profile (cf., Fielding, 2011 *vs* Zhu et al., 2012) affects quantification: apparent measures of dip length and progradation distance overestimate true values whereas apparent progradation angles underestimate true values.
- Depositional-tract shoreline trajectories and parasequence progradation angles are also affected by problems relating to variability in data types and density, choice of datum in actively deforming basins, parasequence-top erosion, differential sediment compaction, and along-strike variations in sedimentary architectures (see discussions in: Hampson et al., 2009; Helland-Hansen & Hampson, 2009; Bhattacharya, 2011; Jordan et al., 2016; Madof et al., 2016; Hutsky & Fielding, 2017; Pattison, 2020).
- Although the case studies considered in this meta-analysis are globally distributed and cover Phanerozoic successions of different ages, there exists bias towards Upper Cretaceous

successions of the Western Interior Seaway of North America (48% of the studied parasequences). This reflects how research delivering data suited to this study has been conducted to date by the wider community.

RESULTS

Parasequence geometries and stacking patterns

Differences in the characteristics of parasequences across parasequence-set types are assessed first. Parasequence sets are successions made of genetically related parasequences arranged in a distinctive stacking pattern (Van Wagoner et al., 1988). Only parasequence sets classified as 'progradational', 'aggradational', or 'retrogradational', according to the definitions by Van Wagoner et al. (1988) are employed for this analysis; other denominations (e.g., 'aggradational to progradational set') are excluded.

In total, the database contains data on 416 parasequences contained in 120 classified parasequence sets suitable for this part of the analysis. The majority of parasequences assigned to classified parasequence sets (ca. 58%) are arranged according to a progradational stacking pattern, whereas ca. 26% of parasequences are from sets with backstepping pattern and ca. 16% from aggradational parasequence sets (Fig. 4A).

Some observations can be made on distributions of parasequence parameters for parasequence-set stacking patterns (Fig. 4B-G, Tab. 2). Parasequences in progradational sets are on average thicker than those in aggradational or retrogradational sets, to a level that is statistically significant based on results of Welch's one-way ANOVA with Games-Howell post-hoc tests (Fig. 4B, Tab. 2). Parasequence sand belts in progradational sets are on average thicker and longer along the depositional dip profile than those in aggradational or retrogradational sets, to a statistically significant level (Fig. 4C-D, Tab. 2). The stratigraphic rise of parasequences in progradational sets is on average larger than that of aggradational or retrogradational sets; differences in mean stratigraphic rise between progradational and retrogradational sets are statistically significant (Fig. 4E, Tab. 2). The progradation distances of parasequences in progradational sets are on average larger than those of aggradational sets, themselves larger than those of retrogradational sets; differences are statistically significant (Fig. 4F, Tab. 2). The progradation angles of parasequences in aggradational sets are on average steeper than those of retrogradational sets, whereas progradational sets display progradation angles that tend to be the smallest; however these differences are not statistically significant (Fig. 4G, Tab. 2).

Table 2: Descriptive statistics for parasequences grouped by parasequence-set type and results of statistical tests. St. dev.: standard deviation; N: number of parasequences; ANOVA: analysis of variance; psT: parasequence thickness; sstT: parasequence sand-belt thickness; sstL: parasequence sand-belt dip length; sR: parasequence stratigraphic rise; pD: parasequence progradation distance; α: parasequence progradation angle; F: F-value, p: p-value. (*) For progradation angles, values of circular mean and circular standard deviation are reported, and ANOVA is performed on corresponding gradient values.

	Progradational set			Aggradational set			Retrogradational set			Welch's one-way ANOVA
	Mean	St. dev.	N	Mean	St. dev.	N	Mean	St. dev.	N	
psT (m)	17.2	12.8	221	10.1	6.6	56	11.7	9	109	F[2, 185.9] = 18.57, p<0.001
sstT (m)	13.8	8.2	156	8.6	6.1	44	6.2	4.7	45	F[2, 103.8] = 33.05, p<0.001
sstL (km)	23.0	25.7	150	11.6	20.4	31	10.9	10.0	37	F[2, 76.4] = 10.75, p<0.001
sR (m)	8.1	6.6	58	5.2	4.9	14	3.6	1.9	7	F[2, 25.6] = 7.78, p = 0.002
pD (km)	11.2	10.9	63	5.0	3.1	11	1.9	1.0	7	F[2, 27.6] = 24.07, p<0.001
α (°)*	0.091	0.099	62	0.193	0.443	14	0.140	0.082	7	F[2, 13.1] = 1.12, p = 0.355

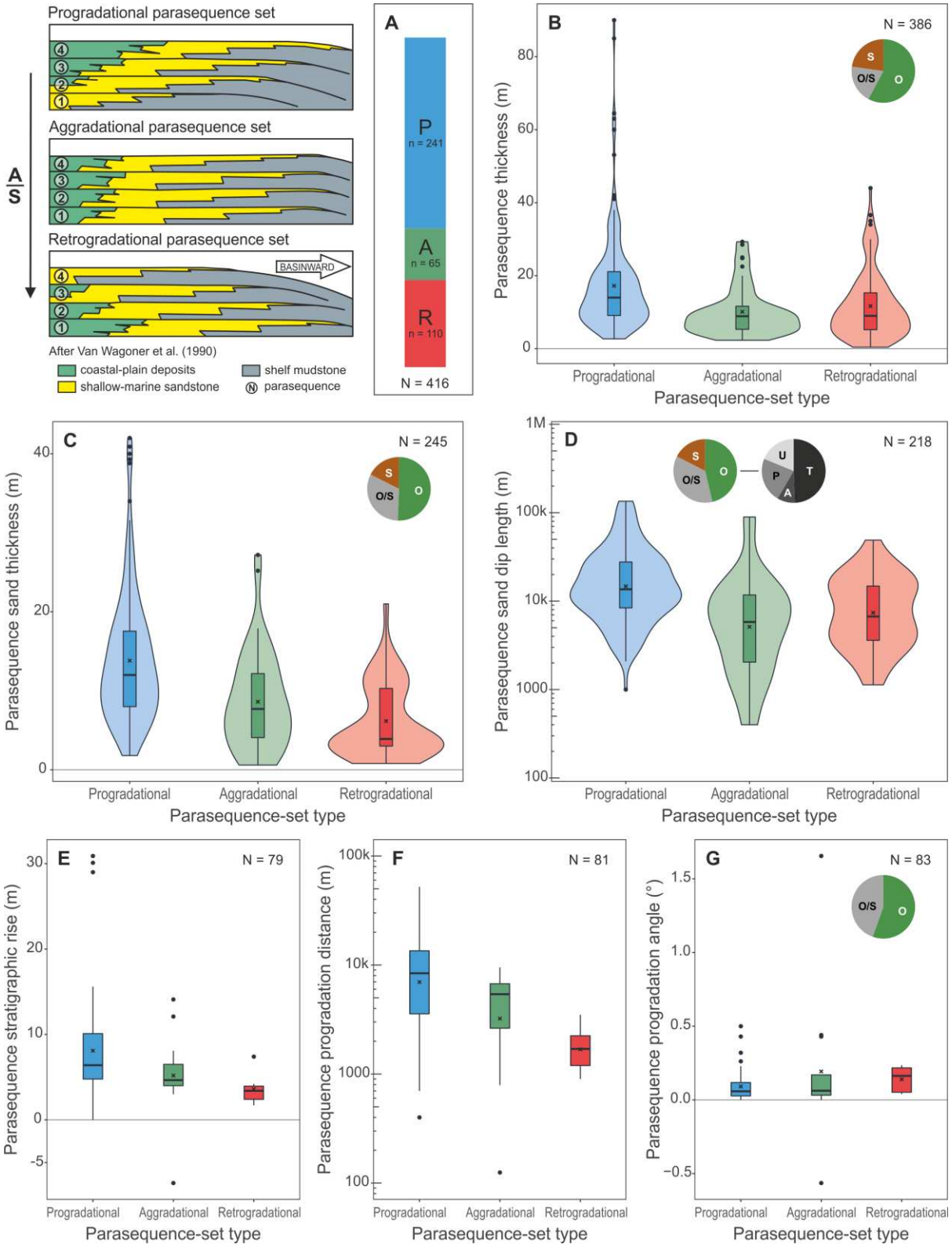

Figure 4: Comparison of parasequence characteristics across different parasequence-set types. (A) Relative proportion of parasequences by type of parent parasequence set. (B-D) Combined violin-box plots of the distribution of parasequence thickness (B), sand-belt thickness (C), and sand-belt dip length (D) in different types of parasequence sets. (E-G) Box plots of the distribution of parasequence stratigraphic rise (E), progradation distance (F), and progradation angle (G) in different types of parasequence sets. Mean values, outliers and kernel densities are computed after log-scale transformations were applied for parts D and F. 'N' denotes the number of parasequences. In box plots, boxes represent interquartile ranges, crosses represent mean values (back-transformed means in parts D and F), horizontal bars represent median values, and dots represent outliers (values

larger than 1.5 times the interquartile range). Violin plots also display kernel density estimates. In parts B, C, D and G, pie charts are included that report the relative proportion of data from outcrop (O), subsurface (S) and mixed outcrop-subsurface (O/S) examples. In part D a pie chart is included that shows the relative proportion of observations on sandstone dip length classified as 'true' (T), 'apparent' (A), 'partial' (P), and 'unlimited' (U) measurements, for outcrop datasets. See Table 2 for a breakdown of dataset size.

Parasequence geometries and systems tracts

A corresponding analysis is undertaken for characteristics of parasequences across different types of systems tracts. Only successions classified as lowstand systems tracts (LSTs), transgressive systems tracts (TSTs), highstand systems tracts (HSTs) or falling-stage systems tract (FSSTs), based on established definitions (cf. Van Wagoner et al., 1988; Hunt & Tucker, 1992; Catuneanu et al., 2009), are considered.

In total, the database contains data on 618 parasequences contained in 153 classified systems tracts suitable for this analysis. Of parasequences assigned to systems tracts, ca. 17% are from LSTs, ca. 24% are from TSTs, ca. 55% are from HSTs, and ca. 4% are from FSSTs (Fig. 5A).

Parasequences tend to be thicker on average (i.e., their mean thickness is larger) in HSTs and LSTs, and particularly thickest in HSTs and thinnest in FSSTs, with differences between HST parasequences and FSST or TST parasequences that are statistically significant, based on Welch's one-way ANOVA and Games-Howell post-hoc tests (Fig. 5B, Tab. 3). Parasequence sand belts tend to be thickest in HSTs, and thicker in LSTs than in TSTs or FSSTs; these differences are statistically significant (Fig. 5C, Tab. 3). The dip length of parasequence sand belts tends to be larger on average in HSTs and LSTs, largest for HSTs, and shortest for FSSTs; differences in mean sand length seen between HST parasequences and those in FSSTs and TSTs are statistically significant at alpha = 0.1 (Fig. 5D, Tab. 3). The stratigraphic rise and progradation angle of parasequences are necessarily negative in FSSTs, and larger in HST or LST parasequences than in TST parasequences; only the stratigraphic rise and progradation angle of FSST parasequences differ to a statistically significant level from those of parasequences in other systems tracts (Fig. 5E, 5G, Tab. 3). The progradation distance of parasequences tend to be largest in FSSTs and smallest in TSTs, but differences in progradation distance between TST and HST parasequences are also statistically significant (Fig. 5F, Tab. 3).

For LSTs and HSTs, changes in progradation angle and progradation distance seen across pairs of adjacent successively stacked parasequences contained in the same systems tract are assessed (Fig. 6). Descriptive statistics of differences in progradation distance and angle quantify the tendency to which systems tracts record variations in shoreline progradation. In particular, differences in progradation angle quantify the development of concave-landward or concave-seaward shoreline trajectories, which might arise from acceleration or deceleration in rates of creation of accommodation or from autogenic dynamics. Dominance of positive differences in progradation angle will reflect a tendency to develop concave landward systems-tract shoreline trajectories (progressive rise). Dominance of positive differences in progradation distance might reflect an increase in shoreline progradation rates or longer parasequence duration (progressive lengthening). This type of quantification describes trends in parasequence regression, but ignores potential trends in transgressive histories. If LSTs and HSTs are considered jointly, differences in the progradation angle of successive parasequences are positive in 44% of the cases, whereas differences in progradation distance are positive 51% of the times. Mean values of progradation distance and angle (circular mean) are both negative (–126 m, –0.030°; Fig. 6), but neither means are significantly different from zero based on one-sample t-tests returning p-values of 0.873 and 0.339 (on equivalent gradients), respectively. Across the studied systems tracts, the sum of differences in progradation angle of successive parasequences within each are positive in four cases out of nine, whereas the sum of differences in progradation distance are positive in three cases out of nine. If LSTs and HSTs are considered separately, differences in the progradation angle of successive parasequences are positive in 41% of the cases in HSTs (circular mean: –0.041°) and in half of the cases in LSTs (circular mean: –0.007°). Differences in progradation distance are positive in 52% of parasequence pairs in HSTs (mean: 127 m) and in half of the cases in LSTs, where their mean value is however negative (mean: –810 m). In SMAKS, 28 highstand and lowstand systems tracts are included

that were originally recognized as displaying aggradational-to-progradational or progradational-to-aggradational stacking patterns: of these, the majority (64%) exhibit aggradational-to-progradational stacking. None of the HSTs (N = 16) was originally classed as demonstrating progradational-to-aggradational stacking; only 17% of these LSTs (N = 12) were recognized as having aggradational-to-progradational stacking.

Similarly, differences in parasequence thickness across consecutive stacked parasequences can be assessed. The difference in parasequence thickness is on average negative for both HSTs (mean: –0.67 m, standard deviation: 8.1 m, N = 229) and LSTs (mean: –0.85 m, standard deviation: 9.3 m, N = 229), i.e., parasequences tend to become thinner through time in both types of systems tract. Instead, the difference in parasequence thickness is on average positive for TSTs (mean: 0.37 m, standard deviation: 6.7 m, N = 112). Nevertheless, these differences are not statistically significant (Welch's one-way ANOVA: F[2, 180.2] = 0.94, p = 0.393). Also, stratigraphic transitions to thinner parasequences are only marginally more common than transitions to thicker parasequences in HSTs (54% *vs* 46 %, N = 229) or LSTs (55% *vs* 45 %, N = 76), and transitions to thicker parasequences are as common as transitions to thinner parasequences in TSTs (50% *vs* 50%, N = 112).

Table 3: Descriptive statistics for parasequences grouped by type of systems tract and results of statistical tests. St. dev.: standard deviation; N: number of parasequences; ANOVA: analysis of variance; psT: parasequence thickness; sstT: parasequence sand-belt thickness; sstL: parasequence sand-belt dip length; sR: parasequence stratigraphic rise; pD: parasequence progradation distance; α: parasequence progradation angle; F: F-value, p: p-value. (*) For progradation angles, values of circular mean and circular standard deviation are reported, and ANOVA is performed on corresponding gradient values.

	LST			TST			HST			FSST			Welch's one-way ANOVA
	Mean	St. dev.	N	Mean	St. dev.	N	Mean	St. dev.	N	Mean	St. dev.	N	
psT (m)	14.0	10.3	109	11.1	8.2	154	15.2	12.1	328	9.8	4.4	21	F[3, 109.3] = 10.03, p<0.001
sstT (m)	9.3	6.0	71	6.3	5.2	63	11.7	8.7	239	6.2	2.6	20	F[3, 101.8] = 21.62, p<0.001
sstL (km)	15.4	13.4	48	13.2	13.9	46	19.8	20.3	181	10.1	7.5	20	F[3, 85.7] = 6.43, p<0.001
sR (m)	5.9	7.2	18	3.9	3.7	11	7.8	7.1	56	–24.4	5.3	4	F[3, 12.9] = 40.27, p<0.001
pD (km)	7.1	8.4	18	3.0	3.1	11	9.4	11.3	59	10.7	7.8	4	F[3, 13.1] = 5.02, p = 0.016
α (°)*	0.159	0.415	18	0.116	0.100	11	0.136	0.165	56	–0.226	0.169	7	F[3, 19.8] = 7.90, p = 0.001

Parasequence geometries, aggradation and progradation

Relationships are assessed that may exist between parameters that describe parasequence geometry and measures of the style of parasequence aggradation and progradation, consisting of stratigraphic rise, progradation distance, the resulting progradation angle, and associated rates of shoreline progradation and aggradation at the shoreline.

Moderate direct correlations are seen between positive values of parasequence stratigraphic rise and thickness (Pearson's R = 0.526, p<0.001; Fig. 7A) and between progradation distance and thickness (R = 0.546, p<0.001; Fig. 7C). Modest positive correlation is also seen between stratigraphic rise and progradation distance for normal-regressive parasequences (R = 0.406, p<0.001).

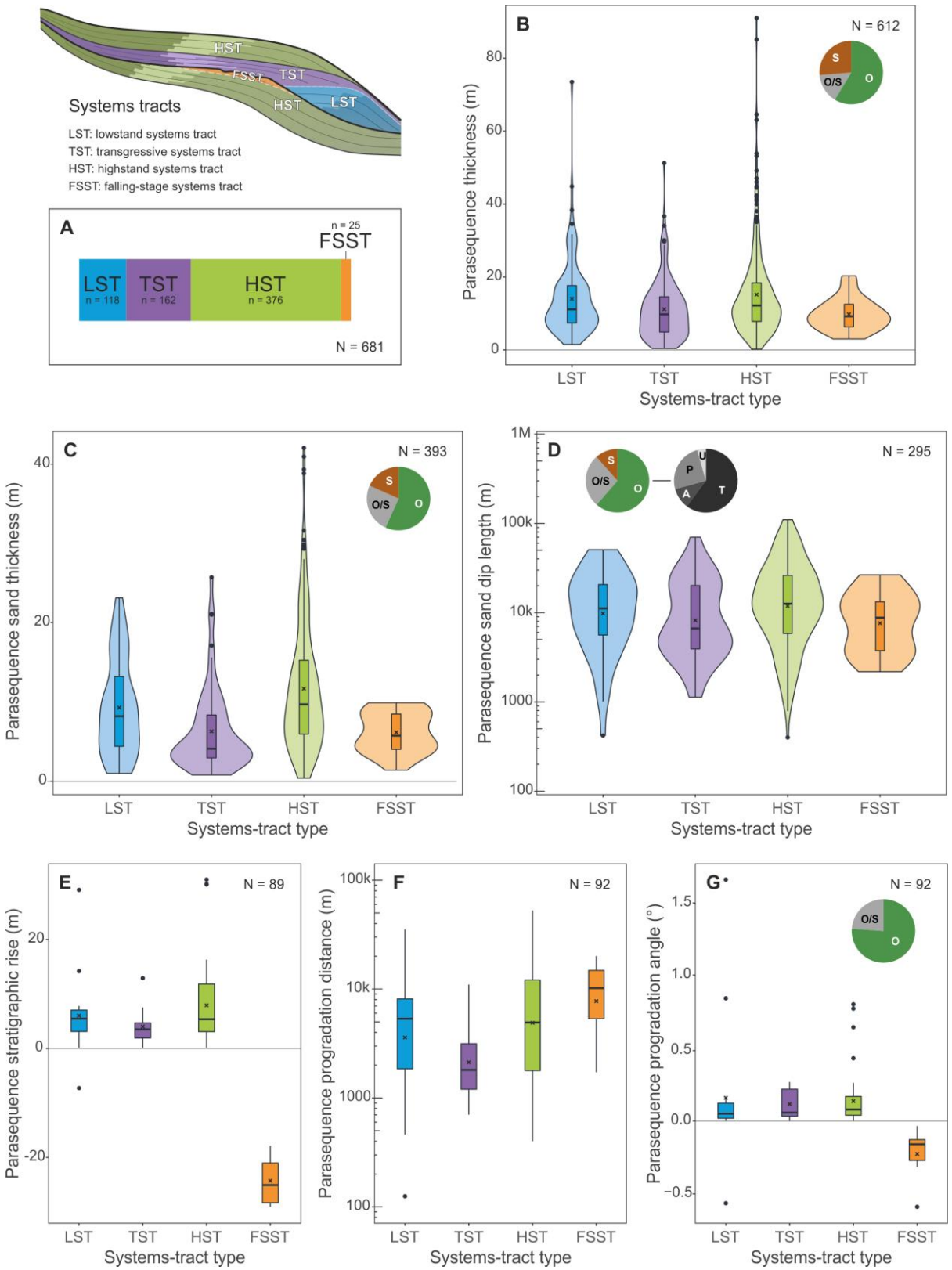

Figure 5: Comparison of parasequence characteristics across different types of systems tracts. (A) Relative proportion of parasequences by type of systems tract. (B-D) Combined violin-box plots of the distribution of parasequence thickness (B), sand-belt thickness (C), and sand-belt dip length (D) in different types of systems tracts. (E-G) Box plots of the distribution of parasequence stratigraphic rise (E), progradation distance (F), and progradation angle (G) in different types of systems tracts. Mean values, outliers and kernel densities are computed after log-scale transformations were applied for parts D and F. 'N' denotes the number of parasequences. In box plots, boxes represent interquartile ranges, crosses represent mean values (back-

transformed means in parts D and F), horizontal bars represent median values, and dots represent outliers (values larger than 1.5 times the interquartile range). Violin plots also display kernel density estimates. In parts B, C, D and G, pie charts are included that report the relative proportion of data from outcrop (O), subsurface (S) and mixed outcrop-subsurface (O/S) examples. In part D a pie chart is included that shows the relative proportion of observations on sandstone dip length classified as 'true' (T), 'apparent' (A), 'partial' (P), and 'unlimited' (U) measurements, for outcrop datasets. See Table 3 for a breakdown of dataset size.

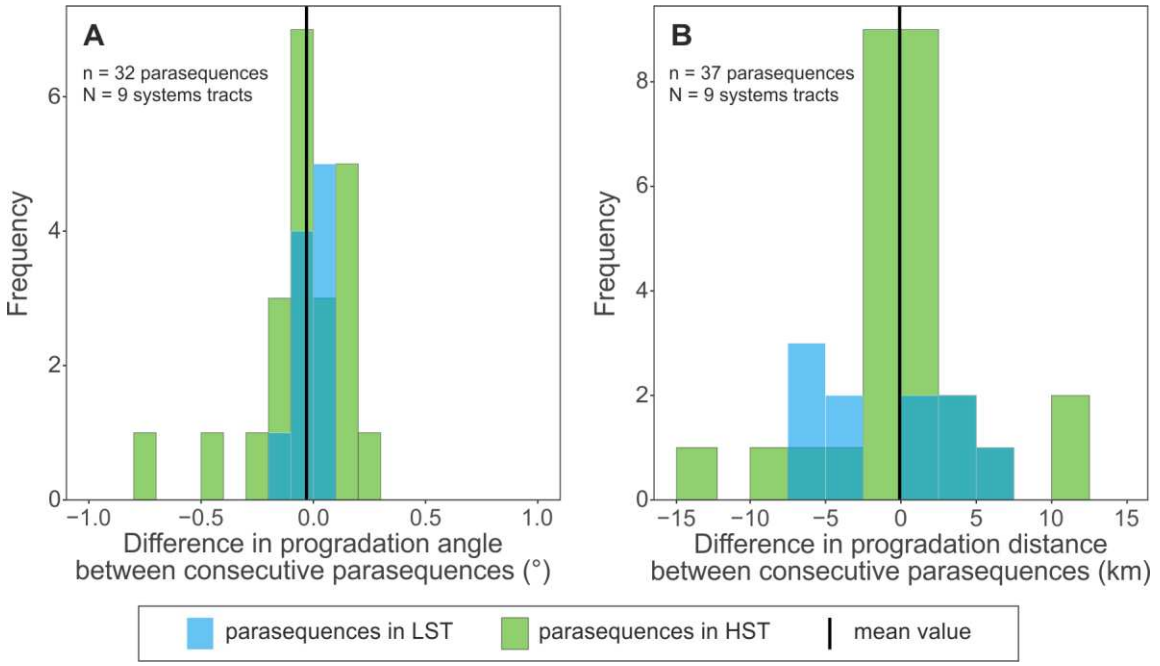

Figure 6: Stratigraphic changes in parasequence progradation in lowstand and highstand systems tracts. Distributions of the difference in progradation angle (A) and progradation distance (B) between pairs of successive parasequences contained in the same systems tract. Distributions are plotted separately for lowstand (blue, transparent) and highstand (green) parasequences. Overall mean values of the parameters are represented as vertical bars.

Parasequence aggradation and progradation rates are affected by so-called Sadler effect (Sadler, 1981), i.e., vary as a function of the length of time over which they are evaluated, in relation to increased average duration of gaps in sedimentation with increasing length of time (Colombera & Mountney, 2020). Thus, relationships between mean parasequence aggradation or progradation rates and parasequence geometries should be assessed with consideration of the timescale of parasequence development (Figs. 7 and 8). Thus, although only weak positive correlation is seen between the thickness of parasequences and their log-transformed mean aggradation rate for the entire data pool (Pearson's $R = 0.292$, $p = 0.058$), stronger positive relationships are separately seen between the same variables for groups of parasequences developed over 10^3 yr and 10^4 yr timescale (10^3 yr: $R = 0.950$, $p<0.001$; 10^4 yr: $R = 0.793$, $p<0.001$; Fig. 7B). Correspondingly, a direct correlation is seen between parasequence thickness and log-transformed mean progradation rate that is weak overall (Pearson's $R = 0.381$, $p = 0.006$), but stronger when evaluated for groups of parasequences of comparable timescales (10^4 yr: $R = 0.671$, $p<0.001$; 10^5 yr: $R = 0.610$, $p = 0.108$; Fig. 7D). Similarly, no correlation is seen between the log-transformed mean progradation rate and parasequence sand or sandstone dip length for the entire data pool (Pearson's $R = –0.048$), but positive relationships are seen between the same variables for groups of parasequences classified on order of magnitude in timescale (10^3 yr: $R = 0.833$, $p<0.001$; 10^4 yr: $R = 0.621$, $p = 0.002$; 10^5 yr: $R = 0.697$, $p = 0.082$; Fig. 8).

For stratigraphic intervals for which basin-wide average aggradation rates can be estimated (e.g., Garrison & van den Bergh, 2004; Zhu et al., 2012; Lin et al., 2019), relationships between the mean

aggradation rate of the intervals and the average thickness of the parasequences they contain can be assessed. A moderate and non-significant positive correlation is seen between aggradation rate and mean parasequence thickness for intervals that encompass orders of magnitude in temporal duration of 10^6 yr (R = 0.563, p = 0.244, N = 6), whereas a weak positive relationship is seen for successions accumulated over 10^5 yr timescales (R = 0.204, p = 0.571, N = 10).

For 'parasequences' that record forced regression (and which therefore do not strictly conform to the definition of parasequence *sensu stricto*; Kamola & Van Wagoner, 1995), characterized by negative progradation angles, moderate positive relationships are seen between their progradation angle and their overall thickness (Pearson's R = 0.535, p = 0.138; Fig. 9A), the thickness of their shallow-water sand belts (R = 0.537, p = 0.136; Fig. 9B), and the true or apparent down-dip length of the sand belts (R = 0.711, p = 0.032; Fig. 9C). Thus, forced-regressive parasequences tend to be thicker and display thicker and longer sand belts for flatter progradation trajectories. However, the dataset size is limited, and direct scaling between negative progradation angle and parasequence sand-belt dip length might reflect spurious correlation due to measurements taken along sections that are variably oblique to the depositional-dip direction.

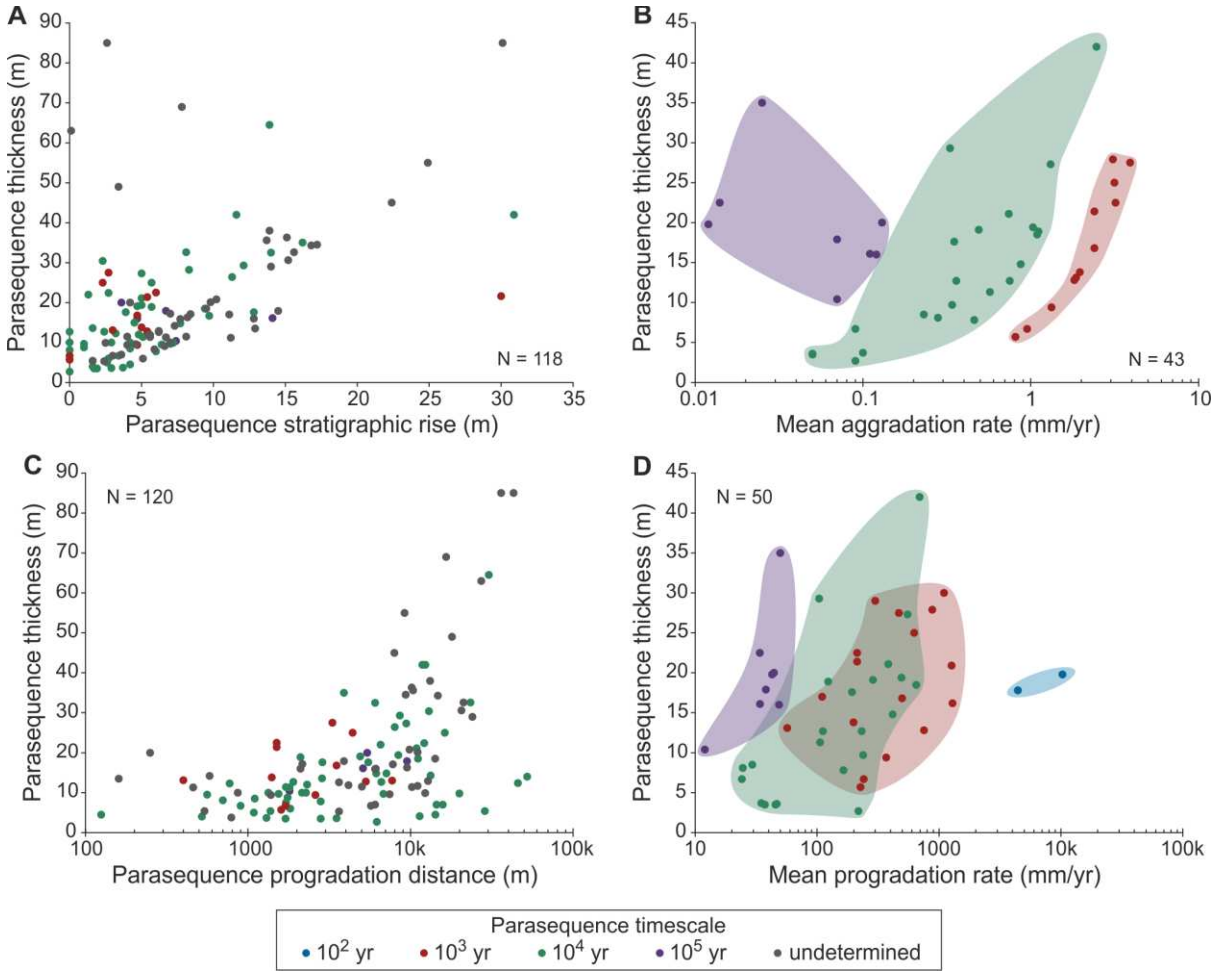

Figure 7: Scatter plots of parasequence thickness against parasequence stratigraphic rise (A), mean nearshore aggradation rate (B), shoreline progradation distance (C) and mean progradation rate (D); spots are colour-coded by the timescale over which parasequences were deposited and rates estimated.

For parasequences that record normal depositional regression, i.e., with positive progradation angle, weak negative relationships are seen between their progradation angle and either their overall thickness (Pearson's R = –0.190, p = 0.042; Fig. 9A) or the thickness of their sand belts (R = –0.171, p = 0.055;

Fig. 9B). A moderate negative relationship is between log-transformed parasequence progradation angle and sand-belt down-dip length (R = –0.463, p<0.001; Fig. 9D). In part this can be explained by underestimation of dip lengths for partial and unlimited observations (see Fig. 9D) and by inverse scaling between apparent values of progradation angle and dip length associated with measurements taken along sections that are oblique to the true depositional dip; the strength in correlation is slightly lower when considered for true dip-length values only (R = –0.385, p<0.001, N = 90). Overall, this means that also normal-regressive parasequences tend, on average, to be thicker and contain thicker and longer sand belts for flatter progradation trajectories. As expected, the relationship between log-transformed positive parasequence progradation angle and progradation distance is negative (R = –0.678, p<0.001). The relationship between log-transformed positive parasequence progradation angle and the difference between sand-belt dip length and progradation distance (a measure of the sand-belt 'pinchout distance' *sensu* Løseth & Helland-Hansen, 2001) is also negative but very weak (R = –0.177, p=0.072).

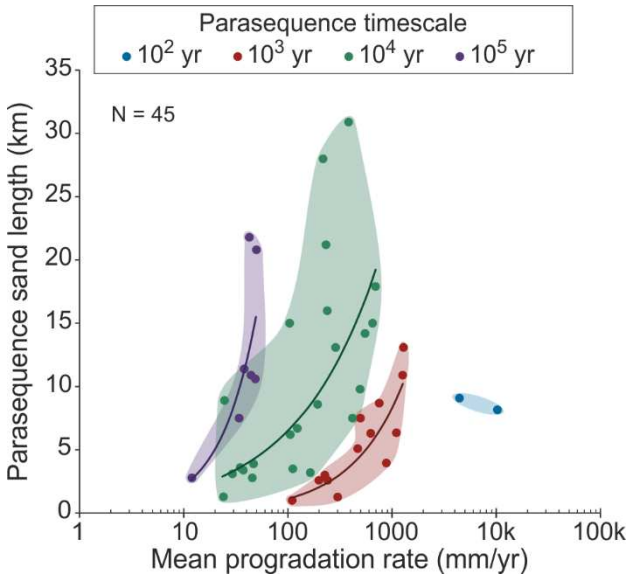

Figure 8: Scatter plot of the downdip length of parasequence shallow-water sand belts against the mean rate of progradation of the parasequence, colour-coded by the timescale over which the parasequence was deposited and the progradation rate estimated. Power-law regressions are shown for parasequences of 103 yr (R2 = 0.755), 104 yr (R2 = 0.534) and 105 yr (R2 = 0.789) timescales.

Positive shoreline trajectories of SMAKS nearshore depositional tracts portray normal depositional regression at a scale comparable to that of parasequence sets, but exclusively for parasequence sand belts that are laterally amalgamated. A positive relationship is seen between the log-transformed values of shoreline trajectories of normal regressive depositional tracts and of the mean progradation angle of their associated parasequences (R = 0.722, p = 0.001, based on 142 parasequences and 18 depositional tracts); this quantifies the degree to which parasequence-scale shoreline advances, of possible local and more temporally restricted significance, map onto larger-scale progradational trends. A moderate negative relationship is seen between log-transformed depositional-tract shoreline trajectories and the mean down-dip length of the parasequence sand belts that form each depositional tract (R = –0.402, p = 0.057; Fig. 10).

Parasequence thickness and top type

Top-truncated parasequences are on average thinner than others with non-erosional or unclassified tops (mean values of 13.8 m vs 15.7; Fig. 11), but this difference is only statistically significant at alpha = 0.1 based on two-sample t-test (T-value = 1.92, p-value = 0.057, d.f. = 152). Parasequences that are truncated at their top by ravinement surfaces tend to be more markedly thinner on average (mean value of 9.7 m; Fig. 11); their difference with other parasequences is statistically significant (two-sample t-test: T = 6.57, p<0.001, d.f. = 64).

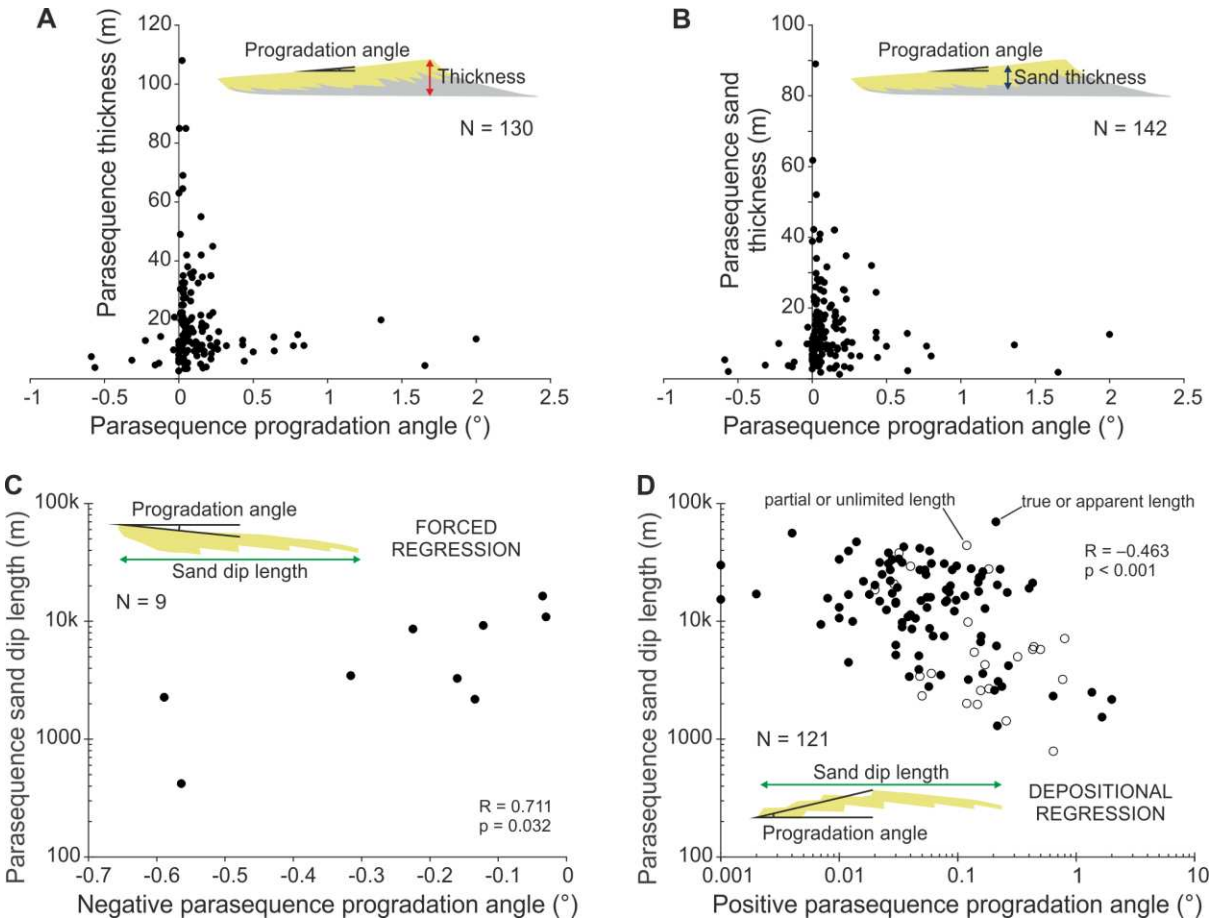

Figure 9: Relationships between metrics of parasequence progradation style and morphometric parameters. (A-B) Scatter plots of parasequence thickness (A) and parasequence sand-belt thickness (B) against parasequence progradation angle. (C-D) Scatter plots of parasequence sand-belt down-dip length against negative (C) and positive (D) regressive progradation angles. For sand-body length values, complete (true or apparent) and incomplete (partial or unlimited, sensu Geehan & Underwood, 1993) observations are differentiated. The data are from the Battfjellet Formation, Blackhawk Formation, Castlegate Sandstone, Cliff House Sandstone, Cozzette Sandstone, Ferron Sandstone ('Last Chance Delta' and 'Notom Delta' intervals), Fox Hills Formation, Frontier Formation, Gallup Formation, Hosta Tongue, Iles Formation, Star Point Sandstone, and from the Quaternary of the Paraná coastal plain (see Table 1). R indicates the Pearson's correlation coefficient and p its p-value for the reported variables (C) or their log-transformed values (D).

Parasequence thickness-to-sand-fraction ratio and A/S proxies

Values of parasequence thickness-to-sand-fraction ratios (T/SF ratios) can be obtained from recorded thicknesses of parasequences and of their sand belts of shallow-water origin. The terms 'sand fraction' is used in the sense of Ainsworth et al. (2018, 2020): it is the ratio between sand-belt thickness and parasequence thickness, and as such it is an estimate of the fraction of sand for the part of parasequence containing nearshore deposits. The way these ratios are computed in this work differ from the quantification that is recommended for the so-called T/SF analysis, a technique that can be employed to reveal parasequence stacking patterns quantitatively based on changes in T/SF in 1D datasets (Ainsworth et al. 2018), in part because the scope of this work is not to assess the predictive power of this method, but rather to determine the sensibility of considering the T/SF ratio as a proxy for A/S at parasequence scale. Unlike Ainsworth et al. (2018, 2020), thickness-to-sand-fraction ratios are based on single values of maximum observed thicknesses, which may be measured at different locations. It should be noted that estimations of sand or sandstone fractions based on multiple measurements over the dip profile of a parasequence (cf. Ainsworth et al. 2018) are necessarily more accurate than the estimations employed in this work. Notwithstanding, values of parasequence thickness-to-sand-fraction

ratios used in the following results are closely correlated to T/SF ratios computed as recommended for scopes of T/SF analysis, based on a comparison of the two metrics in corresponding datasets (R = 0.836, p<0.001, N = 57).

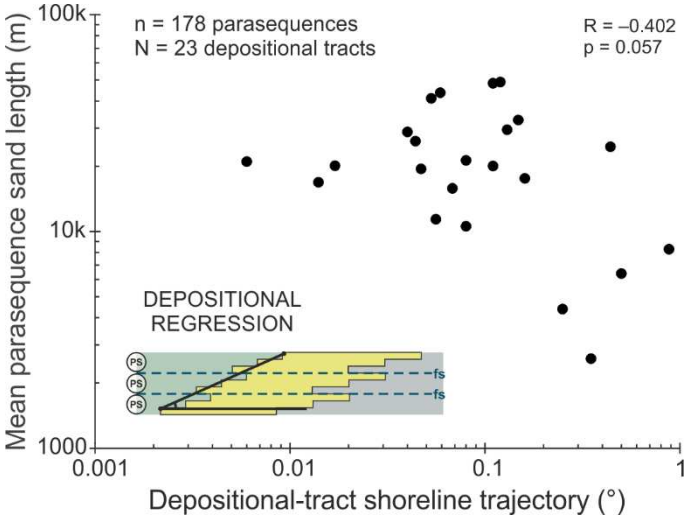

Figure 10: Scatter plot of mean dip length of parasequence shallow-water sand belts in SMAKS depositional tracts (i.e., facies belts) against positive regressive (i.e., <90°) depositional-tract shoreline trajectories. Each spot represents a SMAKS depositional tract (see Colombera et al., 2016). R indicates the Pearson's correlation coefficient and p its p-value for log-transformed values.

Figure 11: Combined violin-box plots of the distribution of parasequence thickness for parasequences that are truncated at the top by erosional surfaces (wave or tidal ravinements, sequence boundaries, or regressive surfaces of marine erosion), in green, parasequences that are specifically topped by ravinement surfaces, in orange, and parasequences with non-erosional or unclassified tops, in brown. 'N' denotes the number of parasequences. Boxes represent interquartile ranges, crosses represent mean values, horizontal bars represent median values, and dots represent outliers (values larger than 1.5 times the interquartile range); kernel density is displayed on the sides of box plots.

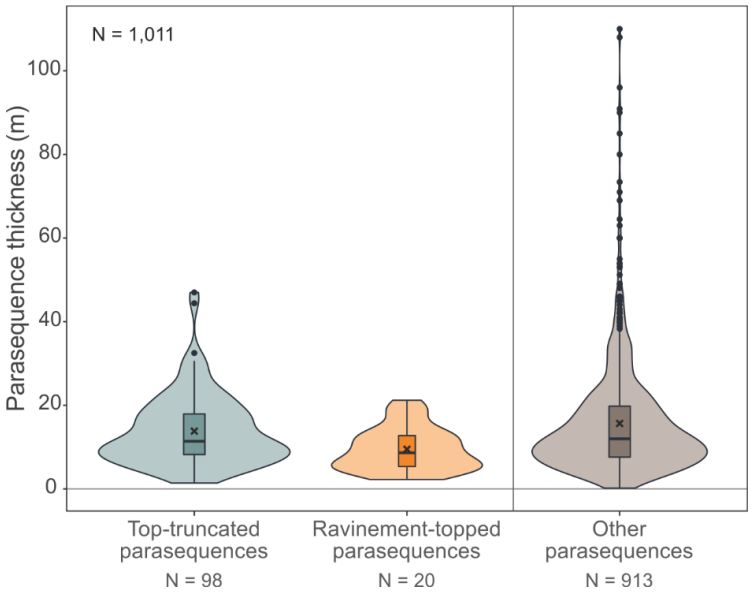

For parasequences that record normal depositional regression, i.e., with positive progradation angle, a weak negative relationship is seen between their log-transformed progradation angle and their thickness-to-sand-fraction (T/SF) ratios (Pearson's R = –0.263, p = 0.005; Fig. 12A). A moderate positive relationship is seen between parasequence progradation distance and T/SF ratio (R = 0.646, p<0.001, N = 114), whereas no significant correlation exists between progradation distance and sand fraction (R = –0.160, p = 0.090). No relationship is seen between the log-transformed shoreline trajectory of depositional tracts that contain parasequence sand belts and the mean T/SF ratio of the parasequences (R = –0.079, p = 0.734; Fig. 12B). It could be argued that a direct measure for the rate of creation of accommodation, at least for the regressive evolution of a parasequence, is given by its stratigraphic rise (Fig. 3A), i.e., by the amount of aggradation taking place at the shoreline during regression (albeit not corrected for compaction). A possible rough estimator for the rate of sediment

supply is instead given by the product of parasequence thickness and progradation distance (Fig. 3A), which crudely approximates the volume of sediment (per unit shoreline length) accreting in the nearshore during the parasequence history. Where these quantities and sand-belt thickness can all be constrained, the ratio between stratigraphic rise and the product of parasequence thickness and progradation distance does not demonstrate any significant correlation with the thickness-to-sand-fraction ratio (R = –0.140, p = 0.153, N = 106).

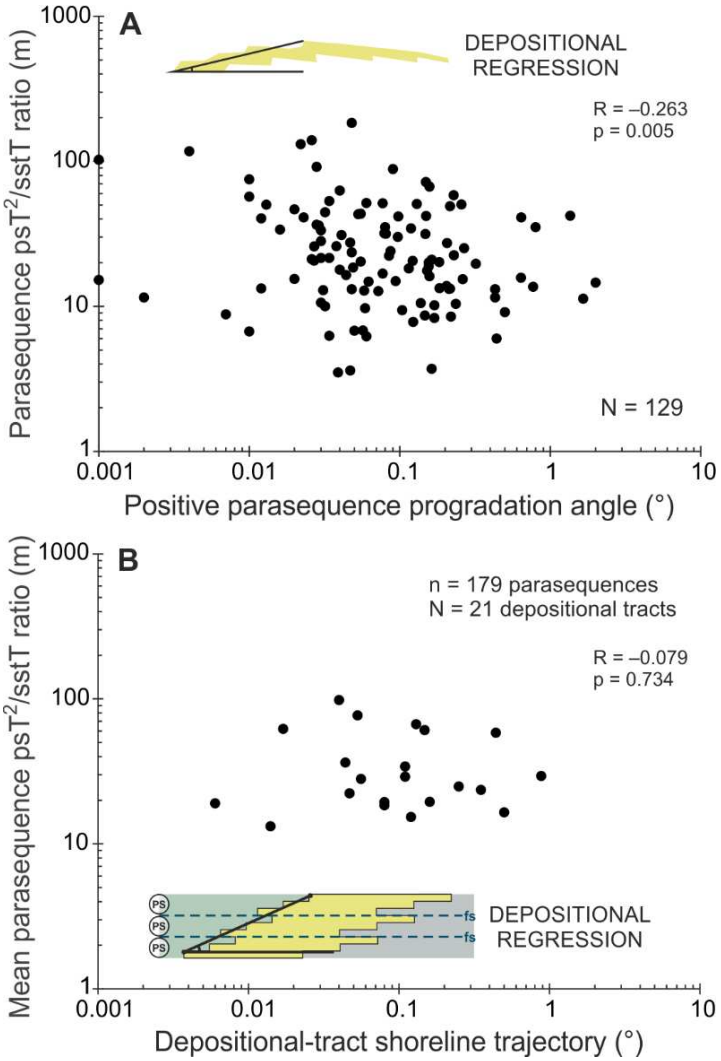

Figure 12: elationships between metrics of progradation style and parasequence thickness-to-sand-fraction ratio, computed on the basis of maximum observed thickness values (see text). (A) Scatter plot of parasequence thickness-to-sand-fraction ratio against positive regressive (i.e., <90°) progradation angle. (B) Scatter plot of mean parasequence thickness-to-sand-fraction ratio in SMAKS depositional tracts (i.e., facies belts) against positive regressive (i.e., <90°) depositional-tract shoreline trajectories. Quantities psT and sstT indicate parasequence thickness and shallow-marine sandstone thickness, respectively (see Fig. 3). R indicates the Pearson's correlation coefficient and p its p-value for log-transformed values.

Across parasequence sets classified on their stacking pattern (Fig. 13A), the parasequence T/SF ratio is on average largest for progradational sets (mean: 30.6 m, standard deviation: 32.6 m, N = 143) and smallest for retrogradational set (mean: 19.4 m, standard deviation: 20.0 m, N = 45). Differences in mean T/SF ratio between progradational and retrogradational sets are significant, based on Welch's one-way ANOVA with Games-Howell post-hoc tests (F[2, 91.5] = 3.98, p = 0.022).

Across classified systems tracts (Fig. 13B), the parasequence T/SF ratio is on average largest for HSTs (mean: 34.8 m, standard deviation: 44.8 m, N = 196) and smallest for FSSTs (mean: 13.4 m, standard deviation: 8.3 m, N = 19). LST and TST parasequences have similar mean values of T/SF ratio (23.9 m and 22.0 m, respectively), which differ significantly from those of HST and FSST parasequences (Welch's one-way ANOVA with Games-Howell post-hoc tests; F[3, 109.3] = 12.13, p<0.001).

When variations in T/SF ratios across stacked consecutive parasequences are considered in HSTs and TSTs (cf. Ainsworth et al., 2018), the difference in parasequence T/SF ratio is on average negative for

HSTs (mean: –7.8 m, standard deviation: 49.9 m, N = 106), i.e., parasequences tend to have lower T/SF ratios than underlying ones, whereas the difference in T/SF ratio is on average positive for TSTs (mean: 5.6 m, standard deviation: 18.3 m, N = 35). This difference is statistically significant (two-sample t-test: T = –2.33, p-value = 0.021, d.f. = 137). In HSTs, stratigraphic transitions to parasequences with lower T/SF ratios are more common than transitions to parasequences with higher T/SF ratios (61% *vs* 39 %, N = 106). In TSTs, stratigraphic transitions to parasequences with higher T/SF ratios are instead more common (63% *vs* 37 %, N = 35). Differences in sand fraction across stacked consecutive parasequences are also separately considered: these differences are on average close to zero for both HSTs (mean: 0.035, standard deviation: 0.261, N = 106) and TSTs (mean: 0.035, standard deviation: 0.292, N = 35).

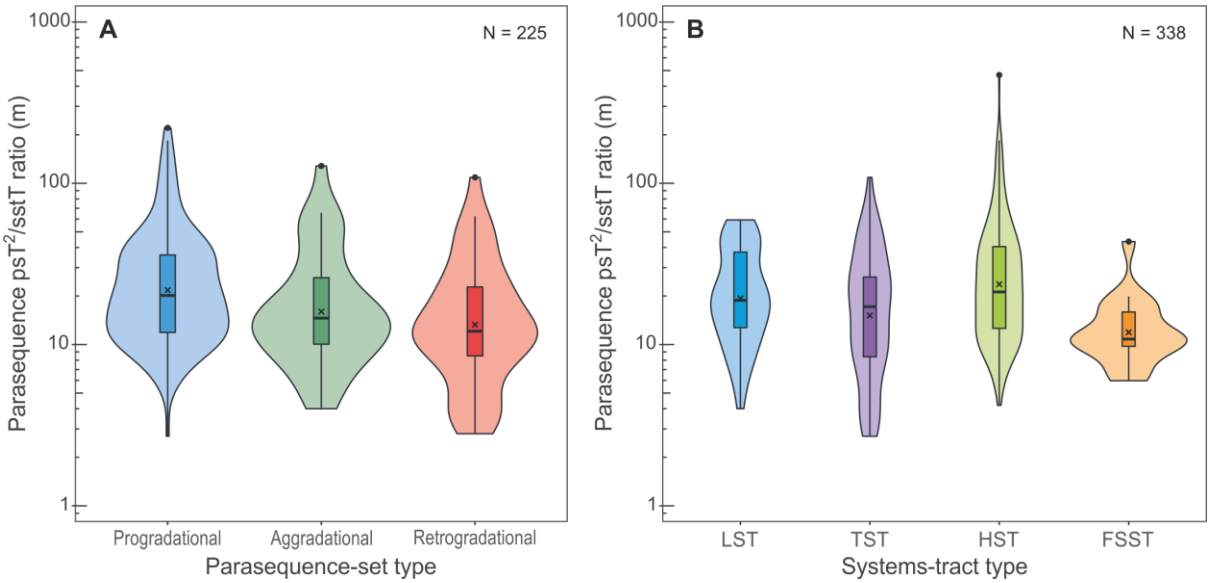

Figure 13: Comparison of distributions in parasequence thickness-to-sand-fraction ratios, computed on the basis of maximum observed thickness values (see text), across different types of parasequence sets and systems tracts. (A) Combined violin-box plots of the distribution of parasequence thickness-to-sand-fraction ratio in parasequence sets classified on stacking pattern. (B) Combined violin-box plots of the distribution of parasequence thickness-to-sand-fraction ratio in different types of systems tracts (cf. results in Fig. 9 in Ainsworth et al., 2018). See text for discussion of stratigraphic changes in parasequence thickness-to-sand-fraction ratios within systems tracts. Kernel density estimates are displayed on the sides of the box plots. Mean values, outliers and kernel densities shown here are computed after log-scale transformations were applied. 'N' denotes the number of parasequences. Boxes represent interquartile ranges, crosses represent back-transformed mean values, horizontal bars represent median values, and dots represent outliers (values larger than 1.5 times the interquartile range). Quantities psT and sstT indicate parasequence thickness and shallow-marine sandstone thickness, respectively (see Fig. 3).

Parasequence origin, process dominance and sequence-stratigraphic architectures

Differences in the abundance of clastic parasequences associated with different formative environments and processes can be assessed across types of parasequence sets and systems tracts.

Wave-dominated parasequences are the most common in the database (ca. 67% of classified parasequences; Colombera & Mountney, 2020), as well as in the studied parasequence sets and systems tracts (ca. 70% of classified parasequences; Fig. 14A). In parasequence sets with progradational stacking patterns, river-dominated parasequences are markedly more common (ca. 28%, and ca. 32% of classified parasequences; Fig. 14A) than in aggradational or retrogradational sets (<2%, and <3% of classified parasequences; Fig. 14A). River-dominated parasequences are also most abundant in the studied HSTs (ca. 21%, and ca. 31% of classified parasequences; Fig. 14B), and more common in LSTs (ca. 13%) than in FSSTs or TSTs (<7%).

Shoreface parasequences are slightly more common than deltaic ones across the database (42% vs 34% of all parasequences in SMAKS; Colombera & Mountney, 2020), but markedly more abundant than deltaic ones in the studied parasequence sets (ca. 46% vs ca. 26%) and systems tracts (ca. 46% vs ca. 29%). Deltaic parasequences are more common in progradational parasequence sets (ca. 33%, and ca. 41% of classified parasequences; Fig. 15A) than in aggradational or retrogradational sets (ca. 17%, and ca. 21% of classified parasequences; Fig. 15A). Deltaic parasequences are also most abundant in the studied LSTs (ca. 32%, and ca. 44% of classified parasequences; Fig. 15B), and more common in HSTs (ca. 29%) and TSTs (ca. 27%) than in FSSTs (12%).

The dip length of shallow-water sand belts is larger on average for deltaic parasequences (means: 21.4 km vs 18.1 km, N = 358), but not to a statistically significant level (two-sample t-test: T = 1.08, p = 0.283, d.f. = 163), and the shoreline progradation distance is larger on average for shoreface parasequences instead (means: 12.7 km vs 4.7 km, N = 91; Colombera & Mountney, 2020). For normal-regressive conditions, deltaic parasequences tend to display steeper progradation angles than shoreface ones (circular means: 0.30° vs 0.10°, N = 89); this difference is statistically significant (two-sample t-test on equivalent gradients: T = 2.15, p-value = 0.040, d.f. = 30).

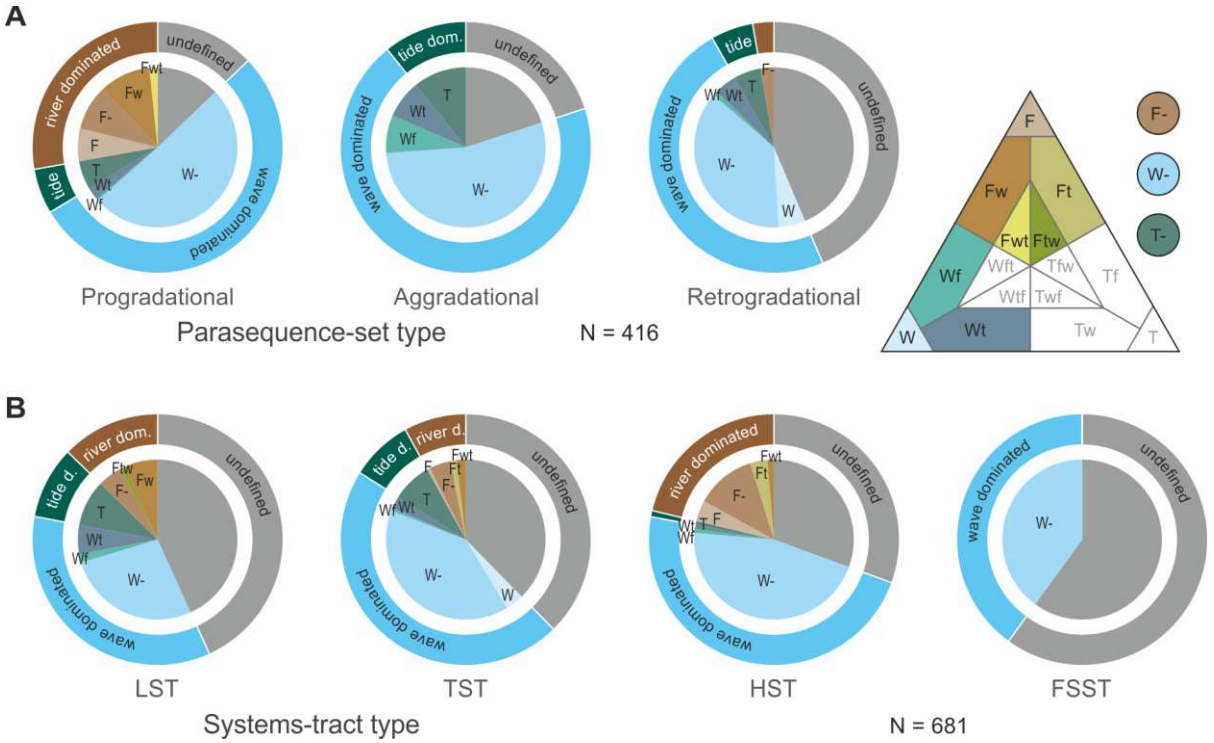

Figure 14: Proportions of parasequences classified on dominant process regime in different types of parasequence sets and systems tracts. (A) Pie charts of the proportion of parasequence types in parasequence sets classified on stacking pattern. (B) Pie charts of the proportion of parasequence types in different types of systems tracts. The parasequences are classified on a scheme that includes the 15 categories of Ainsworth et al. (2011; e.g., 'W' = wave dominated; 'Wt' = wave dominated, tide influenced; 'Ftw' = river dominated, tide influenced, wave affected) together with three generic categories that are used when only the main dominant process is inferred (i.e., 'W-' = wave dominated; 'T-' = tide dominated; 'F-' = fluvial dominated; each possibly recording the influence of other processes). Other labels in charts are as follows: 'F' = river dominated; 'Fw' = river dominated, wave influenced; 'Ft' = river dominated, tide influenced; 'Fwt' = river dominated, wave influenced, tide affected; 'Wf' = wave dominated, river influenced. 'N' denotes the number of parasequences.

Parasequence geometries and river-system size

Where shallow-marine successions can be related to up-dip broadly coeval alluvial and river-dominated coastal-plain successions, relationships between the dip length of shallow-marine sands and the size of

associated river systems can be investigated. These relationships are studied here for parasequences recognized in the shallow subsurface of two active deltas (rivers Po and Rhône) and in ancient successions from the Cretaceous of the Western Interior Seaway (WIS) that are correlative to time-equivalent strata representing the preserved record of coastal plains traversed by rivers of variable size. Although temporal variations in tectonic forcing on parasequence architectures may have been important (cf. Aschoff & Steel, 2011; Fielding, 2011), limiting the analysis to data from the same tectonic context, by focussing on examples from the WIS, makes the comparison meaningful. However, by exclusively considering WIS successions, the range in river-system scales that is taken into account is limited, since it reflects the relatively limited distance of the seaway margin from the source orogen and does not encompass continental-scale catchments and rivers.

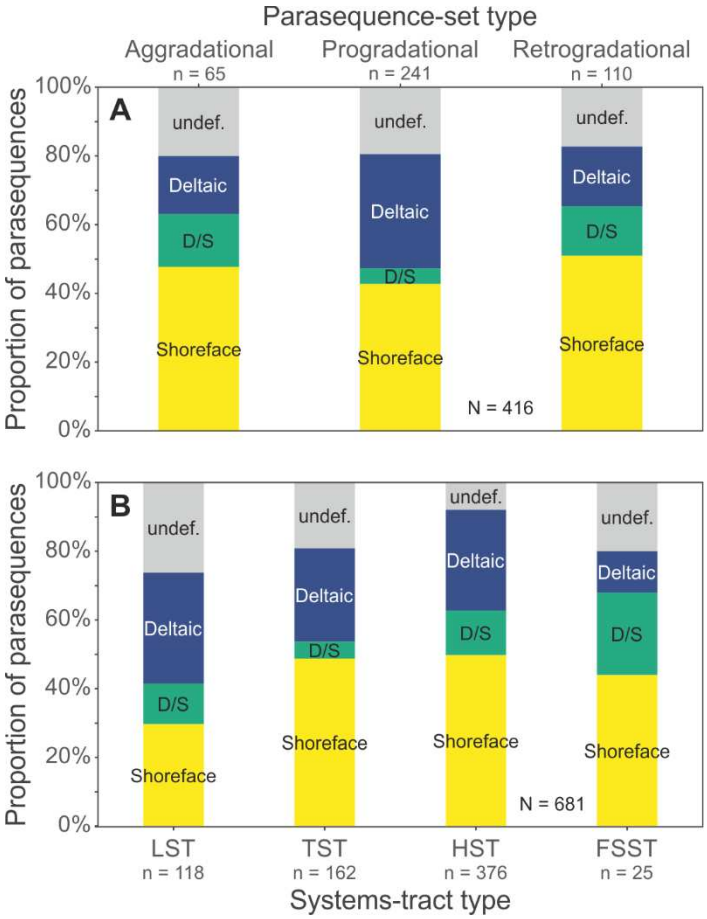

Figure 15: Proportion of parasequences, classified according to their interpreted formative littoral depositional environment, in different types of parasequence sets and systems tracts. (A) Bar charts of the proportion of parasequence types in parasequence sets classified on stacking pattern. (B) Bar charts of the proportion of parasequence types in different types of systems tracts. The term 'shoreface' is used to refer generally to deposits of non-deltaic linear coasts (e.g., strandplains, barriers). 'D/S' identifies 'deltaic-shoreface' parasequences, which are interpreted to have been deposited by both shoreface (sensu lato) and deltaic systems. 'Undef.' = undefined. 'N' denotes the number of parasequences.

Existing estimates of the size of drainage areas feeding the palaeo-shorelines based on palaeogeographic reconstructions (Bhattacharya & Tye, 2004; Bhattacharya & MacEachern, 2009; Carvajal & Steel, 2012; Szwarc et al., 2015; Bhattacharya et al., 2016; Hutsky & Fielding, 2016; Lin & Bhattacharya, 2017) can be related to the down-dip length of shallow-marine sand belts in groups of parasequences (Fig. 16A). Overall, a modest positive relationship is seen between estimated catchment areas (or the mid value of the range of estimations in catchment size) and mean parasequence sand-belt dip lengths (Pearson's $R = 0.551$, $p = 0.063$, $N = 12$). Correlation between the same variables is only marginally stronger and not statistically significant if separately considered for outcrop ($R = 0.574$, $p = 0.312$, $N = 5$) and subsurface ($R = 0.669$, $p = 0.217$, $N = 5$) WIS examples.

The mean dip length of shallow-marine sand belts in parasequences can also be related to measures of central tendency in channel maximum bankfull depth (either the mean value or the mid value of a range; Fig 16B). Data on inferred maximum bankfull depths of channels of coastal or alluvial rivers are based on observation of the thickness of architectural elements interpreted as preserved macroforms or

channel fills (cf. Bridge & Tye, 2000; Mohrig et al., 2000; Hajek & Heller, 2012); the resulting figures are sometime corroborated by inferences of mean bankfull depths based on application of empirical relationships relating flow depth to dune-scale cross-set thicknesses (cf. Leclair & Bridge, 2001). Data on estimated channel depth employed in this analysis (Shanley & McCabe, 1993; Plint, 2002; Plint & Wadsworth, 2003; Adams & Bhattacharya, 2005; Garrison and van den Bergh, 2006; McLaurin & Steel, 2007; Li et al., 2010; Hampson et al., 2012, 2013; Bhattacharyya et al., 2015; Chentnik et al., 2015; Flood & Hampson, 2015; Bhattacharya et al., 2016; Gooley et al., 2016; Lin & Bhattacharya, 2017, 2020; Wang & Bhattacharya, 2017; Shiers et al., 2019) may variably relate to trunk rivers, tributaries, or distributaries and to rivers with both single-thread and braided planform. These quantities may therefore not represent accurate proxies for the bankfull discharge of rivers draining into the WIS. For the Cretaceous successions, the correlation between measures of central tendency in maximum bankfull depth and mean parasequence sand-belt dip lengths is positive, but weak and not statistically significant (Pearson's R = 0.351, p = 0.263, N = 12), even if the analysis is restricted to the parasequences characterized in outcrop (R = 0.140, p = 0.700, N = 10).

Corresponding analyses of relationships between river-system scale and parasequence progradation distance or angle have not been undertaken because of data paucity.

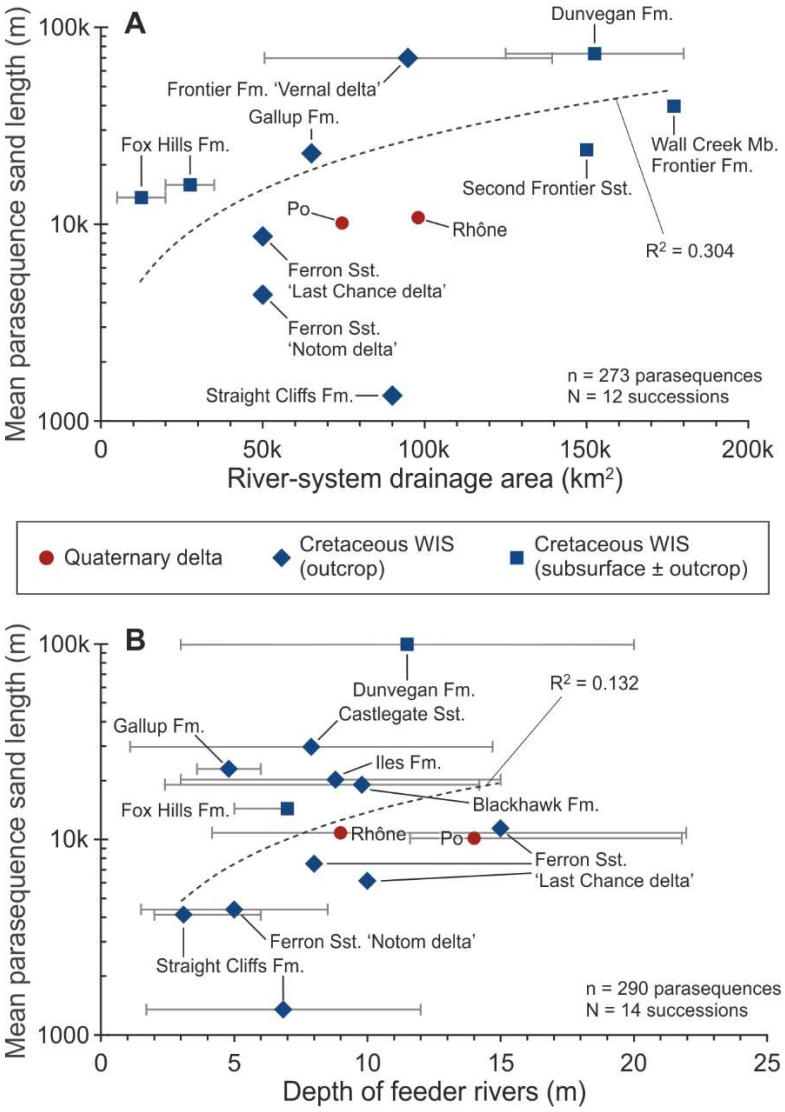

Figure 16: Relationships between river-system size and parasequence nearshore sand-belt length, for successions from the Cretaceous Western Interior Seaway and for the shallow subsurface of the Po and Rhône deltas. (A) Scatter plot of mean dip length of parasequence shallow-marine sand belts in different successions against the drainage area of the river systems that directly fed the formative coasts. Horizontal bars represent ranges of estimated catchment sizes, and associated data points represent mid values of the range. (B) Scatter plot of mean dip length of parasequence shallow-marine sand belts in different successions against the depth of the rivers that directly fed the formative coasts. Depth values for data points relating to ancient successions represent either means of estimated maximum bankfull depths or mid values of ranges in estimated maximum bankfull depths; depth values for data points relating to modern deltas represent mean values of mean bankfull depths. Horizontal bars represent ranges of channel depth. Dashed lines indicate linear (A) and power-law (B) best-fit curves.

DISCUSSION

Analyses of parameters that describe parasequences and associated shallow-marine sand belts can be interpreted with respect to how parasequence properties are controlled by accommodation and rates of sediment supply. The possibility of using inferences of geological controls to attempt predictions of parasequence architectures in the subsurface is also discussed.

Controls on parasequence geometries and stacking patterns

The thickness of parasequences is expected to reflect a number of factors: (i) the accommodation provided by the pre-existing bathymetry into which a coastal system builds out, (ii) the amount of aggradation taking place along the dip profile of the parasequence during its deposition in response to accommodation generation (quantified by the stratigraphic rise in the nearshore), (iii) possible partial erosion, and (iv) sediment compaction (cf. Driscoll & Karner, 1999; Lee et al., 2007b; Emery & Myers, 2009; Ainsworth et al., 2020; Fig. 1C).

Pre-existing accommodation is a primary control on parasequence thickness: parasequences are expected to typically record shoreline progradation into progressively deeper shelf areas, and as such parasequences embodying depositional systems that have prograded further offshore are expected to be thicker on average (Emery & Myers, 2009; Ainsworth et al., 2020). This behaviour appears to be reflected in relations between parasequence thickness and progradation distance, and between parasequence thickness and rates of progradation for units of comparable timescale (Fig. 7C-D). The positive relationship between parasequence thickness and progradation distance is statistically significant, but not strong: the weakness in correlation might be due to (i) the limiting effect of bathymetry on rates of shelf transit, whereby steeper continental shelves – typically with deeper margins – generate thicker parasequences but arising from slower rates of shoreline advance (Bijkerk et al., 2016; Ainsworth et al., 2020), and/or (ii) to the fact that higher rates of sediment delivery over timescales longer than that of a single parasequence may result in a shallower receiving shelf (Swift & Thorne, 1991). The positive correlation between parasequence progradation distance and thickness might also in part reflect the observed scaling between progradation distance and stratigraphic rise (i.e., aggradation), since both quantities depend on the length of time recorded in a parasequence; however, the same observations may otherwise be due to unrecognized lateral and vertical amalgamation of shingled units that are not differentiatied as parasequences, especially for subsurface datasets (see Colombera & Mountney, 2020).

The role of the increase in accommodation space in controlling parasequence thickness (Posamentier & Allen, 1999; Emery & Myers, 2009; Ainsworth et al., 2018) is reflected in relationships between parasequence thickness and stratigraphic rise, and between parasequence thickness and rates of aggradation evaluated across groups of units deposited over a comparable timescale (Fig. 7A-B). However, parasequences tend to be thinner than average in TSTs and retrogradational parasequence sets, i.e., for conditions under which rates of accommodation creation should be largest (Figs. 4C and 5C). This may reflect the anticipated role of transgressive marine erosion of the upper portions of parasequences on their preserved thickness (as also observed in the data pool of parasequences with classified tops; Fig. 11), more limited progradation into deeper shelf areas (Figs. 4F, 5F; see below), and/or a characteristically reduced bathymetry of transgressive seas (cf. Cross & Lessenger, 1997).

Rates of creation of accommodation can also be considered with respect to how accommodation varies relative to changes in rates of sediment supply to depositional shorelines. The parasequence progradation angle represents the net effect of the ratio between the rate of aggradation in the nearshore and the rate of shoreline progradation, as recorded during the regressive evolution of a parasequence, and can therefore be employed as a proxy for the ratio between rate of creation of accommodation and rate of sediment supply (at least for a given shelf depth) at parasequence scale (A/S; Helland-Hansen & Martinsen, 1996; Helland-Hansen & Hampson, 2009). For both normal-regressive parasequences and units termed parasequences but recording forced-regressive progradation (and thus not parasequences *sensu stricto*; Kamola & Van Wagoner, 1995), weak but statistically significant relationships are observed between thickness and progradation angle (Fig. 9A), according to which parasequences with flatter progradation trajectories tend to be thicker. This observation suggests that the rate of shore migration into deeper shelf areas may be more important than the rate of aggradation in the nearshore

domain in determining parasequence thickness. On this basis, rates of sediment supply may act as a stronger control on parasequence thickness than rates of accommodation creation, contrary to what might be expected (cf. Løseth & Helland-Hansen, 2001; Emery & Myers, 2009).

Differences in stratigraphic trends of parasequence thickness are seen between HSTs (dominantly thinning upward) and TSTs (dominantly thickening upward), which are overall consistent with variations in accommodation through a cycle that might be expected theoretically (i.e., respectively undergoing decreasing and increasing rates of accommodation generation; Posamentier & Allen, 1999; Ainsworth et al., 2018); however, these differences are typically modest, and frequently opposite to what is anticipated. The notion that parasequences in LSTs might typically be arranged in thickening-upward fashion in response to accelerating rates of accommodation creation (Posamentier et al., 1988; Emery & Myers, 2009) is not supported by the data, since a dominance of upward-thinning transitions is seen instead. It is likely that discrepancies between models and observations arise in part because of the variability in the length of time over which successive parasequences are generated (cf. Colombera & Mountney, 2020) and because of irregular (non-sinusoidal) relative sea-level change.

In the same way as the parasequence thickness, the thickness of shoreline-shelf parasequence sand belts is also limited by the pre-existent accommodation (shelf depth) and affected by erosive processes, but is additionally determined by the depth of sand-mud transition on the shelf, itself a function of the grainsize distribution of the sediment that reaches the shelf and of the process regime controlling sediment dispersal and offshore sand advection (Niedoroda et al., 1985; Hampson & Storms, 2003; Dunbar & Barrett, 2005; Storms & Hampson, 2005; George & Hill, 2008; and references therein).

Parasequence shallow-marine sands or sandstones are thinner on average in retrogradational parasequence sets and in FSSTs and TSTs (Figs. 4C, 5C), likely in relation to erosion by ravinement processes (Fig. 11) and during forced regression. No significant relationships are seen between the thickness of sand belts and the progradation angle of their parasequences, which indicates that A/S variations are not important in controlling sand-belt thickness.

The length of parasequence sand-belts along the depositional dip profile is expected to result from the interplay of three factors: (i) the amount of continuous progradation experienced by the shoreline during deposition of the parasequence (i.e., the progradation distance; cf. Ainsworth et al., 2020), (ii) the distance of the shelf sand-mud transition from the shoreline (cf. ‘pinchout distance’ of Løseth & Helland-Hansen, 2001), and (iii) possible erosional truncation.

Parasequence sand belts are on average narrower in sets with retrogradational stacking pattern and in TSTs or FSSTs, compared to those of aggradational or progradational sets and of HSTs and LSTs (Figs. 4D, 5D). The progradation distance of parasequences also tends to be lower in retrogradational sets and in TSTs; however, FSST parasequences display on average the longest progradation distance, albeit based on a very limited dataset (Figs. 4F, 5F). In part, these observations suggest that rapid shifts in shoreline position are likely to determine punctuation in parasequence organization that affects the dip length of parasequence sand bodies (cf. Cant, 1989; Hunt & Tucker, 1992; Cattaneo & Steel 2003), and that transgressive and regressive marine erosion may be responsible for significant cannibalization of nearshore sand belts (cf. Posamentier & Allen, 1999).

Results indicate that normal-regressive parasequences with flatter progradation trajectories tend to have more extensive sand belts particularly because of increased progradation, and not as a result of sand-mud transitions being deeper (and resulting pinchout distances longer) on average. This is in agreement with positive relationships between parasequence sand-belt dip length and rates of progradation, when evaluated for units of comparable timescale (Fig. 8), and can be explained by controls exerted by sediment-supply rates and shelf bathymetry, whereby both shallower shelves and faster sediment-delivery rates can drive more rapid progradation. Results relating sand-body length to both parasequence progradation angles and depositional-tract shoreline trajectories (Figs. 9 and 10) can be interpreted in terms of these controls, which appear to be expressed over a range of spatial and temporal scales. Similarly, for forced-regressive parasequences, positive scaling between sand-body dip length and progradation angle (Fig. 9C) could reflect the effect of progradation driven by sediment supply (leading to increased progradation distance and therefore to gentler negative progradation angle) superimposed on forced regression; it is also possible however that this direct scaling is merely due to

the variable orientation of observation windows at an angle with the depositional dip direction.

These results show that where shoreline trajectories of facies belts and of sets of clinothems can be observed in seismic data, or progradation angles of parasequences can be inferred in subsurface successions, predictions can be attempted of the likely range of dimensions of parasequence-scale stratigraphic compartments in shallow-marine hydrocarbon reservoirs and in successions targeted for carbon-dioxide sequestration by underground storage.

Data on parasequence progradation angles can also provide insight into whether parasequence stacking in systems tracts is sensitive to forms of self-organization or to intrinsic behaviours in the variations of allogenic controls. It is claimed that the progradation angles of successive parasequences should portray concave-landward shoreline trajectories in response to the autogenic dynamics that drive shoreline autoretreat, and which occur in relation to temporal variations in sediment storage on coastal plains and in sediment volumes required to sustain shore progradation (Jervey 1988; Muto & Steel, 1992, 1997, 2002, 2014; Muto et al., 2007; Hampson, 2016; Ainsworth et al., 2020; Fig. 1F). In LSTs, similar concave-landward shoreline trajectories may also develop in response to inherently accelerating relative sea-level rise, under the assumption of simple sinusoidal cycles of variations in sea level (Catuneanu, 2019a). On the contrary, concave-seaward shoreline trajectories are expected to develop in HSTs in response to decelerating relative sea-level rise (Posamentier et al., 1988; Posamentier & Allen, 1999; Catuneanu, 2019a; Fig. 1E). However, the presented quantitative assessments of variations in progradation angles for parasequences in HSTs and LSTs, where autoretreat behaviours might be expected to emerge, indicate that there is no evident preferential pattern of shoreline trajectory (Fig. 6). Meanwhile, only a weak tendency to develop concave-seaward shoreline trajectories is seen for parasequences in HSTs. These observations could reflect the interference of these intrinsic dynamics, the overwhelming control of sediment supply, non-sinusoidal variations in accommodation generation, and/or variance in the temporal duration of parasequences. Equally, it is possible that these results merely reflect the difficulty in accurately constraining parameters that describe parasequence accretion histories in a quantitative manner: where qualitative descriptors are used, propensity towards aggradational-to-progradational or progradational-to-aggradational stacking are seen in HSTs and LSTs respectively.

Parasequence thickness-to-sand-fraction ratio as A/S predictor

Thickness-to-sand-fraction (T/SF) analysis is a technique that employs stratigraphic *variations in* T/SF ratios, as evaluated based on estimated values of mean parasequence thickness and sand fraction, to make inferences of parasequence stacking patterns (and, implicitly, of A/S across groups of parasequences); this type of analysis is particularly useful for 1D datasets (Ainsworth et al., 2018, 2020). It is however also claimed (Ainsworth, 2005; Ainsworth et al., 2018, 2020) that the thickness-to-sand-fraction (T/SF) ratio of parasequences acts – of itself, not just as variation thereof – as a direct measure of the ratio between rates of creation of accommodation and rate of sediment supply (A/S), where accommodation generation is considered for both the transgressive and regressive history of a parasequence (Ainsworth et al., 2018), since "parasequence thickness can be used as a proxy for accommodation at the time of deposition and parasequence sandstone fraction can be used as a proxy for sediment supply" (Ainsworth et al. 2018, p. 1915). This assumption is being specifically examined here. The current analysis supports the view that the thickness of a parasequence does not just reflect variations in accommodation generation (Ainsworth et al., 2018) but also any extant accommodation relating to seabed bathymetry, as recognized by Ainsworth et al. (2020). Also, there is no process-oriented justification for considering the sand fraction indicative of the rate of sediment supply (Ainsworth, 2005; Ainsworth et al., 2018, 2020), since the sand-belt thickness depends on the calibre of sediment being supplied, on its fractionation through subenvironments (cf. Anthony, 2015; Korus & Fielding, 2015; van der Vegt et al., 2020), and on the sand-mud transition depth (Dunbar & Barrett, 2005; George & Hill, 2008), that is, it depends on the process regime that operates in marine environments. From this perspective, it is also necessary to consider how parasequence thickness and sand fraction could covary because of relationships that exist between shelf depth and sand-dispersal mechanisms, for example in relation to the fact that typically the coasts of shallower shelves are exposed to less energetic waves but experience larger storm surges (Resio & Westerlink, 2008; Immenhauser, 2009). Furthermore, our analysis indicates that higher rates of sediment supply, by driving more rapid

progradation into deeper water, ultimately recorded as thicker parasequences, could even determine inverse proportionality between A/S and T/SF ratio. Positive correlation between parasequence progradation distance (a proxy for progradation rate and proportional to the rate of sediment supply) and thickness-to-sand-fraction ratio is indeed seen, and our analysis shows that this likely reflects the positive relationship between parasequence progradation distance and thickness (Fig. 7C). More fundamentally, no correlation exists between potential indicators of A/S ratio at parasequence scale (at least for their regressive part) and depositional-tract scales, respectively given by parasequence progradation angles and depositional-tract shoreline trajectories (Fig. 12). At the parasequence-set and systems-tract scale, mean values of thickness-to-sand-fraction ratios are smaller on average for conditions under which A/S ratio is expected to be highest (TSTs and retrogradational sets), contrary to what might be expected if the absolute value in T/SF ratio had the supposed predictive power as direct A/S proxy (Fig. 13).

It is also useful to consider stratigraphic variations in thickness-to-sand-fraction ratios, in view of their use for T/SF analysis. Thickness-to-sand-fraction changes across successive parasequences are on average consistent with what is predicted in Ainsworth et al. (2018, 2020; Fig. 1D): dominantly increasing in TSTs and dominantly decreasing in HSTs; our analysis suggests that this behaviour reflects exclusively variations in parasequence thickness, and not variations in sand fraction. These variations in parasequence thickness may indeed reflect variations in accommodation as theorized by Ainsworth et al. (2018; Fig. 1D), supporting the application of T/SF analysis for revealing stacking patterns, but are frequently limited in magnitude or opposite in sign: the uncertainty in systems-tract classification based on related observations from well data may be significant.

Parasequence architecture and depositional-system configuration

In view of results demonstrating emerging relationships between parasequence sand-body dip length and proxies for rates of sediment delivery to ancient shorelines or parasequence-scale A/S ratio, the predictive value of metrics that describe controls on the sediment budget of a shoreline-shelf system on parasequence architectures can be considered.

For Cretaceous examples from the North-American western interior, the weak positive relationships that are seen between the length of parasequence sandstones in shoreline-shelf successions and estimates of hydraulic geometry and catchment size for river systems that fed the palaeo-shorelines could represent a signature of the control exerted by sediment flux on sediment supply and shoreline shelf transit (cf. Swift & Thorne, 1991; Aadland & Helland-Hansen, 2019). The weakness in scaling between river systems and parasequence sand bodies could be due to inherent error in the data (particularly in interpretations and estimations; Colombera & Mountney, 2020) and to interference of other geological controls on sediment supply and sedimentary architectures (e.g., shelf physiography, temporal variations in longshore drift, processes controlling sand-mud transition depth). Because of the narrow focus of this analysis and the limited strength of the observed scaling relationships, predictive tools suitable for subsurface characterization, which could be applied based on insight from source-to-sink studies and river palaeohydrology, cannot yet be proposed. Exploration of relationships based on a larger database covering a wider range of scales of linked depositional systems is necessary, and should be undertaken with consideration of the autogenic or allogenic origin of the units and of their timescale and hierarchy.

Realistically, a control by sediment-supply rates should translate to differences in parasequence architecture between deltaic depositional systems and littoral systems associated with linear coasts, based on the intuition that sediment supply rates to deltaic systems should be typically higher, although perhaps also more variable in time and space. At the scale of individual parasequences, however, this assumption is at odds with data on progradation distance and angles and not evidently reflected in data on sand dip length, even though these observations might partly be affected by the fact that the studied deltaic parasequences embody shorter development time on average, possibly because of influence by autogenic mechanisms of parasequence generation (e.g., trunk-river avulsion; Colombera & Mountney, 2020). At the scale of groups of parasequences (sets and systems tracts) though, some association seems to exist between stacking patterns and shoreline type, whereby deltas and river-dominated systems are more commonly associated with progradational patterns. In part, these results may reflect the supposed

intimate relationship between shoreline type and relative-sea level state (Heward 1981; Boyd et al., 1992; James & Dalrymple, 2010), and/or the fact that increased sediment flux favours the development of fully developed river deltas while simultaneously acting as a driver of depositional regression (Caldwell et al., 2019). At the same time, these results support the idea that intrinsic along-strike variations in sediment supply and associated differences in depositional-system type can cause lateral variability in parasequence architecture that may affect the application of sequence stratigraphic categories (cf. Wehr, 1993; Martinsen & Helland-Hansen, 1995; Krystinik & DeJarnett, 1995; Madof et al., 2016).

CONCLUSIONS

With the caveat that any such analysis is affected by the varied geological significance of parasequences and by subjectivity in their definition, a statistical analysis of the properties of parasequences from many siliciclastic successions has been attempted to infer the record of accommodation, sediment supply, and autogenic behaviours as controls on parasequence architecture, considering how these factors vary across depositional settings and over multiple scales.

Selected findings of this quantitative assessment can be summarized as follows:

- Parasequence thickness – a partial record of shelf or ramp bathymetry – is related to rates of accommodation generation, but may be especially influenced by the degree of shore progradation into deeper waters, and is also affected by top truncation, especially by ravinement. These factors also explain observed variations in parasequence thickness across systems tracts and parasequence sets of different types.
- Inverse proportionality between the dip length of parasequence sand bodies and proxies of A/S ratio at parasequence and ‘depositional-tract’ (i.e., large-scale facies belt) scales is interpreted to reflect the influence of sediment-supply rates on progradation rates; this control also seems to be expressed in stacking patterns.
- In systems tracts, stratigraphic trends in parasequence progradation angles that could be interpreted as due to autogenic dynamics or to predictably varying rates of relative sea-level change are not seen. Qualitative classifications of stacking patterns, however, indicate that further study based on a larger dataset is desired.
- Associations exist between deltaic or river-dominated parasequences and progradational stacking, but correlation between metrics of river-system size and dip lengths of shallow-marine parasequence sand bodies is modest.

The quantification presented in this work can be referred to when attempting predictions of likely volume, geometry and compartmentalization of shallow-marine sand bodies, on the basis of constraints of accommodation and sediment supply that may be available in subsurface studies, particularly from those based on regional seismic stratigraphy and source-to-sink analyses.

There is scope for future work, which could focus on complementary analyses to be undertaken with improved consideration of tectonic setting, sediment-delivery mechanisms and the type of shoreline dynamics (autogenic *vs* allogenic, local *vs* regional) recorded in the parasequences.

CONFLICT OF INTEREST

The authors declare that they have no known competing financial interests or personal relationships that could have appeared to influence the work reported in this paper.

ACKNOWLEDGEMENTS

The SMAKS database has been funded by the sponsors of the Shallow-Marine Research Group (De Beers and Engie [now Neptune]) and by NERC (Catalyst Fund award NE/M007324/1; Follow-on Fund

NE/N017218/1). We also thank the sponsors of the Fluvial & Eolian Research Group (AkerBP, Areva [now Orano], BHPBilliton, Cairn India [Vedanta], ConocoPhillips, Chevron, Equinor, Murphy Oil, Nexen-CNOOC, Occidental, Petrotechnical Data Systems [PDS], Saudi Aramco, Shell, Tullow Oil, Woodside and YPF) for financial support to our research. Ru Wang and Soma Budai are thanked for help with data collection. Editors Ian Kane and Chris Fielding and reviewers Bruce Ainsworth, Gary Hampson and Boyan Vakarelov are thanked for their thoughtful comments and detailed reviews, which significantly improved the article.

DATA AVAILABILITY STATEMENT

The data that support the findings of this study are available from the corresponding author upon reasonable request.

REFERENCES

Aadland, T. and **Helland-Hansen, W.** (2019) Progradation Rates Measured at Modern River Outlets: A First-Order Constraint on the Pace of Deltaic Deposition. *J. Geophys. Res. Earth Surf.*, **124**, 347-364.

Adams, M.M. and **Bhattacharya, J.P.** (2005) No change in fluvial style across a sequence boundary, Cretaceous Blackhawk and Castlegate Formations of central Utah, USA. *J. Sed. Res.*, **75**, 1038-1051.

Ainsworth, R.B. (2005) Sequence stratigraphic-based analysis of reservoir connectivity: influence of depositional architecture–a case study from a marginal marine depositional setting. *Petrol. Geosci.*, **11**, 257-276.

Ainsworth, R.B., Flint, S.S. and **Howell, J.A.** (2008) Predicting coastal depositional style: Influence of basin morphology and accommodation to sediment supply ratio within a sequence-stratigraphic framework. In: *Recent advances in models of shallow-marine stratigraphy* (Eds G.J. Hampson, R.J. Steel, P.M. Burgess and R.W. Dalrymple), *SEPM Spec. Publ.*, **90**, 237-263.

Ainsworth, R.B., Vakarelov, B.K. and **Nanson, R.A.** (2011) Dynamic spatial and temporal prediction of changes in depositional processes on clastic shorelines: toward improved subsurface uncertainty reduction and management. *AAPG Bull.*, **95**, 267-297.

Ainsworth, R.B., Payenberg, T.H.D., Willis, B.J., Sixsmith, P.J., Yeaton, J.W., Sykiotis, N. and **Lang, S.C.** (2016) Predicting Shallow Marine Reservoir Heterogeneity Using a High Resolution Mapping Approach, Brigadier Formation, NWS, Australia. Society of Petroleum Engineers, Asia Pacific Oil and Gas Conference and Exhibition, Perth, Australia, SPE-182355-MS, 13

Ainsworth, R.B., McArthur, J.B., Lang, S.C. and **Vonk, A.J.** (2018) Quantitative sequence stratigraphy. *AAPG Bull.*, **102**, 1913-1939.

Ainsworth, R.B., Vakarelov, B.K., Eide, C.H., Howell, J.A. and **Bourget, J.** (2019) Linking the high-resolution architecture of modern and ancient wave-dominated deltas: Processes, products, and forcing factors. *J. Sed. Res.*, **89**, 168-185.

Ainsworth, R.B., McArthur, J.B., Lang, S.C. and **Vonk, A.J.** (2020) Parameterizing parasequences: Importance of shelf gradient, shoreline trajectory, sediment supply, and autoretreat. *AAPG Bull.*, **104**, 53-82.

Amorosi, A., Centineo, M.C., Colalongo, M.L. and **Fiorini, F.** (2005) Millennial-scale depositional cycles from the Holocene of the Po Plain, Italy. *Mar. Geol.*, **222**, 7-18.

Amorosi, A., Sarti, G., Rossi, V. and **Fontana, V.** (2008) Anatomy and sequence stratigraphy of the late quaternary Arno valley fill (Tuscany, Italy). In: *Advances in Application of Sequence Stratigraphy in Italy* (Eds A. Amorosi, B.U. Haq and L. Sabato), *GeoActa Spec. Publ.*, **1**, 117-128.

Amorosi, A., Rossi, V., Sarti, G. and **Mattei, R.** (2013) Coalescent valley fills from the late Quaternary record of Tuscany (Italy). *Quatern. Int.*, 288, 129-138.

Amorosi, A., Bruno, L., Campo, B., Morelli, A., Rossi, V., Scarponi, D., Hong, W., Bohacs, K.M. and **Drexler, T.M.** (2017) Global sea-level control on local parasequence architecture from the Holocene record of the Po Plain, Italy. *Mar. Petrol. Geol.*, **87**, 99-111.

Angulo, R.J., Lessa, G.C. and **Souza, M.C.** (2009) The Holocene barrier systems of Paranaguá and northern Santa Catarina coasts, Southern Brazil. In: *Geology and Geomorphology of Holocene Coastal Barriers of Brazil* (Eds S.R. Dillenburg and P.A. Hesp), *Lecture Notes in Earth Sciences*, **107**, Springer, Berlin, 135-176.

Anthony, E.J. (2015) Wave influence in the construction, shaping and destruction of river deltas: A review. *Mar. Geol.*, **361**, 53-78.

Arnott, R.W.C. (1995) The parasequence definition; are transgressive deposits inadequately addressed?. *J. Sed. Res.*, **65**, 1-6.

Aschoff, J.L. and **Steel, R.J.** (2011) Anatomy and development of a low-accommodation clastic wedge, upper Cretaceous, Cordilleran Foreland Basin, USA. *Sed. Geol.*, **236**, 1-24.

Balsley, J.K. (1983) *Cretaceous Wave-Dominated Delta Systems: Book Cliffs, East Central Utah*. Oklahoma City Geological Society, Continuing Education Short Course, 219 pp.

Bartek, L.R., Carbote, B.S., Young, T. and **Schroeder, W.** (2004) Sequence stratigraphy of a continental margin subjected to low-energy and low-sediment-supply environmental boundary conditions; late Pleistocene–Holocene deposition offshore Alabama, U.S.A.. In: *Late Quaternary stratigraphic evolution of the northern Gulf of Mexico margin* (Eds J.B. Anderson and R.H. Fillon) *SEPM Spec. Publ.*, **79**, 85-109.

Bassetti, M.A., Jouet, G., Dufois, F., Berné, S., Rabineau, M. and **Taviani, M.** (2006) Sand bodies at the shelf edge in the Gulf of Lions (Western Mediterranean): Deglacial history and modern processes. *Mar. Geol.*, **234**, 93-109.

Bassetti, M.A., Berné, S., Jouet, G., Taviani, M., Dennielou, B., Flores, J.A., Gaillot, A., Gelfort, R., Lafuerza, S. and **Sultan, N.** (2008) The 100-ka and rapid sea level changes recorded by prograding shelf sand bodies in the Gulf of Lions (western Mediterranean Sea). *Geochem. Geophys. Geosyst.*, **9**, Q11R05.

Berné, S., Lericolais, G., Marsset, T., Bourillet, J.F. and **De Batist, M.** (1998) Erosional offshore sand ridges and lowstand shorefaces: examples from tide-and wave-dominated environments of France. *J. Sed. Res.*, **68**, 540-555.

Berné, S., Jouet, G., Bassetti, M.A., Dennielou, B. and **Taviani, M.** (2007) Late Glacial to Preboreal sea-level rise recorded by the Rhône deltaic system (NW Mediterranean). *Mar. Geol.*, **245**, 65-88.

Berton, F., Guedes, C.C.F., Vesely, F.F., Souza, M.C., Angulo, R.J., Rosa, M.L.C.C. and **Barboza, E.G.** (2019) Quaternary coastal plains as reservoir analogs: Wave-dominated sand-body heterogeneity from outcrop and ground-penetrating radar, central Santos Basin, southeast Brazil. *Sed. Geol.*, **379**, 97-113.

Bhattacharya, J. (1989) Allostratigraphy and river- and wave-dominated depositional systems of the Upper Cretaceous (Cenomanian) Dunvegan Formation, Alberta [Ph.D. Thesis]. McMaster University, Hamilton, Ontario, 588

Bhattacharya, J.P. (1992) Regional to subregional facies architecture of river-dominated deltas in the Alberta subsurface, Upper Cretaceous Dunvegan Formation. In: *The three-dimensional facies architecture of terrigenous clastic sediments, and its implications for hydrocarbon discovery and recovery* (Eds A.D. Miall and N. Tyler), *SEPM Concepts in Sedimentology and Paleontology*, **3**, 189-206.

Bhattacharya, J.P. (2011) Practical problems in the application of the sequence stratigraphic method and key surfaces: integrating observations from ancient fluvial–deltaic wedges with Quaternary and modelling studies. *Sedimentology*, **58**, 120-169.

Bhattacharya, J.P. and **MacEachern, J.A.** (2009) Hyperpycnal rivers and prodeltaic shelves in the

Cretaceous Seaway of North America. *J. Sed. Res.*, **79**, 184-209.

Bhattacharya, J.P. and **Posamentier, H.W.** (1994) Sequence stratigraphic and allostratigraphic applications in the Alberta Foreland Basin. In: *Geological Atlas of the Western Canada Sedimentary Basin* (Eds G.D. Mossop and I. Shetsen), pp. 407-412. Canadian Society of Petroleum Geologists and Alberta Research Council Calgary, Alberta, Canada.

Bhattacharya, J.P. and **Tye, R.S.** (2004) Searching for modern Ferron analogs and application to subsurface interpretation. In: *The Fluvial-Deltaic Ferron Sandstone: Regional to Wellbore-Scale Outcrop Analog Studies and Application to Reservoir Modeling* (Eds T.C. Chidsey, R.D. Adams and T.H. Morris), AAPG Stud. Geol., **50**, 39-57.

Bhattacharya, J. and **Walker, R.G.** (1991a) Allostratigraphic subdivision of the Upper Cretaceous Dunvegan, Shaftesbury and Kaskapau formations in the northwestern Alberta subsurface. *Bull. Can. Petrol. Geol.*, **39**, 145-164.

Bhattacharya, J. and **Walker, R.G.** (1991b) River-and wave-dominated depositional systems of the Upper Cretaceous Dunvegan Formation, northwestern Alberta. *Bull. Can. Petrol. Geol.*, **39**, 165-191.

Bhattacharya, J.P., Copeland, P., Lawton, T.F. and **Holbrook, J.** (2016) Estimation of source area, river paleo-discharge, paleoslope, and sediment budgets of linked deep-time depositional systems and implications for hydrocarbon potential. *Earth-Sci. Rev.*, **153**, 77-110.

Bhattacharyya, P., Bhattacharya, J.P. and **Khan, S.D.** (2015) Paleo-channel reconstruction and grain size variability in fluvial deposits, Ferron Sandstone, Notom Delta, Hanksville, Utah. *Sed. Geol.*, **325**, 17-25.

Bhattacharya, J.P., Miall, A.D., Ferron, C., Gabriel, J., Randazzo, N., Kynaston, D., Jicha, B.R. and **Singer, B.S.** (2019) Time-stratigraphy in point sourced river deltas: Application to sediment budgets, shelf construction, and paleo-storm records. *Earth-Sci. Rev.*, **199**, article 102985.

Bijkerk, J.F., Eggenhuisen, J.T., Kane, I.A., Meijer, N., Waters, C.N., Wignall, P.B. and **McCaffrey, W.D.** (2016) Fluvio-marine sediment partitioning as a function of basin water depth. *J. Sed. Res.*, **86**, 217-235.

Blondel, T.J.A., Gorin, G.E. and **Chene, J.D.** (1993) Sequence stratigraphy in coastal environments: sedimentology and palynofacies of the Miocene in central Tunisia. In: *Sequence Stratigraphy and Facies Associations* (Eds H.W. Posamentier, C.P. Summerhayes, B.U. Haq and G.P. Allen), *Int. Assoc. Sedimentol. Spec. Publ.*, **18**, 161-179.

Boreen, T. and **Walker, R.G.** (1991) Definition of allomembers and their facies assemblages in the Viking Formation, Willesden Green area, Alberta. *Bull. Can. Petrol. Geol.*, **39**, 123-144.

Bowman, A.P. (2003) *Sequence Stratigraphy and Reservoir Characterisation in the Columbus Basin, Trinidad*. Ph.D. Thesis, Imperial College London, 243 pp.

Bowman, A. (2016) Outcrop analogues for hydrocarbon reservoirs in the Columbus Basin, offshore east Trinidad. In: *The value of outcrop studies in reducing subsurface uncertainty and risk in hydrocarbon exploration and production* (Eds M. Bowman, H.R. Smyth, T.R. Good, S.R. Passey, J.P.P. Hirst and C.J. Jordan), *Geol. Soc. London Spec. Publ.*, **436**, 151-192.

Bowman, A.P. and **Johnson, H.D.** (2014) Storm-dominated shelf-edge delta successions in a high accommodation setting: The palaeo-Orinoco Delta (Mayaro Formation), Columbus Basin, South-East Trinidad. *Sedimentology*, **61**, 792-835.

Boyd, R., Dalrymple, R. and **Zaitlin, B.A.** (1992) Classification of clastic coastal depositional environments. *Sed. Geol.*, **80**, 139-150.

Boyer, J., Duvail, C., Le Strat, P., Gensous, B. and **Tesson, M.** (2005) High resolution stratigraphy and evolution of the Rhône delta plain during Postglacial time, from subsurface drilling data bank. *Mar. Geol.*, **222**, 267-298.

Bridge, J.S. and **Tye, R.S.** (2000) Interpreting the dimensions of ancient fluvial channel bars, channels,

and channel belts from wireline-logs and cores. *AAPG Bull.*, **84**, 1205-1228.

Brenchley, P.J., Pickerill, R.K. and **Stromberg, S.G.** (1993) The role of wave reworking on the architecture of storm sandstone facies, Bell Island Group (Lower Ordovician), eastern Newfoundland. *Sedimentology*, **40**, 359-382.

Burgess, P.M. and **Allen, P.A.** (1996) A forward-modelling analysis of the controls on sequence stratigraphical geometries. In: *Sequence Stratigraphy in British Geology* (Ed S.P. Hesselbo and D.N. Parkinson), *Geol. Soc. London Spec. Publ.*, **103**, 9-24.

Burpee, A.P., Slingerland, R.L., Edmonds, D.A., Parsons, D., Best, J., Cederberg, J., McGuffin, A., Caldwell, R., Nijhuis, A. and **Royce, J.** (2015) Grain-size controls on the morphology and internal geometry of river-dominated deltas. *J. Sed. Res.*, **85**, 699-714.

Caldwell, R.L., Edmonds, D.A., Baumgardner, S., Paola, C., Roy, S. and **Nienhuis, J.H.** (2019) A global delta dataset and the environmental variables that predict delta formation on marine coastlines. *Earth Surf. Dynam.*, **7**, 773-787.

Campo, B., Amorosi, A. and **Vaiani, S.C.** (2017) Sequence stratigraphy and late Quaternary paleoenvironmental evolution of the Northern Adriatic coastal plain (Italy). *Palaeogeogr. Palaeoclimatol. Palaeoecol.*, **466**, 265-278.

Cant, D.J. (1989) Simple equations of sedimentation: applications to sequence stratigraphy. *Basin Res.*, **2**, 73-81.

Cant, D.J. (1991) Geometric modelling of facies migration: theoretical development of facies successions and local unconformities. *Basin Res.*, **3**, 51-62.

Cant, D.J. (1993) The stratigraphic and paleogeographic context of shoreline—shelf reservoirs. In: *Marine clastic reservoirs: examples and analogues* (Eds E.G. Rhodes and T.F. Moslow), *Frontiers in Sedimentary Geology*, pp. 3-20. Springer, New York, NY.

Carter, R.M., Fulthorpe, C.S. and **Naish, T.R.** (1998). Sequence concepts at seismic and outcrop scale: the distinction between physical and conceptual stratigraphic surfaces. *Sed. Geol.*, **122**, 165-179.

Carvajal, C. and **Steel, R.** (2009) Shelf-edge architecture and bypass of sand to deep water: influence of shelf-edge processes, sea level, and sediment supply. *J. Sed. Res.*, **79**, 652-672.

Carvajal, C. and **Steel, R.** (2012) Source-to-sink sediment volumes within a tectono-stratigraphic model for a Laramide shelf-to-deep-water basin: methods and results. In: *Tectonics of Sedimentary Basins: Recent Advances* (Eds C. Busby and A. Azor Perez), pp. 131-151. Wiley-Blackwell, Oxford, UK.

Cattaneo, A. and **Steel, R. J.** (2003). Transgressive deposits: a review of their variability. *Earth-Sci. Rev.*, **62**, 187-228.

Catuneanu, O. (2019a) Model-independent sequence stratigraphy. *Earth-Sci. Rev.*, **188**, 312-388.

Catuneanu, O. (2019b) Scale in sequence stratigraphy. *Mar. Petrol. Geol.*, **106**, 128-159.

Catuneanu, O., Abreu, V., Bhattacharya, J.P., Blum, M.D., Dalrymple, R.W., Eriksson, P.G., Fielding, C.R., Fisher, W.L., Galloway, W.E., Gibling, M.R. and **Giles, K.A.** (2009) Towards the standardization of sequence stratigraphy. *Earth-Sci. Rev.*, **92**, 1-33.

Catuneanu, O., Bhattacharya, J.P., Blum, M.D., Dalrymple, R.W., Eriksson, P.G., Fielding, C.R., Fisher, W.L., Galloway, W.E., Gianolla, P., Gibling, M.R. and **Giles, K.A.** (2010) Thematic Set: Sequence stratigraphy: common ground after three decades of development. *First Break*, **28**, 41-54.

Charvin, K., Hampson, G.J., Gallagher, K.L. and **Labourdette, R.** (2010) Intra-parasequence architecture of an interpreted asymmetrical wave-dominated delta. *Sedimentology*, **57**, 760-785.

Charvin, K., Hampson, G.J., Gallagher, K.L., Storms, J.E. and **Labourdette, R.** (2011) Characterization of controls on high-resolution stratigraphic architecture in wave-dominated shoreface–shelf parasequences using inverse numerical modeling. *J. Sed. Res.*, **81**, 562-578.

Chentnik, B.M., Johnson, C.L., Mulhern, J.S. and **Stright, L.** (2015) Valleys, estuaries, and lagoons: paleoenvironments and regressive–transgressive architecture of the Upper Cretaceous Straight Cliffs Formation, Utah, USA. *J. Sed. Res.*, **85**, 1166-1196.

Christie-Blick, N. and **Driscoll, N. W.** (1995) Sequence stratigraphy. *Ann. Rev. Earth. Planet. Sci.*, **23**, 451-478.

Coleman, J.M. and **Gagliano, S.M.** (1964) Cyclic Sedimentation in the Mississippi River Deltaic Plain. *Gulf Coast Ass. Geol. Soc. Trans.*, **14**, 67-80

Colombera, L. and **Mountney, N.P.** (2020) On the geological significance of clastic parasequences. *Earth-Sci. Rev.*, **201**, article 103062.

Colombera, L., Mountney, N.P., Hodgson, D.M. and **McCaffrey, W.D.** (2016) The Shallow-Marine Architecture Knowledge Store: A database for the characterization of shallow-marine and paralic depositional systems. *Mar. Petrol. Geol.*, **75**, 83-99.

Crandall, G.A. (1992) Fluvial influence on high-frequency sedimentary cycle geometry: The transition from strandplain to deltaic deposition in the Cretaceous Point Lookout Sandstone, San Juan Basin, Colorado [MA Thesis]. Rice University, Houston, 140 pp.

Cross, T.A. and **Lessenger, M.A.** (1997) Sediment volume partitioning: rationale for stratigraphic model evaluation and high-resolution stratigraphic correlation. In: *Sequence Stratigraphy – Concepts and Applications* (Eds F.M. Gradstein, K.O. Sandvik and N.J. Milton), *Norw. Petrol. Soc. Spec. Publ.*, **8**, 171-195.

Dam, G. and **Surlyk, F.** (1995) Sequence stratigraphic correlation of Lower Jurassic shallow marine and paralic successions across the Greenland-Norway seaway. In: *Sequence stratigraphy on the northwest European margin* (Eds R.J. Steel, V.L. Felt, E.P. Johannessen and C. Mathieu), *Norw. Petrol. Soc. Spec. Publ.*, **5**, 483-509.

Devine, P.E. (1991) Transgressive Origin of Channeled Estuarine Deposits in the Point Lookout Sandstone, Northwestern New Mexico: A Model for Upper Cretaceous, Cyclic Regressive Parasequences of the US Western Interior. *AAPG Bull.*, **75**, 1039-1063.

Driscoll, N.W. and **Karner, G.D.** (1999) Three-dimensional quantitative modeling of clinoform development. *Mar. Geol.*, **154**, 383-398.

Dunbar, G.B. and **Barrett, P.J.** (2005) Estimating palaeobathymetry of wave-graded continental shelves from sediment texture. *Sedimentology*, **52**, 253-269.

Edwards, C.M., Howell, J.A. and **Flint, S.S.** (2005) Depositional and stratigraphic architecture of the Santonian Emery Sandstone of the Mancos Shale: Implications for Late Cretaceous evolution of the Western Interior foreland basin of central Utah, USA. *J. Sed. Res.*, **75**, 280-299.

Eide, C.H., Howell, J.A., Buckley, S.J., Martinius, A.W., Oftedal, B.T. and **Henstra, G.A.** (2016) Facies model for a coarse-grained, tide-influenced delta: Gule Horn Formation (early Jurassic), Jameson Land, Greenland. *Sedimentology*, **63**, 1474-1506.

Embry, A.F. (2009) *Practical Sequence Stratigraphy*. Canadian Society of Petroleum Geologists, 81 pp.

Embry, A.F. and **Johannessen, E.P.** (2017) Two approaches to sequence stratigraphy. In: *Stratigraphy & Timescales, Vol. 2, Advances in Sequence Stratigraphy* (Ed M. Montenari), Academic Press, 85-118.

Emery, D. and **Myers, K.J.** (2009) *Sequence Stratigraphy*. Blackwell Science, Oxford, 297 pp.

Engkilde, M. and **Surlyk, F.** (2003) Shallow marine syn-rift sedimentation: Middle Jurassic Pelion Formation, Jameson Land, East Greenland. In: *The Jurassic of Denmark and Greenland* (Eds J.R. Ineson and F. Surlyk), *Geol. Surv. Den. Greenl. Bull.*, **1**, 813-863.

Eriksson, K.A., McClung, W.S. and **Simpson, E.L.** (2019) Sequence stratigraphic expression of greenhouse, transitional and icehouse conditions in siliciclastic successions: Paleozoic examples from the central Appalachian basin, USA. *Earth-Sci. Rev.*, **188**, 176-189.

Feldman, H.R., Fabijanic, J.M., Faulkner, B.L. and **Rudolph, K.W.** (2014) Lithofacies, parasequence stacking, and depositional architecture of wave- to tide-dominated shorelines in the Frontier Formation, western Wyoming, USA. *J. Sed. Res.*, **84**, 694-717.

Fielding, C.R. (2011) Foreland basin structural growth recorded in the Turonian Ferron Sandstone of the Western Interior Seaway Basin, USA. *Geology*, **39**, 1107-1110.

Fitzsimmons, R. and **Johnson, S.** (2000) Forced regressions: recognition, architecture and genesis in the Campanian of the Bighorn Basin, Wyoming. In: *Sedimentary responses to forced regressions* (Eds D. Hunt and R.L. Gawthorpe), *Geol. Soc. London Spec. Publ.*, **172**, 113-139.

Flood, Y.S. and **Hampson, G.J.** (2015) Quantitative analysis of the dimensions and distribution of channelized fluvial sandbodies within a large outcrop dataset: upper Cretaceous Blackhawk Formation, Wasatch Plateau, Central Utah, U.S.A. *J. Sed. Res.*, **85**, 315-336.

Forzoni, A., Storms, J.E., Whittaker, A.C. and **de Jager, G.** (2014) Delayed delivery from the sediment factory: modeling the impact of catchment response time to tectonics on sediment flux and fluvio-deltaic stratigraphy. *Earth Surf. Proc. Land.*, **39**, 689-704.

Forzoni, A., Hampson, G. and **Storms, J.** (2015). Along-strike variations in stratigraphic architecture of shallow-marine reservoir analogues: Upper Cretaceous Panther Tongue delta and coeval shoreface, Star Point Sandstone, Wasatch Plateau, Central Utah, USA. *J. Sed. Res.*, **85**, 968-989.

Frazier, D.E. (1974) Depositional episodes: their relationship to Quaternary framework in the northwestern portion of the Gulf Basin. The University of Texas, Austin, Bureau of Economic Geology, Geologic Circular, 74-1, 28 pp.

Galloway, W.E. (1989) Genetic stratigraphic sequences in basin analysis I: architecture and genesis of flooding-surface bounded depositional units. *AAPG Bull.*, **73**, 125-142.

Games, P.A. and **Howell, J.F.** (1976) Pairwise multiple comparison procedures with unequal n's and/or variances: a Monte Carlo study. *J. Educ. Stat.*, **1**, 113-125.

Gani, M.R. and **Bhattacharya, J.P.** (2007) Basic building blocks and process variability of a Cretaceous delta: internal facies architecture reveals a more dynamic interaction of river, wave, and tidal processes than is indicated by external shape. *J. Sed. Res.*, **77**, 284-302.

Garrison, J.R. Jr and **van den Bergh, T.C.V.** (2004) High-resolution depositional sequence stratigraphy of the Upper Ferron Sandstone, Last Chance Delta: an application of coal zone stratigraphy. In: *The Fluvial-Deltaic Ferron Sandstone: Regional to Wellbore-Scale Outcrop Analog Studies and Application to Reservoir Modeling* (Eds T.C. Chidsey, R.D. Adams and T.H. Morris), AAPG Stud. Geol., **50**, 125-192.

Garrison, J.R. Jr and **van den Bergh, T.C.V.** (2006) Effects of sedimentation rate, rate of relative rise in sea level, and duration of sea-level cycle on the filling of incised valleys: examples of filled and "overfilled" incised valleys from the Upper Ferron Sandstone, Last Chance Delta, east-central Utah, USA. In: *Incised Valleys in Time and Space* (Eds R.W. Dalrymple, D.A. Leckie, D. A and R.W. Tillman), *SEPM Spec. Publ.*, **85**, 239-279.

Geehan, G. and **Underwood, J.** (1993) The use of length distributions in geological modeling. In: *The Geologic Modelling of Hydrocarbon Reservoirs and Outcrop Analogs* (Eds S.S. Flint and I.D. Bryant), *Int. Assoc. Sedimentol. Spec. Publ.*, **15**, 205-212.

George, D.A. and **Hill, P.S.** (2008) Wave climate, sediment supply and the depth of the sand–mud transition: a global survey. *Mar. Geol.*, **254**, 121-128.

Ghinassi, M. (2007) The effects of differential subsidence and coastal topography on high-order transgressive–regressive cycles: Pliocene nearshore deposits of the Val d'Orcia Basin, Northern Apennines, Italy. *Sed. Geol.*, **202**, 677-701.

Gjelberg, H.K. (2010) Facies analysis and sandbody geometry of the Paleogene Battfjellet Formation, Central Western Nordenskiöld Land, Spitsbergen [MSc Thesis]. University of Bergen, Bergen, 172 pp.

Gonzalez, R., Dias, J.M.A., Lobo, F. and **Mendes, I.** (2004) Sedimentological and paleoenvironmental characterisation of transgressive sediments on the Guadiana Shelf (Northern Gulf of Cadiz, SW Iberia). *Quatern. Int.*, **120**, 133-144.

Gooley, J.T., Johnson, C.L. and **Pettinga, L.** (2016) Spatial and temporal variation of fluvial architecture in a prograding clastic wedge of the Late Cretaceous Western Interior Basin (Kaiparowits Plateau), USA. *J. Sed. Res.*, **86**, 125-147.

Grundvåg, S.A., Helland-Hansen, W., Johannessen, E.P., Olsen, A.H. and **Stene, S.A.** (2014) The depositional architecture and facies variability of shelf deltas in the Eocene Battfjellet Formation, Nathorst Land, Spitsbergen. *Sedimentology*, **61**, 2172-2204.

Gruenwald, R. (2001) The hydrocarbon prospectivity of lower Oligocene deposits in the Maragh Trough, SE Sirt Basin, Libya. *J. Petrol. Geol.*, **24**, 213-231.

Hajek, E.A. and **Heller, P.L.** (2012) Flow-depth scaling in alluvial architecture and nonmarine sequence stratigraphy: example from the Castlegate Sandstone, central Utah, USA. *J. Sed. Res.*, **82**, 121-130.

Hajek, E., Paola, C., Petter, A., Alabbad, A. and **Kim, W.** (2014) Amplification of shoreline response to sea-level change by back-tilted subsidence. *J. Sed. Res.*, **84**, 470-474.

Hampson, G.J. (2000) Discontinuity surfaces, clinoforms, and facies architecture in a wave-dominated, shoreface-shelf parasequence. *J. Sed. Res.*, **70**, 325-340.

Hampson, G.J. (2010) Sediment dispersal and quantitative stratigraphic architecture across an ancient shelf. *Sedimentology*, **57**, 96-141.

Hampson, G.J. (2016) Towards a sequence stratigraphic solution set for autogenic processes and allogenic controls: upper Cretaceous strata, Book Cliffs, Utah, USA. *J. Geol. Soc.*, **173**, 817-836.

Hampson, G.J. and **Howell, J.A.** (2005) Sedimentologic and geomorphic characterization of ancient wave-dominated deltaic shorelines: Upper Cretaceous Blackhawk Formation, Book Cliffs, Utah, U.S.A. In: *River Deltas; Concepts, Models and Examples* (Eds L. Giosan and J.P. Bhattacharya), *SEPM Spec. Publ.*, **83**, 133-154.

Hampson, G.J. and **Storms, J.E.** (2003) Geomorphological and sequence stratigraphic variability in wave-dominated, shoreface-shelf parasequences. *Sedimentology*, **50**, 667-701.

Hampson, G.J., Rodriguez, A.B., Storms, J.E.A., Johnson, H.D. and **Meyer, C.T.** (2008) Geomorphology and high-resolution stratigraphy of wave-dominated shoreline deposits: impact on reservoir-scale facies architecture. In: *Recent advances in models of shallow-marine stratigraphy* (Eds G.J. Hampson, R.J. Steel, P.M. Burgess and R.W. Dalrymple), *SEPM Spec. Publ.*, **90**, 117-142.

Hampson, G.J., Sixsmith, P.J., Kieft, R.L., Jackson, C.L. and **Johnson, H.D.** (2009) Quantitative analysis of net-transgressive shoreline trajectories and stratigraphic architectures: mid-tolate Jurassic of the North Sea rift basin. *Basin Res.*, **21**, 528-558.

Hampson, G.J., Gani, M.R., Sharman, K.E., Irfan, N. and **Bracken, B.** (2011) Along-strike and down-dip variations in shallow-marine sequence stratigraphic architecture: Upper Cretaceous Star Point Sandstone, Wasatch Plateau, Central Utah, USA. *J. Sed. Res.*, **81**, 159-184.

Hampson, G.J., Royhan Gani, M., Sahoo, H., Rittersbacher, A., Irfan, N., Ranson, A., Jewell, T.O., Gani, N.D., Howell, J.A. and **Buckley, S.J.** (2012) Controls on large-scale patterns of fluvial sandbody distribution in alluvial to coastal plain strata: upper Cretaceous Blackhawk Formation, Wasatch Plateau, Central Utah, USA. *Sedimentology*, **59**, 2226-2258.

Hampson, G.J., Jewell, T.O., Irfan, N., Gani, M.R. and **Bracken, B.** (2013) Modest change in fluvial style with varying accommodation in regressive alluvial-to-coastal-plain wedge: Upper Cretaceous Blackhawk Formation, Wasatch Plateau, central Utah, USA. *J. Sed. Res.*, **83**, 145-169.

Hansen, J.P.V. and **Rasmussen, E.S.** (2008) Structural, sedimentologic, and sea-level controls on sand distribution in a steep-clinoform asymmetric wave-influenced delta: Miocene Billund sand, eastern

Danish North Sea and Jylland. *J. Sed. Res.*, **78**, 130-146.

Harms, J.C., Mackenzie, D.B. and **McCubbin, D.G.** (1965) Depositional environment of the Fox Hills Sandstone near Rock Springs, Wyoming. *Rocky Mtn. Ass. Geologists 19th Field Conf. Gdbk*, 113-130.

Hassan, M.H.A., Sim, Y.B., Peng, L.C. and **Rahman, A.H.A.** (2013) Facies analysis of the Uppermost Kubang Pasu Formation, Perlis: a wave-and storm-influenced coastal depositional system. *Sains Malays.*, **42**, 1091-1100.

Hassan, M.H.A., Al Zamruddin, N.N.S., Sim, Y.B. and **Samad, A.S.S.A.** (2017) Sedimentology of the Permian Monodiexodina-bearing bed of the uppermost Kubang Pasu Formation, northwest Peninsular Malaysia: interpretation as storm-generated, transgressive lag deposits. *Geol. Soc. Malays. Bull.*, **64**, 51-58.

Hein, C.J., FitzGerald, D.M., de Souza, L.H., Georgiou, I.Y., Buynevich, I.V., Klein, A.H.D.F., de Menezes, J.T., Cleary, W.J. and **Scolaro, T.L.** (2016) Complex coastal change in response to autogenic basin infilling: An example from a sub-tropical Holocene strandplain. *Sedimentology*, **63**, pp.1362-1395.

Helland-Hansen, W. (2010) Facies and stacking patterns of shelf-deltas within the Palaeogene Battfjellet Formation, Nordenskiold Land, Svalbard: implications for subsurface reservoir prediction. *Sedimentology*, **57**, 190-208.

Helland-Hansen, W. and **Hampson, G.J.** (2009) Trajectory analysis: concepts and applications. *Basin Res.*, **21**, 454-483.

Helland-Hansen, W. and **Martinsen, O.J.** (1996) Shoreline trajectories and sequences: description of variable depositional-dip scenarios. *J. Sed. Res.*, **B66**, 670-688.

Herbert, C. (1997) Relative sea level control of deposition in the Late Permian Newcastle Coal Measures of the Sydney Basin, Australia. *Sed. Geol.*, **107**, 167-187.

Heward, A.P. (1981) A review of wave-dominated clastic shoreline deposits. *Earth-Sci. Rev.*, **17**, 223-276.

Holgate, N.E. (2014) Geological characterisation of shallow marine-to-deltaic sandstone reservoir targets, Krossfjord and Fensfjord formations, Troll Field, Norwegian North Sea [PhD Thesis]. Imperial College, London, 335 pp.

Holgate, N.E., Jackson, C.A.-L., Hampson, G.J. and **Dreyer, T.** (2013) Sedimentology and sequence stratigraphy of the Middle–Upper Jurassic Krossfjord and Fensfjord formations, Troll Field, northern North Sea. *Petrol. Geosci.*, **19**, 237-258.

Holgate, N.E., Jackson, C.A.-L., Hampson, G.J. and **Dreyer T.** (2015) Seismic stratigraphic analysis of the Middle Jurassic Krossfjord and Fensfjord formations, Troll oil and gas field, northern North Sea. *Mar. Petrol. Geol.*, **68**, 352-380.

Hollenshead, C.T. and **Pritchard, R.I.** (1961) Geometry of producing Mesaverde sandstones, San Juan Basin. In: *Geometry of Sandstone Bodies* (Eds J.A. Peterson and J.C. Osmond), *AAPG Spec. Publ.*, **22**, 98-118.

Holz, M. (2003) Sequence stratigraphy of a lagoonal estuarine system—an example from the lower Permian Rio Bonito Formation, Paraná Basin, Brazil. *Sed. Geol.*, **162**, 305-331.

Holz, M. and **Kalkreuth, W.** (2004) Sequence Stratigraphy and Coal Petrology Applied to the Early Permian Coal-bearing Rio Bonito Formation, Paraná Basin, Brazil. In: *Sequence stratigraphy, paleoclimate, and tectonics of coal-bearing strata* (Eds J.C. Pashin and R.A. Gastaldo), *AAPG Stud. Geol.*, **51**, 147-167.

Holz, M., Küchle, J., Philipp, R.P., Bischoff, A.P. and **Arima, N.** (2006) Hierarchy of tectonic control on stratigraphic signatures: base-level changes during the Early Permian in the Paraná Basin, southernmost Brazil. *J. S. Am. Earth Sci.*, **22**, 185-204.

Houston, W.S., Huntoon, J.E. and **Kamola, D.L.** (2000) Modeling of Cretaceous foreland-basin parasequences, Utah, with implications for timing of Sevier thrusting. *Geology*, **28**, 267-270.

Hunt, D. and **Tucker, M.E.** (1992) Stranded parasequences and the forced regressive wedge systems tract: deposition during base-level fall. *Sed. Geol.*, **81**, 1-9.

Hutsky, A.J. and **Fielding, C.R.** (2016) The offshore bar revisited: A new depositional model for isolated shallow marine sandstones in the Cretaceous Frontier Formation of the northern Uinta Basin, Utah, USA. *J. Sed. Res.*, **86**, 38-58.

Hutsky, A.J. and **Fielding, C.R.** (2017) Tectonic control on deltaic sediment dispersal in the middle to upper Turonian Western Cordilleran Foreland Basin, USA. *Sedimentology*, **64**, 1540-1571.

Hutsky, A.J., Fielding, C.R. and **Frank, T.D.** (2016) Evidence for a petroleum subsystem in the Frontier Formation of the Uinta–Piceance Basin petroleum province. *AAPG Bull.*, **100**, 1033-1059.

Ilgar, A. (2015) Miocene sea-level changes in northernmost Anatolia: Sedimentary record of eustasy and tectonism at the peri-Pontide fringe of Eastern Paratethys. *Sed. Geol.*, **316**, 62-79.

Ilgar, A. and **Nemec, W.** (2005) Early Miocene lacustrine deposits and sequence stratigraphy of the Ermenek Basin, Central Taurides, Turkey. *Sed. Geol.*, **173**, 233-275.

Immenhauser, A. (2009) Estimating palaeo-water depth from the physical rock record. *Earth-Sci. Rev.*, **96**, 107-139.

Isla, M.F., Schwarz, E. and **Veiga, G.D.** (2018) Bedset characterization within a wave-dominated shallow-marine succession: an evolutionary model related to sediment imbalances. *Sed. Geol.*, **374**, 36-52.

Jaiswal, S., Bhattacharya, B. and **Chakrabarty, S.** (2018) High resolution sequence stratigraphy of Middle Eocene Hazad Member, Jambusar-Broach Block, Cambay Basin, India. *Mar. Petrol. Geol.*, **93**, 79-94.

James, N.P. and **Dalrymple, R.W.** (2010) *Facies models 4*. GEOtext 6, Geological Association of Canada, St John's, 586 pp.

Jervey, M.T. (1988) Quantitative geological modeling of siliciclastic rock sequences and their seismic expression. In: *Sea-Level Changes: An Integrated Approach* (Eds C.K. Wilgus, B.S. Hastings, C.G.St.C Kendall, H.W. Posamentier, C.A. Ross and J.C. Van Wagoner), *SEPM Spec. Publ.*, **42**, 47-69.

Jordan, O.D., Gupta, S., Hampson, G.J. and **Johnson, H.D.** (2016) Preserved stratigraphic architecture and evolution of a net-transgressive mixed wave-and tide-influenced coastal system: the Cliff House Sandstone, northwestern New Mexico, USA. *J. Sed. Res.*, **86**, 1399-1424.

Jorissen, E.L., de Leeuw, A., van Baak, C.G., Mandic, O., Stoica, M., Abels, H.A. and **Krijgsman, W.** (2018) Sedimentary architecture and depositional controls of a Pliocene river-dominated delta in the semi-isolated Dacian Basin, Black Sea. *Sed. Geol.*, **368**, 1-23.

Jouët, G. (2007) Enregistrements stratigraphiques des cycles climatiques et glacio-eustatiques du Quaternaire terminal: modélisations de la marge continentale du Golfe du Lion [PhD Thesis]. Université de Bretagne Occidentale, Brest, 444 pp.

Jouet, G., Berné, S., Rabineau, M., Bassetti, M.A., Bernier, P., Dennielou, B., Sierro, F.J., Flores, J.A. and **Taviani, M.** (2006) Shoreface migrations at the shelf edge and sea-level changes around the Last Glacial Maximum (Gulf of Lions, NW Mediterranean). *Mar. Geol.*, **234**, 21-42.

Kamola, D.L., and **Van Wagoner, J.C.** (1995) Stratigraphy and facies architecture of parasequences with examples from the Spring Canyon Member, Blackhawk Formation, Utah. In: *Sequence Stratigraphy of Foreland Basin Deposits: Outcrop and Subsurface Examples from the Cretaceous of North America* (Eds J.C. Van Wagoner and G.T. Bertram), *AAPG Mem.*, **64**, 27-54.

Katzman, D.R. and **Wright-Dunbar, R.** (1992) Parasequence geometry and facies architecture in the upper Cretaceous Point Lookout Sandstone, Four Corners platform, southwestern Colorado. In: *San Juan Basin IV* (Eds S.G. Lucas, B.S. Kues, T.E. Williamson and A.P. Hunt), New Mexico Geological

Society 43rd Annual Fall Field Conference Guidebook, 187-197.

Ketzer, J.M., Holz, M., Morad, S. and **Al-Aasm, I.S.** (2003) Sequence stratigraphic distribution of diagenetic alterations in coal-bearing, paralic sandstones: evidence from the Rio Bonito Formation (early Permian), southern Brazil. *Sedimentology*, **50**, 855-877.

Kidwell, S.M. (1993) Influence of subsidence on the anatomy of marine siliciclastic sequences and on the distribution of shell and bone beds. *J. Geol. Soc.*, **150**, 165-167.

Kim, W., Paola, C., Swenson, J.B. and **Voller, V. R.** (2006). Shoreline response to autogenic processes of sediment storage and release in the fluvial system. *J. Geophys. Res. Earth Surf.*, **111**, F04013.

Kirschbaum, M.A. and **Cumella, S.P.** (2015) Stratigraphic Trapping Mechanisms in the Iles Formation, Piceance Basin, Colorado. *Mt. Geol.*, **52**(4), 5-26.

Kirschbaum, M.A. and **Hettinger, R.D.** (2004) Facies analysis and sequence stratigraphic framework of upper Campanian strata (Neslen and Mount Garfield Formations, Bluecastle Tongue of the Castlegate Sandstone, and Mancos Shale), eastern Book Cliffs, Colorado and Utah. *USGS Digital Data Series*, DDS-0069-G.

Klug, B. (1993) Cyclic facies architecture as a key to depositional controls in a distal foredeep: Campanian Mesaverde Group, Wyoming, USA. *Geol. Rundsch.*, **82**, 306-326.

Korus, J.T. and **Fielding, C.R.** (2015) Asymmetry in Holocene river deltas: patterns, controls, and stratigraphic effects. *Earth-Sci. Rev.*, **150**, 219-242.

Krystinik, L.F. and **DeJarnett, B.B.** (1995) Lateral variability of sequence stratigraphic framework in the Campanian and Lower Maastrichtian of the Western Interior Seaway. In: *Sequence Stratigraphy of Foreland Basin Deposits: Outcrop and Subsurface Examples from the Cretaceous of North America* (Eds J.C. Van Wagoner and G.T. Bertram), *AAPG Mem.*, **64**, 11-26.

Labaune, C., Jouet, G., Berné, S., Gensous, B., Tesson, M. and **Delpeint, A.** (2005) Seismic stratigraphy of the Deglacial deposits of the Rhone prodelta and of the adjacent shelf. *Mar. Geol.*, **222**, 299-311.

Labaune, C., Tesson, M. and **Gensous, B.** (2008) Variability of the transgressive stacking pattern under environmental changes control: example from the Post-Glacial deposits of the Gulf of Lions inner-shelf, Mediterranean, France. *Cont. Shelf Res.*, **28**, 1138-1152.

Larsen, M. and **Surlyk, F.** (2003) Shelf-edge delta and slope deposition in the upper Callovian–middle Oxfordian Olympen Formation, east Greenland. In: *The Jurassic of Denmark and Greenland* (Eds J.R. Ineson and F. Surlyk), *Geol. Surv. Den. Greenl. Bull.*. **1**, 931-948.

Leclair, S.F. and **Bridge, J.S.** (2001) Quantitative interpretation of sedimentary structures formed by river dunes. *J. Sed. Res.*, **71**, 713-716.

Lee, K., Zeng, X., McMechan, G.A., Howell Jr., C.D., Bhattacharya, J.P., Marcy, F. and **Olariu, C**. (2005) A ground-penetrating radar survey of a delta-front reservoir analog in the Wall Creek Member, Frontier Formation, Wyoming. *AAPG Bull.*, **89**, 1139-1155.

Lee, K., Gani, M.R., McMechan, G.A., Bhattacharya, J.P., Nyman, S.L. and **Zeng, X.** (2007a) Three-dimensional facies architecture and three-dimensional calcite concretion distributions in a tide-influenced delta front, Wall Creek Member, Frontier Formation, Wyoming. *AAPG Bull.*, **91**, 191-214.

Lee, K., McMechan, G.A., Gani, M.R., Bhattacharya, J.P., Zeng, X. and **Howell, C.D.** (2007b) 3-D architecture and sequence stratigraphic evolution of a forced regressive top-truncated mixed-influenced delta, Cretaceous Wall Creek Sandstone, Wyoming, U.S.A. *J. Sed. Res.*, **77**, 303-323.

Leva López, J.L., Kim, W. and **Steel, R.J.** (2014) Autoacceleration of clinoform progradation in foreland basins: theory and experiments. *Basin Res.*, **4**, 489-504.

Li, L., Walstra, D.J.R. and **Storms, J.E.** (2015) The Impact of Wave-Induced Longshore Transport On A Delta–Shoreface System. *J. Sed. Res.*, **85**, 6-20.

Li, W., Bhattacharya, J.P. and **Campbell, C.** (2010) Temporal evolution of fluvial style in a compound incised-valley fill, Ferron "Notom Delta", Henry Mountains Region, Utah (USA). *J. Sed. Res.*, **80**, 529-549.

Li, W., Bhattacharya, J.P. and **Zhu, Y.** (2011a) Architecture of a forced regressive systems tract in the Turonian Ferron "Notom Delta", southern Utah, U.S.A.. *Mar. Petrol. Geol.*, **28**, 1517-1529.

Li, W., Bhattacharya, J.P., Zhu, Y., Garza, D. and **Blankenship, E.** (2011b) Evaluating delta asymmetry using three-dimensional facies architecture and ichnological analysis, Ferron 'Notom Delta', Capital Reef, Utah, USA. *Sedimentology*, **58**, 478-507.

Li, W., Bhattacharya, J.P. and **Zhu, Y.** (2012) Stratigraphic uncertainty in sparse versus rich data sets in a fluvial–deltaic outcrop analog: Ferron Notom delta in the Henry Mountains region, southern Utah. *AAPG Bull.*, **96**, 415-438.

Lin, W. and **Bhattacharya, J.P.** (2017) Estimation of source-to-sink mass balance by a fulcrum approach using channel paleohydrologic parameters of the Cretaceous Dunvegan Formation, Canada. *J. Sed. Res.*, **87**, 97-116.

Lin, W. and **Bhattacharya, J.P.** (2020) Depositional facies and the sequence stratigraphic control of a mixed-process influenced clastic wedge in the Cretaceous Western Interior Seaway: The Gallup System, New Mexico, USA. *Sedimentology*, **67**, 920-950.

Lin, W., Bhattacharya, J.P. and **Stockford, A.** (2019) High-resolution Sequence Stratigraphy and Implications For Cretaceous Glacioeustasy of the Late Cretaceous Gallup System, New Mexico, USA. *J. Sed. Res.*, **89**, 552-575.

Lobo F.J., Hernández-Molina, F.J., Somoza, L. and **Díaz del Río, V.** (2001) The sedimentary record of the post-glacial transgression on the Gulf of Cadiz continental shelf (Southwest Spain). *Mar. Geol.*, **178**, 171-195.

Løseth, T.M. and **Helland-Hansen, W.** (2001) Predicting the pinchout distance of shoreline tongues. *Terra Nova*, **13**, 241-248.

Løseth, T.M., Steel, R.J., Crabaugh, J.P. and **Schellpeper, M.** (2006) Interplay between shoreline migration paths, architecture and pinchout distance for siliciclastic shoreline tongues: evidence from the rock record. *Sedimentology*, **53**, 735-767.

Madof, A.S., Christie-Blick, N. and **Anders, M.H.** (2015) Tectonically controlled nearshore deposition: Cozzette Sandstone, Book Cliffs, Colorado, USA. *J. Sed. Res.*, **85**, 459-488.

Madof, A.S., Harris, A.D. and **Connell, S.D.** (2016) Nearshore along-strike variability: Is the concept of the systems tract unhinged?. *Geology*, **44**, 315-318.

Martinsen, O.J. and **Helland-Hansen, W.** (1994) Sequence Stratigraphy and Facies Model of an Incised Valley Fill: The Gironde Estuary, France: Discussion. *J. Sed. Res.*, **B64**, 78-80.

Martinsen, O.J. and **Helland-Hansen, W.** (1995) Strike variability of clastic depositional systems: Does it matter for sequence-stratigraphic analysis?. *Geology*, **23**, 439-442.

McCabe, P.J. and **Shanley, K.W.** (1992) Organic control on shoreface stacking patterns: bogged down in the mire. *Geology*, **20**, 741-744.

McClung, W.S., Eriksson, K.A., Terry Jr., D.O. and **Cuffey, C.A.** (2013) Sequence stratigraphic hierarchy of the Upper Devonian Foreknobs Formation, central Appalachian Basin, USA: Evidence for transitional greenhouse to icehouse conditions. *Palaeogeogr. Palaeoclimatol. Palaeoecol.*, **387**, 104-125.

McClung, W.S., Cuffey, C.A., Eriksson, K.A. and **Terry Jr., D.O.** (2016) An incised valley fill and lowstand wedges in the Upper Devonian Foreknobs Formation, central Appalachian Basin: Implications for Famennian glacioeustasy. *Palaeogeogr. Palaeoclimatol. Palaeoecol.*, **446**, 125-143.

McIlroy, D., Flint, S., Howell, J.A. and **Timms, N.** (2005) Sedimentology of the tide-dominated Jurassic Lajas Formation, Neuquén Basin, Argentina. In: *The Neuquén Basin, Argentina: a case study*

in sequence stratigraphy and basin dynamics (Eds G.D. Veiga, L.A. Spalletti, J.A. Howell and E. Schwarz), *Geol. Soc. London Spec. Publ.*, **252**, 83-107.

McLaurin, B.T. and **Steel, R.J.** (2007) Architecture and origin of an amalgamated fluvial sheet sand, lower Castlegate Formation, Book Cliffs, Utah. *Sed. Geol.*, **197**, 291-311.

Merletti, G.D., Steel, R.J., Olariu, C., Melick, J.J., Armitage, P.J. and **Shabro, V.** (2018) The last big marine transgression of the Western Interior Seaway: Almond Formation development from barrier spits across south Wyoming. *Mar. Petrol. Geol.*, **98**, 763-782.

Mohrig, D., Heller, P.L., Paola, C. and **Lyons, W.J.** (2000) Interpreting avulsion process from ancient alluvial sequences: Guadalope-Matarranya system (northern Spain) and Wasatch Formation (western Colorado). *Geol. Soc. Am. Bull.*, **112**, 1787-1803.

Muto, T. and **Steel, R.J.** (1992) Retreat of the front in a prograding delta. *Geology*, **20**, 967-970.

Muto, T. and **Steel, R.J.** (1997) Principles of regression and transgression: the nature of the interplay between accommodation and sediment supply. *J. Sed. Res.*, **67**, 994-1000.

Muto, T. and **Steel, R.J.** (2002) Role of autoretreat and A/S changes in the understanding of deltaic shoreline trajectory: a semi-quantitative approach. *Basin Res.*, **14**, 303-318.

Muto, T. and **Steel, R.J.** (2014) The autostratigraphic view of responses of river deltas to external forcing: a review of the concepts. In: *From Depositional Systems to Sedimentary Successions on the Norwegian Continental Margin* (Eds A.W. Martinius, R. Ravnas, J.A. Howell, R.J. Steel and J.P. Wonham), *Int. Assoc. Sedimentol. Spec. Publ.*, 46, 139-148.

Muto, T., Steel., R.J. and **Swenson, J.B.** (2007) Autostratigraphy: a framework norm for genetic stratigraphy. *J. Sed. Res.*, **77**, 2-12.

Neal, J.E., Abreu, V., Bohacs, K.M., Feldman, H.R. and **Pederson, K.H.** (2016) Accommodation succession (δA/δS) sequence stratigraphy: observational method, utility and insights into sequence boundary formation. *J. Geol. Soc.*, **173**, 803-816.

Nichol, S.L., Boyd, R. and **Penland, S.** (1996) Sequence stratigraphy of a coastal-plain incised valley estuary, Lake Calcasieu, Louisiana. *J. Sed. Res.*, **66**, 847-857.

Niedoroda, A.W., Swift, D.J.P. and **Hopkins, T.S.** (1985) The shoreface. In: *Coastal Sedimentary Environments* (Ed R.A. Davis), pp.533-624. Springer, New York.

Nouidar, M. and **Chellaï, E.H.** (2002) Facies and sequence stratigraphy of a Late Barremian wave-dominated deltaic deposit, Agadir Basin, Morocco. *Sed. Geol.*, **150**, 375-384.

O'Byrne, C.J. and **Flint, S.** (1993) High-resolution sequence stratigraphy of Cretaceous shallow marine sandstones, Book Cliffs outcrops, Utah, USA—application to reservoir modelling. *First Break*, **11**, 445-459.

Olariu, M.I., Carvajal, C.R., Olariu, C. and **Steel, R.J.** (2012) Deltaic process and architectural evolution during cross-shelf transits, Maastrichtian Fox Hills Formation, Washakie Basin, Wyoming. *AAPG Bull.*, **96**, 1931-1956.

Patruno, S. and **Helland-Hansen, W.** (2018) Clinoforms and clinoform systems: Review and dynamic classification scheme for shorelines, subaqueous deltas, shelf edges and continental margins. *Earth-Sci. Rev.*, **185**, 202-233.

Pattison, S. (1991) Sedimentology and allostratigraphy of regional, valley-fill, shoreface and transgressive deposits of the Viking Formation (Lower Cretaceous), central Alberta [PhD Thesis]. McMaster University, Hamilton, Ontario, 380 pp.

Pattison, S.A.J. (1992) Recognition and interpretation of estuarine mudstones (Central Basin Mudstones) in the tripartite valley-fill Deposits of the Viking Formation, central Alberta. In: *Applications of ichnology to petroleum exploration – A core workshop* (Ed S.G. Pemberton), *SEPM Core Workshop*, **17**, 223-249.

Pattison, S.A.J. (2010) Alternative sequence stratigraphic model for the Desert Member to Castlegate Sandstone interval, Book Cliffs, eastern Utah: implications for the high-resolution correlation of falling stage nonmarine, marginal-marine, and marine strata. In: *Through the Generations: Geologic and Anthropogenic Field Excursions in the Rocky Mountains from Modern to Ancient* (Eds L.A. Morgan and S.L. Quane), *Geol. Soc. Am. Field Guide*, **18**, 163-192.

Pattison, S.A.J. (2018) Rethinking the incised-valley fill paradigm for Campanian Book Cliffs strata, Utah–Colorado, USA: evidence for discrete parasequence-scale, shoreface-incised channel fills. *J. Sed. Res.*, **88**, 1381-1412.

Pattison, S.A.J. (2019a) Re-evaluating the sedimentology and sequence stratigraphy of classic Book Cliffs outcrops at Tusher and Thompson canyons, eastern Utah, USA: Applications to correlation, modelling, and prediction in similar nearshore terrestrial to shallow marine subsurface settings worldwide. *Mar. Petrol. Geol.*, **102**, 202-230.

Pattison, S.A.J. (2019b) Using classic outcrops to revise sequence stratigraphic models: Reevaluating the Campanian Desert Member (Blackhawk Formation) to lower Castlegate Sandstone interval, Book Cliffs, Utah and Colorado, USA. *Geology*, **47**, 11-14.

Pattison, S.A. (2020) Sediment-supply-dominated stratal architectures in a regressively stacked succession of shoreline sand bodies, Campanian Desert Member to Lower Castlegate Sandstone interval, Book Cliffs, Utah–Colorado, USA. *Sedimentology*, **67**, 390-430.

Plint, A.G. (1990) An allostratigraphic correlation of the Muskiki and Marshybank formations (Coniacian-Santonian) in the Foothills and subsurface of the Alberta Basin. *Bull. Can. Petrol. Geol.*, **38**, 288-306.

Plint, A.G. (1991) High-frequency relative sea-level oscillations in Upper Cretaceous shelf clastics of the Alberta foreland basin: possible evidence for a glacio-eustatic control. In: *Sedimentation, tectonics and eustasy—Sea-level changes at active margin* (Ed D.I.M. MacDonald*), Int. Assoc. Sedimentol. Spec. Publ.*, **12**, 409-428.

Plint, A.G. (2002) Paleovalley systems in the Upper Cretaceous Dunvegan Formation, Alberta and British Columbia. *Bull. Can. Petrol. Geol.*, **50**, 277-296.

Plint, A.G. and **Norris, B.** (1991) Anatomy of a ramp margin sequence: facies successions, paleogeography and sediment dispersal patterns in the Muskiki and Marshybank formations, Alberta Foreland Basin. *Bull. Can. Petrol. Geol.*, **39**, 18-42.

Plint, A.G. and **Wadsworth, J.A.** (2003) Sedimentology and palaeogeomorphology of four large valley systems incising delta plains, Western Canada foreland basin; implications for mid-Cretaceous sea-level changes. *Sedimentology*, **50**, 1147-1186.

Posamentier, H.W. and **Allen, G.P.** (1999) *Siliciclastic sequence stratigraphy: concepts and applications*. Concepts in Sedimentology and Paleontology 7, SEPM, 210 pp.

Posamentier, H.W. and **James, D.P.** (1993) An overview of sequence-stratigraphic concepts: uses and abuses. In: *Sequence Stratigraphy and Facies Associations* (Eds H.W. Posamentier, C.P. Summerhayes, B.U. Haq and G.P. Allen), *Int. Assoc. Sedimentol. Spec. Publ.*, **18**, 3-18.

Posamentier, H.W., Jervey, M.T. and **Vail, P.R.** (1988) Eustatic controls on clastic deposition I—conceptual framework. In: *Sea-Level Changes: An Integrated Approach* (Eds C.K. Wilgus, B.S. Hastings, C.G.St.C. Kendall, H.W. Posamentier, C.A. Ross and J.C. Wagoner), *SEPM Spec. Publ.*, **42**, 109-124.

R Core Team (2018) R: a language and environment for statistical computing. R Foundation for Statistical Computing, Vienna, https://www.R-project.org

Rabineau, M., Berné, S., Aslanian, D., Olivet, J.L., Joseph, P., Guillocheau, F., Bourillet, J.F., Ledrezen, E. and **Granjeon, D.** (2005) Sedimentary sequences in the Gulf of Lion: a record of 100,000 years climatic cycles. *Mar. Petrol. Geol.*, **22**, 775-804.

Rasmussen, E.S. (2009) Detailed mapping of marine erosional surfaces and the geometry of clinoforms

on seismic data: a tool to identify the thickest reservoir sand. *Basin Res.*, 21, 721-737.

Rasmussen, E.S. and **Dybkjær, K.** (2005) Sequence stratigraphy of the Upper Oligocene–Lower Miocene of eastern Jylland, Denmark: role of structural relief and variable sediment supply in controlling sequence development. *Sedimentology*, **52**, 25-63.

Rasmussen, E.S., Dybkjær, K. and **Piasecki, S.** (2004) The Billund delta: a possible new giant aquifer in central and western Jutland. In: *Review of Survey activities 2003* (Eds M. Sønderholm and A.K. Higgins), *Geol. Surv. Den. Greenl. Bull.*, **4**, 21-24.

Reading, H.G. and **Collinson, J.D.** (1996) Clastic Coasts. In: *Sedimentary Environments: Processes, Facies and Stratigraphy* (Ed H.G. Reading), pp. 154-231. Blackwell Science, Oxford.

Resio, D.T. and **Westerink, J.J.** (2008) Modeling the physics of storm surges. *Physics Today*, 61, 33-38.

Reynolds, A.D. (1999) Dimensions of paralic sandstone bodies. *AAPG Bull.*, **83**, 211-229.

Reynolds, A.D. (2009) Paralic successions. In: *Sequence Stratigraphy* (Eds D. Emery and K.J. Myers), Blackwell Science, Oxford, 134-177.

Reynolds, A.D. (2017) Paralic reservoirs. In: *Sedimentology of paralic reservoirs: Recent advances* (Eds G.J. Hampson, A.D Reynolds, B. Kostic and M.R. Wells) *Geol. Soc. London Spec. Publ.*, **444**, 7-34.

Rodriguez, A.B., and **Meyer, C.T.** (2006) Sea-level variation during the Holocene deduced from the morphologic and stratigraphic evolution of Morgan Peninsula, Alabama, USA. *J. Sed. Res.*, **76**, 257-269.

Rodriguez, A.B., Anderson, J.B. and **Simms, A.R.** (2005) Terrace inundation as an autocyclic mechanism for parasequence formation: Galveston Estuary, Texas, USA. *J. Sed. Res.*, **75**, 608-620.

Ross, W.C., Watts, D.E. and **May, J.A.** (1995) Insights from stratigraphic modeling: mud-limited versus sand-limited depositional systems. *AAPG Bull.*, **79**, 231-258.

Rossi, V., Amorosi, A., Sarti, G. and **Mariotti, S.** (2017) Late Quaternary multiple incised-valley systems: An unusually well-preserved stratigraphic record of two interglacial valley-fill successions from the Arno plain (northern Tuscany, Italy). *Sedimentology*, **64**, 1901-1928.

Sadeque, J., Bhattacharya, J.P., MacEachern, J.A., Howell, C.D., Bann, K.L., Gingras, M.K. and **Pemberton, S.G.** (2009) Differentiating amalgamated parasequences in deltaic settings using ichnology: an example from the Upper Turonian Wall Creek Member of the Frontier Formation, Wyoming. In: *Applied Ichnology* (Eds J.A. MacEachern, K.L. Bann, M.K. Gingras and S.G. Pemberton), *SEPM Core Workshop*, **52**, 343-362.

Sadler, P.M. (1981) Sediment accumulation rates and the completeness of stratigraphic sections. *J. Geol.*, **89**, 569-584.

Schlager, W. (1993) Accommodation and supply—a dual control on stratigraphic sequences. *Sed. Geol.*, **86**, 111-136.

Schwarz, E., Veiga, G.D., Álvarez Trentini, G., Isla, M.F. and **Spalletti, L.A.** (2018) Expanding the spectrum of shallow-marine, mixed carbonate-siliciclastic systems: processes, facies distribution and depositional controls of a siliciclastic-dominated example. *Sedimentology*, **65**, 1558-1589.

Shanley, K.W. and **McCabe, P.J.** (1993) Alluvial architecture in a sequence stratigraphic framework: a case history from the Upper Cretaceous of southern Utah, USA. In: *Quantitative Description and Modelling of Clastic Hydrocarbon Reservoirs and Outcrop Analogues* (Eds S. Flint and I.D. Bryant), *Int. Assoc. Sedimentol. Spec. Publ.*, **15**, 21-56.

Shelley, D.C. and **Lawton, T.F.** (2005) Sequence stratigraphy of tidally influenced deposits in a salt-withdrawal minibasin: Upper sandstone member of the Potrerillos Formation (Paleocene), La Popa basin, Mexico. *AAPG Bull.*, **89**, 1157-1179.

Shiers, M.N., Mountney, N.P., Hodgson, D.M. and **Colombera, L.** (2019) Controls on the depositional architecture of fluvial point-bar elements in a coastal-plain succession. In: *Fluvial Meanders and Their Sedimentary Products in the Rock Record* (Eds M. Ghinassi, L. Colombera, N.P. Mountney and A.J.H. Reesink), *Int. Assoc. Sedimentol. Spec. Publ.*, **48**, 15-46.

Simms, A.R. and **Rodriguez, A.B.** (2015) The influence of valley morphology on the rate of bayhead delta progradation. *J. Sed. Res.*, **85**, 38-44.

Simpson, E.L. and **Eriksson, K.A.** (1990) Early Cambrian progradational and transgressive sedimentation patterns in Virginia: an example of the early history of a passive margin. *J. Sed. Petrol.*, **60**, 84-100.

Sixsmith, P.J., Hampson, G.J., Gupta, S., Johnson, H.D. and **Fofana, J.F.** (2008) Facies architecture of a net transgressive sandstone reservoir analog: the Cretaceous Hosta Tongue, New Mexico. *AAPG Bull.*, **92**, 513-547.

Soreghan, G.S. and **Dickinson, W.R.** (1994) Generic types of stratigraphic cycles controlled by eustasy. *Geology*, **22**, 759-761.

Souza, M.C., Angulo, R.J., Assine, M.L. and **Castro, D.L.** (2012) Sequence of facies at a Holocene storm-dominated regressive barrier at Praia de Leste, southern Brazil. *Mar. Geol.*, **291**, 49-62.

Storms, J.E. and **Hampson, G.J.** (2005) Mechanisms for forming discontinuity surfaces within shoreface–shelf parasequences: sea level, sediment supply, or wave regime?. *J. Sed. Res.*, **75**, 67-81.

Steel, R.J. (1988) Coarsening-upward and skewed fan bodies: symptoms of strike-slip and transfer fault movement in sedimentary basins. In: *Fan Deltas: Sedimentology and Tectonic Settings* (Eds W. Nemec and R.J. Steel), pp. 75-83. Blackie and Son, Glasgow.

Straub, K.M., Li, Q. and **Benson, W.M.** (2015). Influence of sediment cohesion on deltaic shoreline dynamics and bulk sediment retention: A laboratory study. *Geophys. Res. Lett.*, **42**, 9808-9815.

Surlyk, F. (1991) Sequence stratigraphy of the Jurassic-lowermost Cretaceous of east Greenland. *AAPG Bull.*, **75**, 1468-1488.

Swift, D.J.P. and **Thorne, J.A.** (1991) Sedimentation on continental margins, I: a general model for shelf sedimentation. In: *Shelf sand and sandstone bodies: geometry, facies and sequence stratigraphy* (Eds D.J.P. Swift, G.F. Oertel, R.W. Tillman and J.A. Thorne), *Int. Assoc. Sedimentol. Spec. Publ.*, **14**, 3-31.

Swift, D.J.P., Phillips, S. and **Thorne, J.A.** (1991) Sedimentation on continental margins, V: parasequences. In: *Shelf sand and sandstone bodies: geometry, facies and sequence stratigraphy* (Eds D.J.P. Swift, G.F. Oertel, R.W. Tillman and J.A. Thorne), *Int. Assoc. Sedimentol. Spec. Publ.*, **14**, 153-187.

Szwarc, T.S., Johnson, C.L., Stright, L.E. and **McFarlane, C.M.** (2015) Interactions between axial and transverse drainage systems in the Late Cretaceous Cordilleran foreland basin: evidence from detrital zircons in the Straight Cliffs Formation, southern Utah, USA. *Geol. Soc. Am. Bull.*, **127**, 372-392.

Tamura, T. (2012) Beach ridges and prograded beach deposits as palaeoenvironment records. *Earth-Sci. Rev.*, **114**, 279-297.

Taylor, D.R. and **Lovell, R.W.W.** (1992) Recognition of high-frequency sequences in the Kenilworth Member of the Blackhawk Formation, Book Cliffs, Utah. In: *Sequence stratigraphy applications to shelf sandstone and sandstone reservoirs: outcrop to subsurface examples* (Eds J.C. Van Wagoner, D. Nummedal, C.R. Jones, D.R. Taylor, D.C., Jennette and G.W. Riley), *AAPG Field Conference Guidebook*, unpaginated.

Teng, L.S. and **Tai, P.-C.** (1996) Facies characteristics and sequence stratigraphy of the Oligocene continental shelf deposits of northern Taiwan. In: *Proceedings of the International Symposium on Sequence Stratigraphy in SE Asia* (Eds C.A. Caughey, D.C. Carter, J. Clure, M.J. Gresko, P. Lowry, R.K. Park and A. Wonders), Indonesian Petroleum Association, 421-434.

Thomas, M.A. and **Anderson, J.B.** (1994) Sea-level controls on the facies architecture of the Trinity/Sabine incised-valley system, Texas continental shelf. In: *Incised-Valley Systems: Origin and Sedimentary Sequences* (Eds W. Dalrymple, R. Boyd and B.A. Zaitlin), *SEPM Spec. Publ.*, **51**, 63-82.

Vakarelov, B.K. and **Bhattacharya, J.P.** (2009) Local tectonic control on parasequence architecture: Second Frontier Sandstone, Powder River basin, Wyoming. *AAPG Bull.*, **93**, 295-327.

Vail, P.R., Mitchum, R.M., Jr. and **Thompson, S.** (1977) Seismic stratigraphy and global changes of sea level, Part 4, global cycles of relative changes of sea level. In: *Seismic Stratigraphy, Application to Hydrocarbon Exploration* (Ed C.E. Payton), *AAPG Mem.*, **26**, 83-97.

van den Bergh, T.C.V. and **Garrison Jr., J.R.** (2004) The geometry, architecture, and sedimentology of fluvial and deltaic sandstones within the Upper Ferron Sandstone Last Chance Delta: implications for reservoir modeling. In: *Regional to wellbore analog for fluvial-deltaic reservoir modeling: the Ferron Sandstone of Utah* (Eds T. Chidsey, R.D. Adams and T.H. Morris), *AAPG Stud. Geol.*, **50**, 451-498.

van der Vegt, H., Storms, J.E., Walstra, D.J.R., Nordahl, K., Howes, N.C. and **Martinius, A.W.** (2020) Grain size fractionation by process-driven sorting in sandy to muddy deltas. *Depos. Rec.*, **6**, 217-235.

Van Wagoner, J.C. (1985) Reservoir facies distribution as controlled by sea-level change, SEPM Mid-Year Meeting, Golden, Colorado, 91-92.

Van Wagoner, J.C. (1992) High-frequency sequence stratigraphy and facies architecture of the Sego sandstone in the Book Cliffs of western Colorado and eastern Utah In: *Sequence stratigraphy applications to shelf sandstone and sandstone reservoirs: outcrop to subsurface examples* (Eds J.C. Van Wagoner, D. Nummedal, C.R. Jones, D.R. Taylor, D.C., Jennette and G.W. Riley), *AAPG Field Conference Guidebook*, unpaginated.

Van Wagoner, J.C., Posamentier, H.W., Mitchum, R.M., Vail, P.R., Sarg, J.F., Loutit, T.S. and **Hardenbol, J.** (1988) An overview of the fundamentals of sequence stratigraphy and key definitions. In: *Sea-Level Changes: An Integrated Approach* (Eds C.K. Wilgus, B.S. Hastings, C.G.St.C. Kendall, H.W. Posamentier, C.A. Ross and J.C. Wagoner), *SEPM Spec. Publ.*, **42**, 39-45.

Van Wagoner, J.C., Mitchum, R.M., Campion, K.M. and **Rahmanian, V.D.** (1990) *Siliciclastic sequence stratigraphy in well logs, cores, and outcrops: concepts for high-resolution correlation of time and facies*. Methods in Exploration Series Volume 7, American Association of Petroleum Geologists, Tulsa, 55 pp.

Vosgerau, H., Alsen, P., Carr, I.D., Therkelsen, J., Stemmerik, L. and **Surlyk F.** (2004) Jurassic syn-rift sedimentation on a seawards-tilted fault block, Traill Ø, North-East Greenland. In: *The Jurassic of North-East Greenland* (Eds L. Stemmerik and S. Stouge), *Geol. Surv. Den. Greenl. Bull.*, **5**, 9-18.

Wang, J. and **Bhattacharya, J.P.** (2017) Plan-view Paleochannel Reconstruction of Amalgamated Meander Belts, Cretaceous Ferron Sandstone, Notom Delta, South-central Utah, USA. *J. Sed. Res.*, **88**, 58-74.

Wang, Y., Liu, X., Li, G. and **Zhang, W.** (2016) Stratigraphic variations in the Diaokou lobe area of the Yellow River delta, China: implications for an evolutionary model of a delta lobe. In: *River-dominated shelf sediments of east Asian seas* (Eds P.D. Clift, J. Harff, J. Wu and Y. Qui), *Geol. Soc. London Spec. Publ.*, **429**, 185-195.

Wehr, F.L. (1993) Effects of variations in subsidence and sediment supply on parasequence stacking patterns. In: *Siliciclastic Sequence Stratigraphy: Recent Developments and Applications* (Eds P. Weimer and H.W. Posamentier), *AAPG Mem.*, **58**, 369-379.

Welch, B.L. (1951) On the comparison of several mean values: an alternative approach. *Biometrika*, **38**, 330-336.

Wesolowski, L.J., Buatois, L.A., Mángano, M.G., Ponce, J.J. and **Carmona, N.B.** (2018) Trace fossils, sedimentary facies and parasequence architecture from the Lower Cretaceous Mulichinco

Formation of Argentina: The role of fair-weather waves in shoreface deposits. *Sed. Geol.*, **367**, 146-163.

Wolinsky, M.A., Swenson, J.B., Litchfield, N. and **McNinch, J.E.** (2010) Coastal progradation and sediment partitioning in the Holocene Waipaoa sedimentary system, New Zealand. *Mar. Geol.*, **270**, 94-107.

Wright-Dunbar, R., Zech, R.S., Crandall, G.A. and **Katzman, D.R.** (1992) Strandplain and deltaic depositional models for the Point Lookout Sandstone, San Juan Basin and Four Corners Platform, New Mexico and Colorado. In: *San Juan Basin IV* (Eds S.G. Lucas, B.S. Kues, T.E. Williamson and A.P. Hunt), New Mexico Geological Society 43rd Annual Fall Field Conference Guidebook, 199-206.

Xue, C. (1993) Historical changes in the Yellow River delta, China. *Mar. Geol.*, **113**, 321-330.

Zecchin, M. (2007) The architectural variability of small-scale cycles in shelf and ramp clastic systems: the controlling factors. *Earth-Sci. Rev.*, **84**, 21-55.

Zecchin, M. (2010) Towards the standardization of sequence stratigraphy: is the parasequence concept to be redefined or abandoned?. *Earth-Sci. Rev.*, **102**, 117-119.

Zecchin, M., Mellere, D. and **Roda, C.** (2006). Sequence stratigraphy and architectural variability in growth fault-bounded basin fills: a review of Plio-Pleistocene stratal units of the Crotone Basin, southern Italy. *J. Geol. Soc.*, **163**, 471-486.

Zecchin, M., Catuneanu, O. and **Caffau, M.** (2019) Wave-ravinement surfaces: Classification and key characteristics. *Earth-Sci. Rev.*, **188**, 210-239.

Zhang, X., Dalrymple, R.W. and **Lin, C.-M.** (2017) Facies and stratigraphic architecture of the late Pleistocene to early Holocene tide-dominated paleo-Changjiang (Yangtze River) delta. *Geol. Soc. Am. Bull.*, **130**, 455-483.

Zhu, Y., Bhattacharya, J.P., Li, W., Lapen, T.J., Jicha, B.R. and **Singer, B.S.** (2012) Milankovitch-scale sequence stratigraphy and stepped forced regressions of the Turonian Ferron Notom Deltaic Complex, South-Central Utah, U.S.A. *J. Sed. Res.*, **63**, 723-746.